Stability of solutions of integrable partial differential equations

Jeremy Upsal

A dissertation
submitted in partial fulfillment of the
requirements for the degree of

Doctor of Philosophy

University of Washington

2020

Reading Committee:

Bernard Deconinck, Chair

Anne Greenbaum

Matthew Lorig

Dmitry Pelinovsky

Program Authorized to Offer Degree:
Applied Mathematics

University of Washington

Abstract

Stability of solutions of integrable partial differential equations

Jeremy Upsal

Chair of the Supervisory Committee:
Professor of Applied Mathematics Bernard Deconinck
Department of Applied Mathematics

Stability analysis for solutions of partial differential equations (PDEs) is important for determining the applicability of a model to the physical world. Establishing stability for PDE solutions is often significantly more challenging than for ordinary differential equation solutions. This task becomes tractable for PDEs possessing a Lax pair. In this dissertation, I provide a general framework for computing large parts of the Lax spectrum for periodic and quasiperiodic solutions of a general class of PDEs possessing a Lax pair. This class consists of the AKNS hierarchy admitting a common reduction and generalizations. I then relate the Lax spectrum to the stability spectrum using the squared-eigenfunction connection. Using this, I demonstrate that the subset of the real line which is part of the Lax spectrum maps to stable elements of the linearization.

Several examples that demonstrate the direct applicability of this work are provided. One example is worked out in detail: the stability analysis for the elliptic solutions of the focusing nonlinear Schrödinger (NLS) equation. For the NLS equation, I go further by establishing orbital stability of the elliptic solutions with respect to a class of perturbations of integer multiples of the period of the solution.

TABLE OF CONTENTS

Page

GLOSSARY

$\overline{\mathbb{R}}$: the extended real line, $\overline{\mathbb{R}} = \mathbb{R} \cup \{\infty\}$.

ζ: the Lax parameter.

σ_L: the Lax spectrum.

$\sigma_{\mathcal{L}}$: the stability spectrum.

*: the complex conjugate.

ζ_w: the Weierstrass zeta function.

NLS equation: nonlinear Schrödinger equation, focusing or defocusing.

fNLS equation: focusing nonlinear Schrödinger equation.

dNLS equation: defocusing nonlinear Schrödinger equation.

ACKNOWLEDGMENTS

I first want to thank my supervisory committee for the time and energy they put into reviewing this work: Bernard Deconinck, Anne Greenbaum, Dmitry Pelinovsky, Lucien Brush, and Matt Lorig. I would especially like to thank my advisor Bernard Deconinck. His support and guidance made this work possible. Bernard has been an incredible mentor since I entered graduate school. He immediately invited me into his research group and presented me with many interesting research problems. He guided me when I needed help and let me be when I needed to figure things out on my own. His mentorship helped me get through graduate school and my job search. Further, he taught me almost as much about hiking the PNW as he has about doing research. For that and everything else, I am thankful. The research group that Bernard has established at UW has been an incredibly close and inspiring group to be a part of: Ben Segal, Chris Swierczewski, Jorge Cisneros, Matthew Farkas, Natalie Sheils, Olga Trichtchenko, Ryan Creedon, and Xin Yang. Thank you all for your support, friendship, and for enduring the 8-9 hour weekly meetings with me every week.

When I was an undergraduate student at the University of Colorado at Boulder, I was lucky enough to take a class with Harvey Segur. He taught me so much about differential equations, applied math, and literature. Little did I know at the time that 8 years later I would be writing a thesis that all stems from his influential work in the ‘70s. Harvey, thank you for your mentorship, friendship, and for helping me get to where I am today.

When I was applying to graduate school I had little idea of what I wanted. I decided to come to the University of Washington primarily due to the culture in the department. I have been fortunate to be a part of that culture and to meet and work with some great people over the last six years. I certainly owe thanks to more people than I mention here, so thank you to all. I want to give a special thanks to the AMATH teaching discussion group for providing a fun environment for learning and talking about pedagogy. I also want to give a special thanks to Lauren Lederer for all of the hard work she does in the department and all of the questions she has answered for me and numerous other students.

The majority of my thanks are to the friends I have made since joining the AMATH department.

I remember the immediately strong sense of "being in the right place" I felt upon meeting my cohort. The friendships I developed in that first year have grown and only become more important to me. My favorite part of graduate school was staying in Lewis late into the night with Brian and Weston working on Burke's homework. Without you two, I would not know what a **cone** is. With you two, I still don't know what it is. Thank you two for the camaraderie that started then and continued when we moved in together. The shenanigans continued when Andreas, Brian, Kathleen, and I all began to share on office together. Thank you all for the fun conversations, cabins, and motivation to work. Andreas, thank you for always pushing for beach day: I look forward to more in the future. Although not in my cohort, I also made friends with those in my year in the math department. I especially want to thank Alex Voet whose steadfast Zaire coups have taught me more about stability than anything else I have done in these last six years. Thank you also to my friend from middle school Gavin Medley who was an excellent roommate at the University of Colorado and who taught me that hiking is fun. This may be the most influential lesson I have ever learned in life.

Finally, I want to thank my family. Thank you mom and dad for always supporting and loving me. Thank you for always being interested in what I am doing: it helps keep everything in check. Thank you Isaac for always being a role model in academia. Without you having studied math and physics, I never would have myself. Without you getting a PhD and telling me about it, I never would have gotten there myself. I am constantly amazed and humbled by your work ethic and attitude. I also want to thank my most recent family members: Dana and Olive. Thank you for entering my life and being there for me during my PhD studies. Olive, thank you for being a good study buddy during this thesis writing and for always reminding me to slow down and pay attention to you. Dana, thank you for supporting me, making me laugh, and for everything else you bring into my life. You are an amazing person and scientist and I am lucky to call you my best friend.

DEDICATION

To my parents: Andrea and Chip.

Chapter 1

INTRODUCTION

Stability analysis for solutions of differential equations plays an important rule in relating mathematical models to physical applications. If a solution to a differential equation that appears as a mathematical model is stable, then it is likely to be found in a physical system. One typically first typically learns about stability in a first class on ordinary differential equations (ODEs). Establishing the stability of solutions to partial differential equations (PDEs) is significantly more challenging than establishing the stability of solutions to ODEs. This is because the the solutions of ODEs depend on a finite number of parameters whereas the solutions of PDEs depend on an infinite number of parameters. Nonetheless, many ODE ideas are borrowed for studying the stability of PDE solutions. In this dissertation, I focus on integrable Hamiltonian PDEs for which tools have been developed to make this task tractable [10, 11, 14, 22, 24, 26, 27, 28, 33, 58, 64].

1.1 Stability

The focus of this dissertation is a nonlinear evolution equation

$$u_t = \mathcal{N}(u, u_x, \ldots, u_{Nx}), \tag{1.1}$$

where $u(x,t)$ is a real- or complex-valued function (possibly vector valued) and $\mathcal{N}$ is a nonlinear functional of u and N of its spatial derivatives. Unless otherwise stated, I assume that (1.1) is written in a frame in which there exists a classical nontrivial stationary solution, $u(x,t) = \bar{u}(x)$ which is *periodic* or *quasiperiodic*.

Definition 1.1.1. For the purposes of this work, a complex-valued function f is *quasiperiodic* with period P if $|f(x+P)| = |f(x)|$ for $P \in \mathbb{R}$. If f is a real-valued function, then f is *periodic* with period P.

In order to study the stability of the stationary solution $\bar{u}$, I first linearize (1.1) about $\bar{u}$ by letting $u(x,t) = \bar{u}(x) + \epsilon v(x,t) + \mathcal{O}\left(\epsilon^2\right)$, where $\epsilon > 0$ is a small parameter. Truncating at $\mathcal{O}(\epsilon)$

yields

$$v_t = \mathcal{L}(\bar{u}, \bar{u}_x, \ldots, \bar{u}_{Nx})v, \tag{1.2}$$

where $\mathcal{L}$ is a linear functional. Since $\mathcal{L}(\bar{u}, \bar{u}_x, \ldots, \bar{u}_{Nx})$ is independent of t, (1.2) can be solved with separation of variables by letting

$$v(x,t) = \hat{v}(x;\lambda)e^{\lambda t}, \tag{1.3}$$

yielding a spectral problem for λ:

$$\lambda\hat{v} = \mathcal{L}(\bar{u}, \bar{u}_x, \ldots, \bar{u}_{Nx})\hat{v}. \tag{1.4}$$

Definition 1.1.2. The *stability spectrum* is the set

$$\sigma_{\mathcal{L}} = \{\lambda \in \mathbb{C} : \hat{v} \in S_{\mathcal{L}}\}, \tag{1.5}$$

where $S_{\mathcal{L}}$ is a function space that is chosen later to fit the needs of the specific problem. In essence, $S_{\mathcal{L}}$ is chosen to be the least restrictive space that works in this framework. Typically $C_b^0(\mathbb{R})$, the space of real-valued continuous functions that are bounded on the closed real line, works.

The spectrum $\sigma_{\mathcal{L}}$ for equations (1.1) that are Hamiltonian possess a quadrafold symmetry: if $\lambda \in \sigma_{\mathcal{L}}$, then $-\lambda, \lambda^*, -\lambda^* \in \sigma_{\mathcal{L}}$ (here and throughout * represents the complex conjugate) [44]. There are many different types of stability. The first definition of stability is the weakest type of stability considered in this dissertation.

Definition 1.1.3. A stationary solution $u(x,t) = \bar{u}(x)$ of (1.1) is *spectrally stable* if and only if the stability spectrum of the corresponding operator $\mathcal{L} = \mathcal{L}(\bar{u}, \bar{u}_x, \ldots, \bar{u}_{Nx})$ is a subset of the imaginary axis, $\sigma_{\mathcal{L}} \subset i\mathbb{R}$.

Since spectral stability is determined first by linearizing the equation, it does not tell the whole story. A solution can be spectrally stable and still have perturbations that grow under the full nonlinear dynamics [74]. A stronger notion of stability is one that takes into account the full nonlinear dynamics. Such a result is called a *nonlinear stability* result. Although spectral stability is a good indicator for nonlinear stability, it is not enough to conclude nonlinear stability. A common way to establish a nonlinear stability is to find a Lyapunov function that controls the long-time behavior of the perturbation [74]. This step is not immediate for PDEs since, even if a Lyapunov

functional is found, there are an infinite number of directions that may not necessarily be controlled by the Lyapunov functional. The equations studied in this dissertation are invariant under a group G of symmetries. In other words, if $\tilde{u}$ is a solution of (1.1), then $u = \mathcal{A}(g)\tilde{u}$ is also a solution of (1.1), where $\mathcal{A}(g)$ is the action of an element g of the group of symmetries G. For such equations, the strongest form of nonlinear stability that can exist is *orbital stability* [40].

Definition 1.1.4. A stationary solution $u(x,t) = \bar{u}(x)$ of (1.1) is *orbitally stable* with respect to the norm $||\cdot||$ if for any given $\epsilon > 0$ there exists a $\delta > 0$ such that

$$||u(x,0) - \bar{u}(x)|| < \delta, \tag{1.6}$$

implies that for all $t > 0$,

$$\inf_{g \in G} ||u(x,t) - \mathcal{A}(g)\bar{u}(x)|| < \epsilon, \tag{1.7}$$

where $\mathcal{A}(g)$ is the action of an element g of the group of symmetries G.

Determining the stability, either spectral or orbital, of a stationary solution of a PDE is generally difficult. There exists few orbital stability results in the literature. The stability results in this dissertation rely on the evolution equation (1.1) being an *integrable* PDE, which is defined in the next section. Integrability is used for determining spectral stability and in finding a Lyapunov functional that works to establish orbital stability, using the techniques in [40].

1.2 Integrability

There exists several different definitions for the term *integrable system* [76]. The following definition is used in this dissertation.

Definition 1.2.1. A PDE (1.1) is *integrable* if there exists a *Lax Pair*, *i.e.,* a pair of two linear ODEs,

$$\Phi_x = X\Phi, \qquad\qquad \Phi_t = T\Phi, \tag{1.8}$$

such that the compatibility of mixed derivatives $\partial_t \Phi_x = \partial_x \Phi_t$ holds if (1.1) holds. Here T and X are $n \times n$ matrices depending on the dependent and independent variables in (1.1).

This definition is different from the usual definition for ODEs. For ODEs, integrability is usually defined as there being "enough" conserved quantities to constrain a system to a unique solution

from initial conditions. It is the case, however, that if a PDE possesses a Lax pair, then it possesses an infinite number of conserved quantities and an infinite number of symmetries [7, 76]. For most of this work, the Lax pair is the main aspect of integrable equations that is needed: the Lax pair is used to find spectral stability. The extra conserved quantities are used to show orbital stability by constructing a Lyapunov functional in conjunction with the results of [40]

A surprisingly large number equations of physical significance are integrable and possess a Lax pair [7, 8]. The matrices X and T defining the Lax pair depend on a parameter ζ, called the *Lax parameter*. An important feature of equations with a Lax pair is the Lax spectrum.

Definition 1.2.2. The *Lax spectrum* is the set

$$\sigma_L = \{\zeta \in \mathbb{C} : \Phi \in S_L\}, \tag{1.9}$$

where S_L is a function space to be defined later. It turns out that S_L is related to the space $S_{\mathcal{L}}$.

The squared-eigenfunction connection for a PDE, sometimes referred to as the *strong symmetry* of the PDE or *quadratic eigenfunction expansion*, is a connection between the Lax spectrum, σ_L, and the stability spectrum, $\sigma_{\mathcal{L}}$. This connection usually relates the eigenfunction of the linear stability problem with quadratic combinations of the eigenfunctions of the Lax problem, but it is currently unknown how general this is. There is no general method for finding the squared-eigenfunction connection for a given problem. In fact, it is unknown whether or not every integrable equation possesses a squared-eigenfunction connection [39].

Until recently, the Lax spectrum had only been determined explicitly for decaying potentials on the whole line or for self-adjoint problems with periodic coefficients. For such problems, the Floquet discriminant [4, 14, 31, 33, 45, 58] is a useful, and indeed the most common, tool for numerically computing and giving a qualitative description of the Lax spectrum, but it is not used generally to get an explicit description of the Lax spectrum. A full description of the Lax spectrum can allow one to prove the stability of solutions to integrable equations with respect to certain classes of perturbations. This is accomplished using the squared-eigenfunction connection.

In [28] and Chapter 2 I give a full description of the Lax spectrum for the focusing nonlinear Schrödinger (fNLS) equation using a tool different from the Floquet discriminant. In [71] and Chapters 3 and 4 I provide insight into determining important aspects of the Lax spectrum for a large class of integrable PDEs and provide a generic framework for computing the Floquet discriminant (Appendix B).

1.3 General steps and organization of the dissertation

The general method for establishing stability in this dissertation follows a set of specific steps. Each of these steps is worked out in detail for the fNLS equation in Chapter 2. Some of the steps are worked out for a general class of integrable equations in Chapters 3 and 4.

1. Linearize the PDE (1.1) about the stationary solution $u(x,t) = \bar{u}(x)$ as in Section 1.1.

2. Find the Lax spectrum (Definition 1.2.1) by finding the eigenfunctions Φ and constructing a function whose level set gives the Lax spectrum. This is done in Section 2.2.3 for the fNLS equation.

3. Find and use the squared-eigenfunction connection which provides a map $\Omega : \sigma_L \to \sigma_{\mathcal{L}}$ to find the linear stability spectrum (Definition 1.1.2). Establish whether or not Ω is surjective. It is assumed that Ω is surjective in the following steps.

4. Identify the set $\mathcal{S} \subset \sigma_L$ such that $\Omega : \mathcal{S} \to \sigma_{\mathcal{L}} \cap i\mathbb{R}$. The set $\mathcal{S}$ consists of "stable" elements of the Lax spectrum because they get mapped to stable elements of the stability spectrum. This is done in Section 2.2.4 for the fNLS equation and is the main result of Chapters 3 and 4.

5. If the set $\mathcal{S} \neq \sigma_L$, then the solution $\bar{u}(x)$ is unstable with respect to general perturbations in $\mathcal{S}_{\mathcal{L}}$. The solution, however, may be stable with respect to important subsets of $\mathcal{S}_{\mathcal{L}}$. In order to establish this, $\mathcal{S}$ must be matched with that subset through the squared-eigenfunction connection. For the fNLS equation, this subset is a class of *subharmonic perturbations*. Subharmonic perturbations are those perturbations whose period is an integer multiple of the fundamental period of the solution. This is one of the main results of Chapter 2, see 2.2.18 and 2.2.21.

6. The final step is to prove orbital stability when the solution is spectrally stable. This is done by constructing a Lyapunov functional using the conserved quantities of (1.1). The Lyapunov functional itself is not enough to establish orbital stability for the equations studied here. The functional must also be shown to match several conditions outlined in [40]. This is proven here only for the fNLS equation solutions that are spectrally stable with respect to a class of subharmonic perturbations, Section 2.4.

In Chapter 2 I go through the above steps in detail for the elliptic solutions of the fNLS equation. This work was completed first in [28]. During this work, I noticed some patterns shared by all of the integrable equations whose stability has been studied using these techniques: the real line, as a subset of the Lax spectrum, always gets mapped to stable elements under the squared-eigenfunction connection. This motivated me to find a more general technique that could easily be applied to other integrable equations.

In Chapter 3 I present a general method for determining the Lax spectrum for a large class of integrable PDEs, the AKNS hierarchy. The focus is on elements of the Lax spectrum that give rise to stable elements of the stability spectrum. I provide a number of examples that fit the general description and for which I can say something about spectral stability.

In Chapter 4 I generalize the results presented in Chapter 3 to integrable PDEs that are not in the AKNS hierarchy but that share similar features. This chapter suggests that the results is this dissertation are more widely applicable than to just the AKNS hierarchy.

In Chapter 5 I suggest future work that follows from the results in this dissertation and discuss the difficulties of pushing this work further.

Chapter 2

ORBITAL STABILITY FOR THE FOCUSING NONLINEAR SCHRÖDINGER EQUATION

In this chapter I work through the steps outlined in the Introduction in full detail for the fNLS equation. The work in this chapter appears in [28].

The focusing, one-dimensional, cubic Nonlinear Schrödinger (fNLS) equation,

$$i\Psi_t + \frac{1}{2}\Psi_{xx} + \Psi\,|\Psi|^2 = 0, \tag{2.1}$$

is a universal model for a variety of physical phenomena [16, 41, 52, 65, 69, 78]. In 1972, Zakharov and Shabat [77] found its Lax Pair and the explicit expression for the one-soliton solution. The orbital stability of the soliton was first proved in 1982 by Cazenave and Lions [15] and later by Weinstein [72] using Lyapunov techniques, as used here. Even with such a rich history, a full stability analysis in the periodic setting had not been completed until [28]. The simplest periodic solutions are the genus-one or elliptic solutions (Section 2.1). Rowlands [66] was the first to study their stability using perturbation methods. Since then, Gallay and Hărăgus have examined the stability of small-amplitude elliptic solutions [35] and proven orbital stability with respect to perturbations of the same period as the underlying solution [36] (*i.e.*, coperiodic perturbations). Gustafson, Le Coz, and Tsai [42] establish instability for the elliptic solutions with respect to periodic perturbations of sufficiently large amplitude. The analysis of spectral instability with respect to perturbations of an integer multiple of the period (*i.e.*, subharmonic perturbations) was completed in [27].

In this chapter I build upon the results in [27] to examine the stability of elliptic solutions of arbitrary amplitude. An outline of the steps followed and the conclusions obtained is given below.

1. Spectral stability is considered in Section 2.2 by following the outline in the Introduction. This is motivated by considering the simpler case of the well-known Stokes waves in Section 2.2.2. For these solutions, all operators involved have constant coefficients, and all calculations are explicit. I get to the spectrum of the operator obtained by linearizing about a solution through its connection with the *Lax spectrum*. To this end, I introduce the Lax pair and its spectrum in Section 2.2.3. The setup for determining the Lax spectrum in Section 2.2.3 is from [27]

while the results in Section 2.2.3 and all subsequent sections are new. Section 2.2.4 contains the main spectral stability result: solutions are spectrally stable with respect to subharmonic perturbations if the solution parameters meet a given sufficiency condition (Theorem 2.2.21). This condition is shown to be necessary in most cases and is discussed in Appendix A.3. In essence, Theorem 2.2.21 establishes that solutions of "smaller amplitude" are spectrally stable with respect to a larger class of subharmonic perturbations, *i.e.*, subharmonic perturbations of larger period. The notion of "smaller amplitude" is made more precise in Section 2.2.4.

2. In Section 2.3, I examine how instabilities depend on the parameters of the solution. The orbital stability results of Section 2.4 rely crucially on understanding the spectrum for stable compared to unstable solutions. Thus the transition from stable to unstable dynamics as solution parameters are changed is studied carefully.

3. Finally, in Section 2.4 I use a Lyapunov method [40, 47, 61] to prove (nonlinear) orbital stability in the cases where spectral stability holds. The main result of this chapter is found at the end of the section: I establish the orbital stability of almost all solutions that are spectrally stable. The only solutions for which such a result eludes me are those whose solution parameters are on the boundary of the parameter regions specifying with respect to which subharmonic perturbations the solutions are spectrally stable.

2.1 Elliptic solutions of the fNLS equation

In this chapter I study solutions of (2.1) whose only change in time is through a constant phase-change. Such solutions are stationary solutions of

$$i\psi_t + \omega\psi + \frac{1}{2}\psi_{xx} + \psi\,|\psi|^2 = 0, \tag{2.2}$$

found by defining $\Psi(x,t) = e^{-i\omega t}\psi(x,t)$. Time-independent solutions to (2.2) satisfy

$$\omega\phi + \frac{1}{2}\phi_{xx} + \phi\,|\phi|^2 = 0, \tag{2.3}$$

and are expressed in terms of elliptic functions as

$$\Psi = e^{-i\omega t}\phi(x) = R(x)e^{i\theta(x)}e^{-i\omega t}, \tag{2.4}$$

with

$$R^2(x) = b - k^2\,\mathrm{sn}^2(x,k), \qquad \omega = \frac{1}{2}(1+k^2-3b), \tag{2.5a}$$

$$\theta(x) = c\int_0^x \frac{1}{R^2(y)}\,\mathrm{d}y, \qquad c^2 = b(1-b)(b-k^2), \tag{2.5b}$$

where $\mathrm{sn}(x,k)$ is the Jacobi elliptic sn function with elliptic modulus k [1, Chapter 22]. The parameters b and k are constrained by

$$0 \le k < 1, \qquad k^2 \le b \le 1, \tag{2.6}$$

see Figure 2.1. The solutions formally limit to the soliton as $k \to 1$, which is omitted from these studies [55]. When $k = 0$ and $b \neq 0$, (2.4) reduces to a so-called Stokes wave (Section 2.2.2). The boundary values, $b = k^2$ and $b = 1$, are special cases. In both cases $c = 0$ so $\theta = 0$ and the solutions are said to have trivial phase. When $c \neq 0$, the solutions have non-trivial phase (NTP). I call $\phi(x) = k\,\mathrm{cn}(x,k)$ and $\phi(x) = \mathrm{dn}(x,k)$ the cn and dn solutions corresponding to $b = k^2$ and $b = 1$, respectively. Here $\mathrm{cn}(x,k)$ and $\mathrm{dn}(x,k)$ are the Jacobi elliptic cn and dn functions with elliptic modulus k [1, Chapter 22]. The trivial-phase solutions are periodic, with periods $4K(k)$ and $2K(k)$ for the cn and dn solutions respectively, where

$$K(k) := \int_0^{\pi/2} \frac{\mathrm{d}y}{\sqrt{1-k^2\sin^2(y)}}, \tag{2.7}$$

the complete elliptic integral of the first kind [1, Chapter 19].

Remark 2.1.1. The nontrivial-phase solutions are typically quasi-periodic but only the x-periodic amplitude $R^2(x)$ appears in the analysis. Therefore, unless otherwise stated, any mention of the periodicity of the solutions is in reference to the period of the amplitude which is $T(k) = 2K(k)$ for all solutions.

The elliptic solutions can be written in terms of Weierstrass elliptic functions via

$$\wp(z+\omega_3; g_2, g_3) - e_3 = \left(\frac{K(k)k}{\omega_1}\right)^2 \mathrm{sn}^2\left(\frac{K(k)z}{\omega_1}\right), \tag{2.8}$$

where $\wp(z; g_2, g_3)$ is the Weierstrass elliptic $\wp$ function [1, Chapter 23] with lattice invariants g_2, g_3 and ω_1 and ω_3 are the half-periods of the Weierstrass lattice. Lastly, e_1, e_2, and e_3 are the zeros of

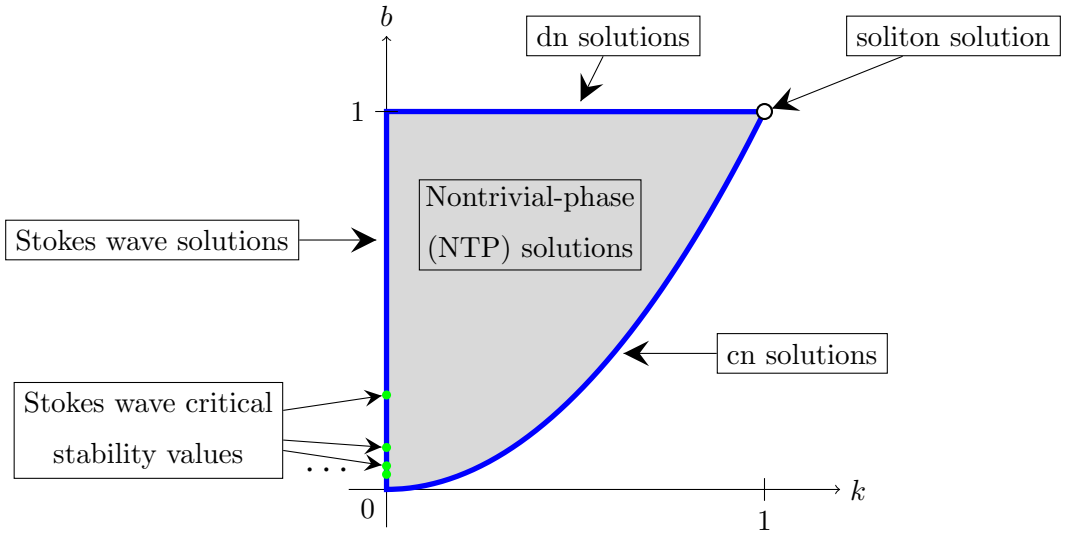

Figure 2.1: The parameter space for the elliptic solutions (2.4) with solution regions labeled. The first 4 Stokes wave stability bounds are plotted in green dots on the line $k = 0$, at which $b = 1/P^2$ for $P \in \{1, 2, 3, 4\}$ (2.28).

the polynomial $4t^3 - g_2 t - g_3$, and

$$e_1 = \frac{1}{3}(2 - k^2), \qquad e_2 = \frac{1}{3}(2k^2 - 1), \qquad e_3 = -\frac{1}{3}(1 + k^2), \tag{2.9a}$$

$$g_2 = \frac{4}{3}(1 - k^2 + k^4), \qquad g_3 = \frac{4}{27}(2 - 3k^2 - 3k^4 + 2k^6), \tag{2.9b}$$

$$\omega_1 = \int_{e_1}^{\infty} \frac{\mathrm{d}z}{\sqrt{4z^3 - g_2 z - g_3}} = K(k), \tag{2.9c}$$

$$\omega_3 = \int_{-e_3}^{\infty} \frac{\mathrm{d}z}{\sqrt{4z^3 - g_2 z - g_3}} = iK\left(\sqrt{1 - k^2}\right). \tag{2.9d}$$

The Weierstrass form of the elliptic solutions is explained in more detail in [21, Section 3.1.3].

2.2 Spectral stability

Spectral stability of elliptic solutions is examined by considering

$$\Psi(x,t) = e^{-i\omega t} e^{i\theta(x)} \left(R(x) + \epsilon u(x,t) + \epsilon i v(x,t)\right) + \mathcal{O}\left(\epsilon^2\right), \tag{2.10}$$

where ϵ is a small parameter and u and v are real-valued functions of x and t. Substituting this into (2.1) and keeping only first-order in ϵ terms gives an autonomous ODE in t. Separating

variables $(u(x,t), v(x,t)) = e^{\lambda t}(U(x), V(x))$ results in the spectral problem

$$\lambda \begin{pmatrix} U \\ V \end{pmatrix} = \begin{pmatrix} -S & \mathcal{L}_- \\ -\mathcal{L}_+ & -S \end{pmatrix} \begin{pmatrix} U \\ V \end{pmatrix} = J \begin{pmatrix} \mathcal{L}_+ & S \\ -S & \mathcal{L}_- \end{pmatrix} \begin{pmatrix} U \\ V \end{pmatrix} = J\mathscr{L} \begin{pmatrix} U \\ V \end{pmatrix} = \mathcal{L} \begin{pmatrix} U \\ V \end{pmatrix}, \tag{2.11}$$

where

$$\mathcal{L} = J\mathscr{L}, \tag{2.12}$$

and

$$\begin{aligned} \mathcal{L}_- &= -\frac{1}{2}\partial_x^2 - R^2(x) - \omega + \frac{c^2}{2R^4(x)}, \\ \mathcal{L}_+ &= -\frac{1}{2}\partial_x^2 - 3R^2(x) - \omega + \frac{c^2}{2R^4(x)}, \\ S &= \frac{c}{R^2(x)}\partial_x - \frac{cR'(x)}{R^3(x)}. \end{aligned} \tag{2.13}$$

The stability spectrum is defined as

$$\sigma_{\mathcal{L}} = \left\{ \lambda \in \mathbb{C} : U, V \in C_b^0(\mathbb{R}) \right\}, \tag{2.14}$$

where $C_b^0(\mathbb{R})$ is the space of real-valued continuous functions, bounded on the closed real line. Due to the Hamiltonian symmetry of the spectrum [44], an elliptic solution is spectrally stable to perturbations in $C_b^0(\mathbb{R})$ if $\sigma_{\mathcal{L}} \subset i\mathbb{R}$.

2.2.1 Stability with respect to subharmonic perturbations

The elliptic solutions are not stable with respect to general bounded perturbations [27]. Therefore, I restrict to *subharmonic perturbations*. Subharmonic perturbations are periodic perturbations whose period is an integer multiple of the fundamental period of a given elliptic solution. Since the operator $\mathcal{L}$ has periodic coefficients (2.13), the eigenfunctions of the spectral problem (2.11) may be decomposed using a Floquet-Bloch decomposition [23],

$$\begin{pmatrix} U(x) \\ V(x) \end{pmatrix} = e^{i\mu x} \begin{pmatrix} \hat{U}_\mu(x) \\ \hat{V}_\mu(x) \end{pmatrix}, \tag{2.15}$$

where $\hat{U}_\mu, \hat{V}_\mu$ are $T(k)$ periodic and $\mu \in [0, 2\pi/T(k))$.

Definition 2.2.1. A *P-subharmonic perturbation* of a solution is a perturbation of integer multiple P times the period of the solution. A 1-subharmonic perturbation is called a *coperiodic perturbation*.

For P-subharmonic perturbations,

$$\mu = m\frac{2\pi}{PT(k)}, \qquad m = 0, \ldots, P-1. \tag{2.16}$$

Note that μ may be defined in any interval of length $2\pi/T(k)$ so the $m = 1$ and $m = P-1$ cases are connected via

$$\mu = -\frac{2\pi}{PT(k)} = (P-1)\frac{2\pi}{PT(k)} \qquad \mod 2\pi/T(k). \tag{2.17}$$

Using the Floquet-Bloch decomposition, $\mathcal{L} \mapsto \mathcal{L}_\mu$ with $\partial_x \mapsto \partial_x + i\mu$ in (2.11). I define the subharmonic stability spectrum with parameter μ,

$$\sigma_\mu = \left\{\lambda \in \mathbb{C} : \hat{U}_\mu, \hat{V}_\mu \in L^2_{\text{per}}\left([-T(k)/2, T(k)/2]\right)\right\}, \tag{2.18}$$

where $L^2_{\text{per}}([-L/2, L/2])$ is the space of square-integrable functions with period L. The spectrum σ_μ consists of isolated eigenvalues of finite multiplicity.

2.2.2 Spectral stability of Stokes Waves

I begin with the simplest case of (2.4). When $k = 0$, the solution is a Stokes wave solution of (2.1). The spectral stability of these solutions is straightforward to analyze, but the analysis is informative for understanding the general features of the stability of other solutions. I choose to work with the Stokes waves in this form to link them with the general elliptic solutions (2.4). The Stokes waves are given by

$$\Psi(x,t) = \sqrt{b}\; e^{ix\sqrt{1-b}}\; e^{-i(1-3b)t/2}, \tag{2.19}$$

with parameter $b \in (0, 1]$. The spectral problem (2.11) becomes

$$\lambda \begin{pmatrix} U \\ V \end{pmatrix} = \begin{pmatrix} -\sqrt{1-b}\;\partial_x & -\frac{1}{2}\partial_x^2 \\ \frac{1}{2}\partial_x^2 + 2b & -\sqrt{1-b}\;\partial_x \end{pmatrix} \begin{pmatrix} U \\ V \end{pmatrix} = \mathcal{L}_S \begin{pmatrix} U \\ V \end{pmatrix}. \tag{2.20}$$

I consider the constant coefficients of $\mathcal{L}_S$ as π-periodic since $2K(k) \to \pi$ as $k \to 0$. This allows the results to match results below for the more general solutions of Section 2.1, but the results for the Stokes waves are independent of this choice of period. Thus the eigenfunctions $(U, V)^\intercal$ of (2.20) may be decomposed via a Floquet-Bloch decomposition (2.15)

$$\begin{pmatrix} U(x) \\ V(x) \end{pmatrix} = e^{i\mu x} \begin{pmatrix} \hat{U}(x) \\ \hat{V}(x) \end{pmatrix}, \tag{2.21}$$

where $\hat{U}$, $\hat{V}$ have period π and $\mu \in [0, 2)$. Since (2.20) has constant coefficients, it suffices to consider each Fourier mode $(\hat{U}_n, \hat{V}_n)^\intercal$ individually:

$$\lambda \begin{pmatrix} \hat{U}_n \\ \hat{V}_n \end{pmatrix} = \begin{pmatrix} -i\sqrt{1-b}\ (\mu+2n) & \frac{1}{2}(\mu+2n)^2 \\ 2b - \frac{1}{2}(\mu+2n)^2 & -i\sqrt{1-b}\ (\mu+2n) \end{pmatrix} \begin{pmatrix} \hat{U}_n \\ \hat{V}_n \end{pmatrix} = \hat{\mathcal{L}}_S^{(n,\mu)} \begin{pmatrix} \hat{U}_n \\ \hat{V}_n \end{pmatrix}, \tag{2.22}$$

where $n \in \mathbb{Z}$. The eigenvalues of $\hat{\mathcal{L}}_S^{(n,\mu)}$ are

$$\lambda_\pm^{(n,\mu)} = \frac{\mu+2n}{2}\left(-2i\sqrt{1-b} \pm \sqrt{4b-(\mu+2n)^2}\right). \tag{2.23}$$

These eigenvalues are imaginary if

$$\mu + 2n = 0 \quad \text{or} \quad b \leq (\mu+2n)^2/4. \tag{2.24}$$

The Stokes wave with amplitude b is spectrally stable with respect to bounded perturbations if (2.24) holds for all $n \in \mathbb{Z}$ and $\mu \in [0, 2)$. For a given b, there exist μ and n such that (2.24) is not satisfied. Consequently, the Stokes waves are not spectrally stable with respect to general bounded perturbations. To examine stability with respect to special classes of perturbations, I consider special values of μ.

Equating $\mu = 0$ corresponds to perturbations with the same period as the solution. The spectral stability criterion (2.24) becomes $n = 0$ or $b \leq n^2$ which is satisfied for all n, independent of b, consistent with [27, 36]. For $\mu \neq 0$, the tightest bound on b from (2.24) is given by

$$b \leq \begin{cases} \mu^2/4, & \mu \in (0, 1], \\ (\mu-2)^2/4, & \mu \in [1, 2). \end{cases} \tag{2.25}$$

With

$$\mu = \frac{2m}{P}, \quad P \in \mathbb{Z}^+, \quad m \in \{0, \ldots, P-1\}, \tag{2.26}$$

the perturbation (2.10) has P times the period of the Stokes wave. The spectral stability criterion (2.25) becomes

$$b \leq \begin{cases} m^2/P^2, & m \in \mathbb{Z} \cap (0, P/2], \\ (m/P-1)^2, & m \in \mathbb{Z} \cap [P/2, P). \end{cases} \tag{2.27}$$

When $P = 1,\ \mu = 0$ for which the spectral stability criterion is always satisfied. When $P > 1$, the bounds on b are tightest when $m = 1$ and when $m = P - 1$ respectively. I call the eigenvalues with $\mu(m = 1) = \mu_1$ and $\mu(m = P - 1) = \mu_{P-1}$ the critical eigenvalues. In either case it must be that

$$b \leq 1/P^2 \tag{2.28}$$

for spectral stability of Stokes waves with respect to P-subharmonic perturbations (see Figure 2.1). This result agrees with [27, Theorem 9.1] but is found in a more direct manner.

Next I examine the process by which solutions transition from a spectrally stable state to a spectrally unstable state with respect to a fixed μ as b increases (see Figure 2.2). For a fixed $P = P_c$, consider a value of b such that (2.28) is satisfied with $b < 1/P_c^2$, *i.e.*, the solution is spectrally stable with respect to P_c-subharmonic perturbations. The above work gives that the instability with respect to P_c-subharmonic perturbations first arises when $b_c = 1/P_c^2$ from the critical eigenvalues with $\mu_1 = 2/P_c$ and with $\mu_{P_c-1} = 2(1 - 1/P_c)$. Defining

$$\lambda_c(b) := i\frac{2}{P_c}\sqrt{1-b} = 2i\sqrt{b_c(1-b)}, \tag{2.29}$$

gives

$$\mathrm{Im}(\lambda_+^{(0,\mu_1)}(b)) < \mathrm{Im}(\lambda_c(b)) < \mathrm{Im}(\lambda_-^{(0,\mu_1)}(b)), \tag{2.30}$$

$$\mathrm{Im}(\lambda_+^{(-1,\mu_{P_c-1})}(b)) > \mathrm{Im}(\lambda_c^*(b)) > \mathrm{Im}(\lambda_-^{(-1,\mu_{P_c-1})}(b)) : \tag{2.31}$$

the critical eigenvalues for $n = 0$ and for $n = -1$ are ordered on the imaginary axis and straddle $\lambda_c(b)$ or $\lambda_c^*(b)$. Increasing b leads to $b = b_c = 1/P_c^2$ where

$$\lambda_+^{(0,\mu_1)} = \lambda_-^{(0,\mu_1)} = \lambda_c = -\lambda_+^{(-1,\mu_{P_c-1})} = -\lambda_-^{(-1,\mu_{P_c-1})} \in i\mathbb{R}, \tag{2.32}$$

and the critical eigenvalues collide at λ_c and $\lambda_c^* = -\lambda_c$ in the upper and lower half planes respectively. At the collision,

$$\lambda_c(b_c) = 2i\sqrt{b_c(1-b_c)}. \tag{2.33}$$

This is the intersection of the top of the figure 8 spectrum and the imaginary axis in the complex λ plane [27, equation (92)]. Instability occurs when two critical imaginary eigenvalues collide along the imaginary axis in a Hamiltonian Hopf bifurcation and enter the right and left half planes along the figure 8, see Figure 2.2. Other such collisions of eigenvalues occur at the top and bottom

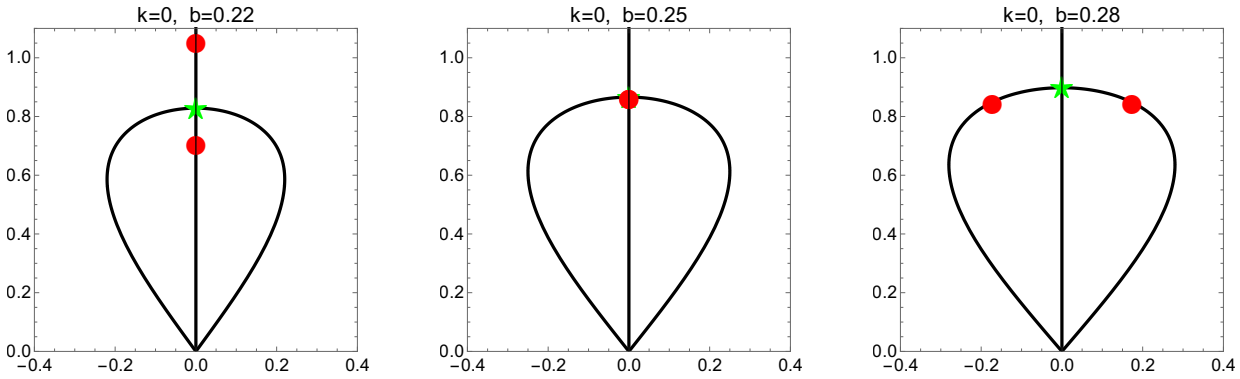

Figure 2.2: The upper half complex λ plane, depicting part of the spectrum for Stokes waves using (2.23) with $b = 0.22$, $b = 0.25$, $b = 0.28$ from left to right. Red dots represent eigenvalues with $P = 2$ and $n = 0$ (using (2.26)). The green star at the intersection of the curve and the imaginary axis represents λ_c (2.29) where the eigenvalues collide.

of the figure 8 leading to unstable modes as b varies, but the classification of spectral stability *vs.* instability is governed by the first unstable modes.

In the rest of Section 2.2, the results for Stokes waves are generalized to the elliptic solutions of (2.1). Doing so is far more technical, but the main idea remains the same: solutions that are spectrally stable with respect to a given subharmonic perturbation become unstable with respect to that subharmonic perturbation when two imaginary eigenvalues collide at the top of the figure 8 spectrum.

2.2.3 The Lax spectrum and the squared-eigenfunction connection

The stability of the elliptic solutions is more difficult to analyze than that of the Stokes waves since $\mathcal{L}$ (2.11) does not have constant coefficients. To determine the spectrum $\sigma_{\mathcal{L}}$, I use the integrability of the fNLS equation and follow step similar to those in Chapter 3. In particular, I use that (2.2) is obtained by requiring that $\Phi_{xt} = \Phi_{tx}$ hold, where

$$\Phi_x = \begin{pmatrix} -i\zeta & \psi \\ -\psi^* & i\zeta \end{pmatrix} \Phi, \qquad \Phi_t = \begin{pmatrix} A & B \\ C & -A \end{pmatrix} \Phi, \tag{2.34a}$$

$$A = -i\zeta^2 + \frac{i}{2}|\psi|^2 + \frac{i}{2}\omega, \qquad B = \zeta\psi + \frac{i}{2}\psi_x, \qquad C = -\zeta\psi^* + \frac{i}{2}\psi_x^*. \tag{2.34b}$$

Equations 2.34 are the Lax pair of the fNLS equation.

Finding the Lax spectrum and the squared eigenfunction connection

I say that $\zeta \in \sigma_L$ (the Lax spectrum) if ζ gives rise to a bounded (for $x \in \mathbb{R}$) eigenfunction of (2.34). To determine these eigenfunctions, restrict the Lax pair (2.34) to the elliptic solutions (2.4) by letting $\psi(x,t) = \phi(x)$. Since now (2.34) are autonomous in t, let $\Phi(x,t) = e^{\Omega t}\varphi(x)$. In order for φ to be nontrivial,

$$\Omega^2 = A^2 + BC = -\zeta^4 + \omega\zeta^2 + c\zeta - \frac{1}{16}\left(4\omega b + 3b^2 + (1-k^2)^2\right). \tag{2.35}$$

For $\Phi(x,t)$ to be a simultaneous solution of (2.34), it must be that

$$\begin{aligned} \Phi(x,t) = \begin{pmatrix} \Phi_1 \\ \Phi_2 \end{pmatrix} &= e^{\Omega t} y(x) \begin{pmatrix} -B(x;\zeta) \\ A(x;\zeta) - \Omega \end{pmatrix}, \\ y(x) &= y_0 \exp\left(-\int \mathcal{I}\, \mathrm{d}x \right), \end{aligned} \tag{2.36}$$

whenever $\langle \mathrm{Re}(\mathcal{I}) \rangle = 0$, *i.e.*, $\mathrm{Re}(\mathcal{I})$ has zero average over one spatial period $T(k)$, and y_0 is a constant. The integrand $\mathcal{I}$ is defined by

$$\begin{aligned} \mathcal{I} &= \frac{i\zeta B(x;\zeta) + (A(x;\zeta) - \Omega)\phi(x) + B_x(x;\zeta)}{B(x;\zeta)} \\ &= \frac{A_x(x;\zeta) - \phi(x)^* B(x;\zeta) - i\zeta(A(x;\zeta) - \Omega)}{A(x;\zeta) - \Omega}. \end{aligned} \tag{2.37}$$

Two seemingly different definitions for $\mathcal{I}$ are given in (2.37). The two definitions arise from the fact that (2.34) defines two linearly dependent differential equations for $y(x)$. The two equivalent definitions for $\mathcal{I}$ follow from Φ_1 and Φ_2 respectively. The average of $\mathcal{I}$ is computed in [27] using the second representation:

$$\begin{aligned} I(\zeta) &= -\int_0^{T(k)} \mathcal{I}\, \mathrm{d}x \\ &= -2i\zeta\omega_1 + \frac{4i(-c + 4\zeta^3 - 2\zeta\omega - 4i\zeta\Omega(\zeta))}{\wp'(\alpha)} \left(\zeta_w(\alpha)\omega_1 - \zeta_w(\omega_1)\alpha\right), \end{aligned} \tag{2.38}$$

where ζ_w is the Weierstrass-Zeta function [1, Chapter 23], and α is any solution of

$$\wp(\alpha) = 2i(\Omega(\zeta) + i\zeta^2 - i\omega/6). \tag{2.39}$$

Note that (2.38) has the opposite sign of [27, equation (69)] in which it is defined inconsistently. Using

$$\left(\wp'(\alpha)\right)^2 = -4\left(-c + 4\zeta^3 - 2\zeta\omega - 4i\zeta\Omega(\zeta)\right)^2, \tag{2.40}$$

(2.38) is given by the simpler form

$$I(\zeta) = -2i\zeta\omega_1 + 2(\zeta_w(\alpha)\omega_1 - \zeta_w(\omega_1)\alpha)\Gamma, \tag{2.41}$$

where

$$\Gamma = \frac{2i\left(-c + 4\zeta^3 - 2\zeta\omega - 4i\zeta\Omega(\zeta)\right)}{\wp'(\alpha)}. \tag{2.42}$$

From (2.40), $|\Gamma| = 1$. The condition for $\zeta \in \sigma_L$ is

$$\zeta \in \sigma_L \Leftrightarrow \mathrm{Re}(I(\zeta)) = 0. \tag{2.43}$$

The derivative

$$\frac{\mathrm{d}I}{\mathrm{d}\zeta} = \frac{2E(k) - (1 + b - k^2 + 4\zeta^2)K(k)}{2\Omega(\zeta)}, \tag{2.44}$$

where

$$E(k) := \int_0^{\pi/2} \sqrt{1 - k^2 \sin^2(y)}\ \mathrm{d}y, \tag{2.45}$$

the complete elliptic integral of the second kind [1, Chapter 19], is used for examining σ_L. Tangent vectors to the curves constituting σ_L are given by the vector

$$\left(\mathrm{Im}\left(\frac{\mathrm{d}I}{\mathrm{d}\zeta}\right), \mathrm{Re}\left(\frac{\mathrm{d}I}{\mathrm{d}\zeta}\right)\right)^{\intercal}, \tag{2.46}$$

in the complex ζ plane.

When $\zeta \in \sigma_L$, the squared-eigenfunction connection [7, 27] gives the spectrum $\lambda = 2\Omega(\zeta)$ and the corresponding eigenfunctions of $\mathcal{L}$ (2.11),

$$\begin{pmatrix} U \\ V \end{pmatrix} = \begin{pmatrix} e^{-i\theta(x)}\varphi_1^2 - e^{i\theta(x)}\varphi_2^2 \\ -ie^{-i\theta(x)}\varphi_1^2 - ie^{i\theta(x)}\varphi_2^2 \end{pmatrix}, \tag{2.47}$$

where $(\varphi_1, \varphi_2)^{\intercal} = e^{-\Omega t}\Phi$. The following theorem establishes that the squared-eigenfunction connection can be used to obtain almost every eigenvalue of $\mathcal{L}$.

Theorem 2.2.2. *All but six solutions of* (2.11) *are obtained through the squared-eigenfunction connection* (2.47). *Specifically, all solutions of* (2.11) *bounded on the whole real line are obtained through the squared-eigenfunction connection, except at* $\lambda = 0$.

Proof. The proof is similar to the proof of [11, Theorem 2]. For a complete proof, see Appendix A.3.4. □

Therefore the condition for spectral stability is that $\Omega(\sigma_L) \subset i\mathbb{R}$.

Remark 2.2.3. The explicit eigenfunction representation (2.47) can be used to construct an explicit representation for the Floquet discriminant which is a commonly used tool for computing σ_L [4, 14, 31, 58]. The Floquet discriminant for the fNLS equation and other integrable equations is constructed and analyzed in Appendix B.

To examine the stability with respect to subharmonic perturbations, I need λ in terms of μ. Except for the Stokes waves (Section 2.2.2), λ cannot be expressed in terms of μ explicitly. Instead, I use an explicit expression for $\mu = \mu(\zeta)$ and the connection between ζ and λ to say something about $\lambda(\mu)$. Equation (112) in [27] gives

$$\begin{aligned} e^{iT(k)\mu(\zeta)} &= \exp\left(-2\int_0^{T(k)} \frac{(A(x)-\Omega)\phi(x) + B_x(x) + i\zeta B(x)}{B(x)}\mathrm{d}x\right) e^{i\theta(T(k))} \\ &= e^{2I(\zeta)+i\theta(T(k))}. \end{aligned} \tag{2.48}$$

It follows that

$$M(\zeta) := T(k)\mu(\zeta) = -2iI(\zeta) + \theta(T(k)) + 2\pi n, \quad n \in \mathbb{Z}. \tag{2.49}$$

Here, $\theta(T(k))$ is defined to be continuous at $b = k^2$ by

$$\theta(T(k)) := \begin{cases} \int_0^{T(k)} \frac{c}{R^2(x)}\ \mathrm{d}x, & b > k^2, \\ \pi, & b = k^2. \end{cases} \tag{2.50}$$

For nontrivial-phase solutions, the Weierstrass integral formula [13, equation 1037.06] gives

$$\begin{aligned} \theta(T(k)) &= \int_0^{2\omega_1} \frac{c}{e_0 - \wp(x; g_2, g_3)}\ \mathrm{d}x = \frac{4c}{\wp'(\alpha_0)}\left(\alpha_0\zeta_w(\omega_1) - \omega_1\zeta_w(\alpha_0)\right) \\ &= -2i\left(\alpha_0\zeta_w(\omega_1) - \omega_1\zeta_w(\alpha_0)\right), \end{aligned} \tag{2.51}$$

where

$$\wp(\alpha_0) = e_0 = -\frac{2\omega}{3} = b + e_3, \tag{2.52}$$

and $\wp'(\wp^{-1}(e_0)) = 2ic$ is obtained from [21, equation (3.51)].

A description of the Lax spectrum

Since the Lax spectrum is used to determine the stability spectrum, a complete description of the Lax spectrum is required for the stability analysis. In what follows, I use the notation

$$\zeta_1 = \frac{1}{2}\left(\sqrt{1-b} + i(\sqrt{b} - \sqrt{b-k^2})\right), \qquad \zeta_2 = \frac{1}{2}\left(-\sqrt{1-b} + i(\sqrt{b} + \sqrt{b-k^2})\right), \tag{2.53a}$$

$$\zeta_3 = \frac{1}{2}\left(-\sqrt{1-b} - i(\sqrt{b} + \sqrt{b-k^2})\right), \qquad \zeta_4 = \frac{1}{2}\left(\sqrt{1-b} - i(\sqrt{b} - \sqrt{b-k^2})\right), \tag{2.53b}$$

for the roots of Ω^2 in the first, second, third, and fourth quadrants of the complex ζ plane, respectively (for cn and NTP solutions). I refer to the roots collectively as ζ_j. I rely heavily on [27, Lemma 9.2] which states that $M(\zeta)$ (2.49) must increase in absolute value along σ_L until a turning point is reached, where $\mathrm{d}I/\mathrm{d}\zeta = 0$. The only turning points occur at $\zeta = \pm\zeta_c$ where

$$\zeta_c^2 := \frac{2E(k) - (1 + b - k^2)K(k)}{4K(k)}. \tag{2.54}$$

Since $\zeta_c^2 \in \mathbb{R}$, ζ_c is real or imaginary depending on the solution parameters (k, b). I refer to ζ_c as the solution to (2.54) with $\mathrm{Re}(\zeta_c) \geq 0$ and $\mathrm{Im}(\zeta_c) \geq 0$. I primarily use $-\zeta_c$ in the analysis to follow since the branch of spectrum in the left half plane maps to the outer figure 8 (see Figure 2.6) which corresponds to the dominant instabilities. Further, $\zeta_c = 0$ when $b = B(k)$ where

$$B(k) := \frac{2E(k) - (1 - k^2)K(k)}{K(k)}. \tag{2.55}$$

For $b > B(k)$, $\zeta_c \in i\mathbb{R} \setminus \{0\}$ and for $b < B(k)$, $\zeta_c \in \mathbb{R} \setminus \{0\}$. The following lemmas concern the shape of the Lax spectrum and are important in the analysis of the stability of solutions.

Lemma 2.2.4. *The Lax spectrum σ_L is symmetric about $\mathrm{Im}\,\zeta = 0$. Further, if $\mu(\zeta)$ increases (decreases) in the upper half plane, then $\mu(\zeta)$ decreases (increases) at the same rate in the lower half plane along σ_L.*

Proof. Though the proof for the symmetry of σ_L comes more directly from the spectral problem, I prove it by other means here to setup the proof for the second part of the lemma.

The tangent line to the curve $\mathrm{Re}(I) = 0$ is given by (2.46), where

$$\mathrm{Re}\left(\frac{\mathrm{d}I}{\mathrm{d}\zeta}\right) = \frac{2E(k)\Omega_r - K(k)\left(8\zeta_i\zeta_r\Omega_i + (1 + b - k^2 + 4(\zeta_r^2 - \zeta_i^2))\Omega_r\right)}{2(\Omega_i^2 + \Omega_r^2)}, \tag{2.56a}$$

$$\mathrm{Im}\left(\frac{\mathrm{d}I}{\mathrm{d}\zeta}\right) = \frac{-2E(k)\Omega_i + K(k)\left(-8\zeta_i\zeta_r\Omega_r + (1 + b - k^2 + 4(\zeta_r^2 - \zeta_i^2))\Omega_i\right)}{2(\Omega_i^2 + \Omega_r^2)}, \tag{2.56b}$$

and Ω_r (Ω_i) and ζ_r (ζ_i) are the real (imaginary) parts of Ω and ζ respectively. Since

$$\mathrm{Re}\left(\Omega^2\right) = -\frac{1}{16}\left(1+3b^2-2k^2+k^4-16c\zeta_r+4b\omega+16(\zeta_i^4+\zeta_r^4-\zeta_r^2\omega+\zeta_i^2(\omega-6\zeta_r^2))\right), \quad (2.57a)$$

$$\mathrm{Im}\left(\Omega^2\right) = \zeta_i\left(-4\zeta_r^3+2\omega\zeta_r+c+4\zeta_i^2\zeta_r\right), \quad (2.57b)$$

only $\mathrm{Im}\left(\Omega^2\right)$ changes sign as $\zeta_i \to -\zeta_i$. It follows that $\Omega_i \to -\Omega_i$ and $\Omega_r \to \Omega_r$ as $\zeta_i \to -\zeta_i$. From (2.46) and (2.56),

$$\left(\mathrm{Im}\left(\frac{\mathrm{d}I}{\mathrm{d}\zeta}\right), \mathrm{Re}\left(\frac{\mathrm{d}I}{\mathrm{d}\zeta}\right)\right) \to \left(-\mathrm{Im}\left(\frac{\mathrm{d}I}{\mathrm{d}\zeta}\right), \mathrm{Re}\left(\frac{\mathrm{d}I}{\mathrm{d}\zeta}\right)\right), \qquad \text{as} \qquad \zeta_i \to -\zeta_i. \quad (2.58)$$

Therefore, σ_L looks qualitatively the same from ζ_j to $-\zeta_c$ as it does from ζ_j^* to $-\zeta_c$.

I calculate the directional derivative of $\mu(\zeta)$ along σ_L:

$$\begin{aligned}\left(\frac{\mathrm{d}\mu(\zeta)}{\mathrm{d}\zeta_r}, \frac{\mathrm{d}\mu(\zeta)}{\mathrm{d}\zeta_i}\right) \cdot \left(\mathrm{Im}\,\frac{\mathrm{d}I}{\mathrm{d}\zeta}, \mathrm{Re}\,\frac{\mathrm{d}I}{\mathrm{d}\zeta}\right) &= 2\left(\frac{\mathrm{d}\,\mathrm{Im}(I)}{\mathrm{d}\zeta_r}, \frac{\mathrm{d}\,\mathrm{Im}(I)}{\mathrm{d}\zeta_i}\right) \cdot \left(\mathrm{Im}\,\frac{\mathrm{d}I}{\mathrm{d}\zeta}, \mathrm{Re}\,\frac{\mathrm{d}I}{\mathrm{d}\zeta}\right) \\ &= 2\left(\left(\mathrm{Im}\,\frac{\mathrm{d}I}{\mathrm{d}\zeta}\right)^2 + \left(\mathrm{Re}\,\frac{\mathrm{d}I}{\mathrm{d}\zeta}\right)^2\right),\end{aligned} \quad (2.59)$$

which is symmetric about $\mathrm{Im}\,\zeta = 0$.

□

Lemma 2.2.5. *When $b \le B(k)$, given in* (2.55)*, the branch of the Lax spectrum in the left half plane (right half plane) intersects the real axis at $\zeta = -\zeta_c$ ($\zeta = \zeta_c$).*

Proof. Let $\zeta_r \in \mathbb{R}$ and $\epsilon > 0$. Since the vector field (2.46) is continuous across the real ζ axis, and since σ_L is vertical at the intersection with the real ζ axis by virtue of (2.58), it must be that

$$\mathrm{Im}\left(\frac{\mathrm{d}I}{\mathrm{d}\zeta}\bigg|_{\zeta=\zeta_r+i\epsilon}\right) = \mathrm{Im}\left(\frac{\mathrm{d}I}{\mathrm{d}\zeta}\bigg|_{\zeta=\zeta_r-i\epsilon}\right), \qquad \text{as } \epsilon \to 0. \quad (2.60)$$

Then

$$\Omega^2(\zeta_r \pm i\epsilon) = \Omega^2(\zeta_r) \pm i\epsilon\left(c-4\zeta_r^3+2\zeta_r\omega\right) + \mathcal{O}\left(\epsilon^2\right), \quad (2.61)$$

so that

$$\Omega(\zeta_r \pm i\epsilon) = \Omega(\zeta_r) \pm \frac{i\epsilon}{2\Omega(\zeta_r)}(c-4\zeta_r^3+2\zeta_r\omega) + \mathcal{O}\left(\epsilon^2\right) = i\Omega_i + \Omega_r + \mathcal{O}\left(\epsilon^2\right), \quad (2.62)$$

where $\Omega_r = \mathcal{O}(\epsilon)$ since $\Omega(\zeta_r) \in i\mathbb{R}$. By (2.56b), equation (2.60) is only satisfied as $\epsilon \to 0$ if

$$\zeta_r = \pm\frac{\sqrt{2E(k)-(1+b-k^2)K(k)}}{2\sqrt{K(k)}} = \pm\zeta_c. \quad (2.63)$$

□

The next lemma details the topology of the Lax spectrum. To my surprise, there exist few rigorous results describing the Lax spectrum in the literature even though it has been used in various contexts (see *e.g.*, [4, 31, 58, 60]). Some representative plots of the Lax spectrum are shown in Figure 2.3.

Lemma 2.2.6. *The Lax spectrum for the elliptic solutions consists only of the real line and two bands, each connecting two of the roots of* Ω.

Proof. The fact that the entire real line is part of the Lax spectrum is proven in [27] but I present a different, simpler proof that does not rely on integrating $\mathcal{I}$ (2.38). If $\zeta \in \mathbb{R}$, the only possibility for a real contribution to the integral of $\mathcal{I}$ over a period $T(k)$ is through

$$\mathcal{E} := \frac{\phi^* B}{A - \Omega}, \tag{2.64}$$

since $A(x)$ is $T(k)$-periodic. Using the definitions for $A,\ B$, and ϕ,

$$\operatorname{Re} \mathcal{E} = \frac{1}{2} \frac{\mathrm{d}}{\mathrm{d}x} \log(R^2 - 2\zeta^2 + \omega + 2i\Omega), \tag{2.65}$$

which has zero average since R^2 is $T(k)$-periodic. It follows that $\mathbb{R} \subset \sigma_L$. That the roots of $\Omega(\zeta)$ are in the Lax spectrum follows from the fact that $M(\zeta_j) \in \mathbb{R}$ (Lemma 2.2.20). Because the coefficients of $\mathcal{L}$ are periodic, there can exist no isolated eigenvalues of $\sigma_{\mathcal{L}}$. It follows that the Lax spectrum can be continued away from the roots of Ω. In what follows, I explain the shape of the spectrum emanating from the roots of Ω and show that these branches and $\mathbb{R}$ constitute the Lax spectrum.

The operator (2.34) is a second-order differential operator, so it has two linearly independent solutions. The solutions obey

$$\Phi_1(x;\zeta) \sim \begin{pmatrix} e^{-i\zeta x} \\ 0 \end{pmatrix}, \qquad \Phi_2(x;\zeta) \sim \begin{pmatrix} 0 \\ e^{i\zeta x} \end{pmatrix}, \qquad \text{as} \qquad |\zeta| \to \infty. \tag{2.66}$$

As $|x| \to \infty$, the above two solutions are bounded if and only if $\zeta \in \mathbb{R}$. Therefore, $\mathbb{R}$ is the only unbounded component of σ_L. I examine all possibilities for the finite components of σ_L in the next two paragraphs.

Finite components of the spectrum can only terminate when $\mathrm{d}I/\mathrm{d}\zeta \to \infty$ by the implicit function theorem. This only occurs at the roots of Ω. A component of the spectrum can only cross another component when $\mathrm{d}I/\mathrm{d}\zeta = 0$. This only occurs at ζ_c which is real if the conditions of Lemma 2.2.5 are satisfied and imaginary otherwise. It follows that the spectral bands emanating from the roots of Ω must intersect either the real or imaginary axis. For the dn solutions, this band lies entirely on

the imaginary axis (see Section 2.2.4). Since there are no other points at which $\mathrm{d}I/\mathrm{d}\zeta = 0$, there can be no other non-closed curves in the spectrum. However, I must still rule out closed curves along which it is not necessary that $\mathrm{d}I/\mathrm{d}\zeta = 0$ anywhere.

Since I is an analytic function away from the roots of Ω and $\zeta = \infty$, $\mathrm{Re}\, I$ is a harmonic function of ζ away from the roots of Ω, which I will deal with next. Therefore, if the spectrum contained a closed curve, it must be that $\mathrm{Re}\, I = 0$ on the interior of that closed curve by the maximum principle for harmonic functions. If this were true, then it must also be that the directional derivative of $I(\zeta)$ vanishes on the interior of the region bounded by the closed curve. However $\mathrm{d}I/\mathrm{d}\zeta = 0$ only at two points which are either on the real or imaginary axis (2.54). It follows that there are no closed curves in σ_L disjoint from the roots of Ω. If there were a closed curve which was tangent to the roots of Ω, the above argument would not hold since $\mathrm{Re}\, I$ is not analytic at the root. However, such a curve would imply that the origin of $\sigma_{\mathcal{L}}$ has multiplicity greater than 4 (the origin has multiplicity 4 since the 4 roots of Ω map to the origin). This is not possible since $\mathcal{L}$ is a fourth-order differential operator, and such a tangent curve can not exist. □

Remark 2.2.7. The above result may also be proven by examining the large-period limit of (2.4) which is the soliton solution of (2.1). The spectrum of the soliton is well known [49]. Using the results of [38, 67, 75], the spectrum of the periodic solutions with large period can be understood. Once the spectrum for solutions with large period is understood, the analysis presented in this chapter applies and can be extended to solutions with smaller period by continuity.

Lemma 2.2.8. $0 \leq M(\zeta) < 2\pi$ *for* $\zeta \in \sigma_L \setminus \mathbb{R}$ *with equality only at the end of the bands, when* $\Omega(\zeta) = 0$.

Proof. See Appendix A.3.3. □

Remark 2.2.9. Lemma 2.2.8 can be rephrased in the language of the Floquet discriminant approach [4, 14, 31, 58] as the nonexistence of *periodic eigenvalues* (those with $M(\zeta) = 0 \mod 2\pi$) on the interior of the complex bands of spectra for the elliptic solutions. Before this result, three things were known about the existence of periodic eigenvalues on the complex bands: (i) The number of periodic eigenvalues on the complex bands was known to have an explicit bound [58]; (ii) for the symmetric solutions (here, the cn and dn solutions), the number of periodic eigenvalues on the complex band is zero [14]; and (iii) the nonexistence of periodic eigenvalues on the complex

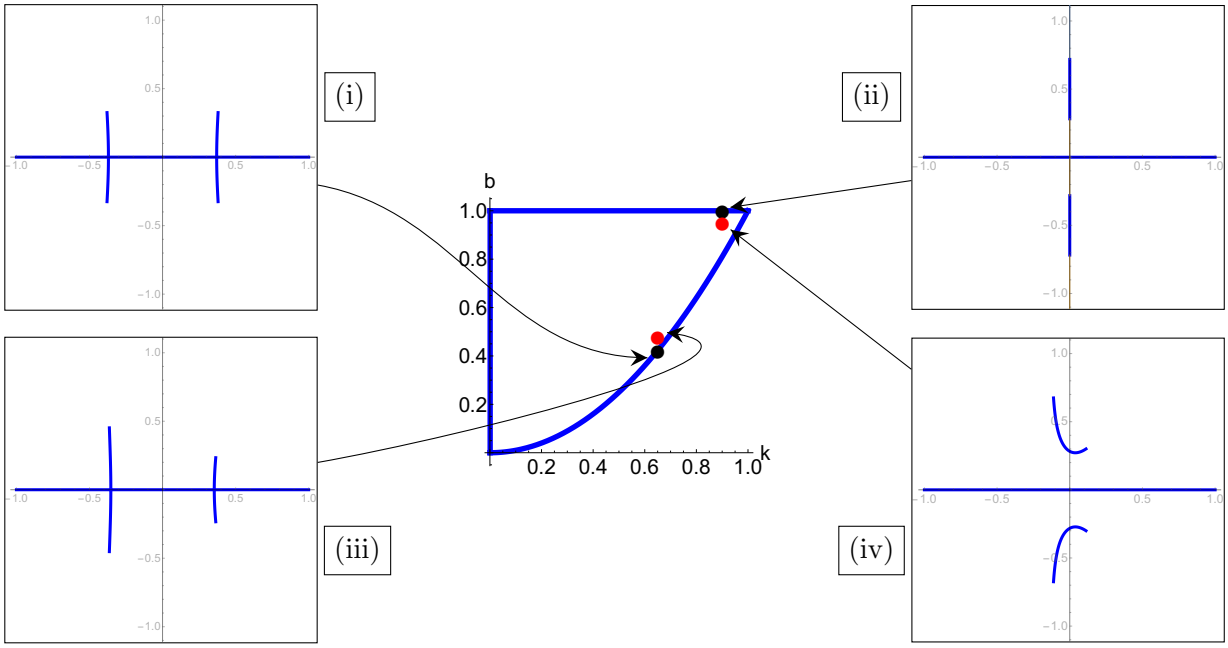

Figure 2.3: Plots of the Lax spectrum. $\mathrm{Re}\,\zeta$ *vs.* $\mathrm{Im}\,\zeta$ for $\zeta \in \sigma_L$. Plots (i) and (ii) are for the cn and dn solutions respectively. Plots (iii) and (iv) are for nontrivial-phase solutions, where the symmetry in all quadrants is broken. Red dots indicate nontrivial-phase solutions, which are plotted in the lower panels. Parameters are chosen close together to contrast nearby solutions of trivial and nontrivial phase.

band had been verified numerically [14, 56]. Lemma 2.2.8 settles this question: there are no periodic eigenvalues on the complex bands of the Lax spectrum for the elliptic solutions of the fNLS equation.

2.2.4 Spectral stability of the elliptic solutions

Results about spectral stability with respect to subharmonic perturbations are found in [27, Section 9]. There, sufficient conditions for stability with respect to subharmonic perturbations are found in Theorems 9.1, 9.3, 9.4, 9.5 and 9.6 for spectra with different topology. In this section I present these known sufficient conditions for spectral stability while providing more detailed proofs. For some choices of parameters I show that the sufficient condition is necessary and comment on progress made towards showing that this condition is necessary for the entire parameter space in Appendix A.3.

I begin by showing that $\Omega : \sigma_L \cap \mathbb{R} \mapsto \sigma_{\mathcal{L}} \cap i\mathbb{R}$, and therefore the real line of the Lax spectrum always maps to stable modes. Showing that these (and the roots of Ω) are the only parts of the Lax spectrum mapping to stable modes is an important challenge (see Appendix A.3).

Lemma 2.2.10. *If $\zeta \in \mathbb{R}$, then $\Omega(\zeta) \in i\mathbb{R}$.*

Proof. If $\zeta \in \mathbb{R}$, then the matrix defining the t-evolution in (2.34) is skew-adjoint, and separation of variables yields imaginary Ω. □

Remark 2.2.11. The above result is proven in [27]. I present the proof above because it is significantly simpler and it is the primary motivation for Chapter 3.

Trivial-phase solutions, $b = 1$ (dn solutions) or $b = k^2$ (cn solutions)

The trivial-phase solutions have $c = 0$ so that

$$\Omega^2(\zeta) = -\zeta^4 + \omega\zeta^2 - \frac{1}{16}\left(4\omega b + 3b^2 + (1-k^2)^2\right), \tag{2.67}$$

and $\Omega^2(\zeta) = \Omega^2(-\zeta)$. Since $\Omega^2(i\mathbb{R}) \subset \mathbb{R}$, $\lambda(\zeta)$ is real or imaginary for $\zeta \in i\mathbb{R}$. Along with Lemmas 2.2.4 and 2.2.6, this implies that trivial-phase solutions have symmetric Lax spectrum across both the real and imaginary axes (see Figure 2.3).

Solutions of dn-type, $b = 1$ When $b = 1$, $\zeta_j \in i\mathbb{R}$ (2.53) and

$$\mathrm{Im}(\zeta_2) > \mathrm{Im}(\zeta_1) > 0 > \mathrm{Im}(\zeta_4) > \mathrm{Im}(\zeta_3), \tag{2.68}$$

with $\zeta_2 = -\zeta_3$ and $\zeta_1 = -\zeta_4$. The following lemmas are needed. The proofs are found in Appendix A.2.

Lemma 2.2.12. *$M(\zeta_j) = T(k)\mu(\zeta_j) = 0 \mod 2\pi$ for the dn solutions.*

Lemma 2.2.13. *Let $\zeta \in i\mathbb{R}$ with either $|\mathrm{Im}(\zeta)| \geq \mathrm{Im}(\zeta_2)$ or $|\mathrm{Im}(\zeta)| \leq \mathrm{Im}(\zeta_1)$. Then $\Omega(\zeta) \in i\mathbb{R}$.*

The above lemmas are used to find necessary and sufficient conditions on the spectral stability of dn solutions.

Theorem 2.2.14. *The dn solutions ($b = 1$) are spectrally stable with respect to perturbations of the same period as the underlying solution and no other subharmonic perturbations.*

Proof. Lemmas 2.2.6, 2.2.13, and the tangent vectors (2.46) show that the complex bands of the Lax spectrum are confined to the imaginary axis between the roots of Ω. Using Lemmas 2.2.8 and 2.2.12 and the fact that $M(\zeta)$ must increase in absolute value between the roots of $\Omega(\zeta)$, $M(\zeta) \in [0, 2\pi]$ on the bands of the Lax spectrum. Equality is attained only at the roots ζ_j. By Lemma 2.2.13, $\Omega(\zeta) \in \mathbb{R}$ on the interior of the bands, so the eigenvalues are unstable. Since $\zeta \in \mathbb{R}$ only maps to stable modes (Lemma 2.2.10), spectral stability only exists for $T(k)\mu = 0$, which is what I wished to show. □

Solutions of cn-type, $b = k^2$ When $b = k^2$, the inequality

$$\Omega^2(i\xi) = -\xi^4 + \frac{1}{2}(2k^2 - 1)\xi^2 - 1/16 < 0, \tag{2.69}$$

is satisfied for all $\xi \in \mathbb{R}$. I need the following lemmas whose proofs can be found in Appendix A.2.

Lemma 2.2.15. *For cn solutions, when $\zeta \in i\mathbb{R}$, $M(\zeta) = \pi \mod 2\pi$.*

Lemma 2.2.16. *$M(\zeta_j) = T(k)\mu(\zeta_j) = 0 \mod 2\pi$ for the cn solutions.*

Lemma 2.2.17. *For $b = k^2$ and $\zeta \in \sigma_L \setminus (\{\zeta_1, \zeta_2, \zeta_3, \zeta_4\} \cup \mathbb{R} \cup i\mathbb{R})$, $\Omega(\zeta) \notin i\mathbb{R}$.*

The above lemmas are used to find necessary and sufficient conditions on the spectral stability of cn solutions.

Theorem 2.2.18. *If $k > k^* \approx 0.9089$ where k^* is the unique root of $2E(k) - K(k)$ for $k \in [0, 1)$, then solutions of cn-type ($b = k^2$), are spectrally stable with respect to coperiodic and 2-subharmonic perturbations, but no other subharmonic perturbations. If instead $k \leq k^*$, then solutions are spectrally stable with respect to perturbations of period $QT(k)$ for all $Q \in \mathbb{N}$ with $Q \leq P \in \mathbb{N}$ if and only if*

$$M(-\zeta_c) \leq \frac{2\pi}{P}, \tag{2.70}$$

defined in the 2π-interval in which $M(\zeta_j) = 0$.

Proof. First choose a solution by fixing k. Then choose a P-subharmonic perturbation. If $k > k^*$, then $2E(k) - K(k) < 0$ so that $b > B(k)$ and $\zeta_c \in i\mathbb{R}$ ((2.55) when $b = k^2$). If $k \leq k^*$, $\zeta_c \in \mathbb{R}$. Consider the band of the spectrum with endpoint ζ_2 at which $M(\zeta_2) = 0$ (Lemma 2.2.16). If $\zeta_c \in i\mathbb{R}$, this band intersects the imaginary axis at $\hat{\zeta} \in i\mathbb{R}$, otherwise it intersects the real axis at $-\zeta_c \in \mathbb{R}$.

Let S represent the band connecting ζ_2 to $\hat{\zeta}$ when $\zeta_c \in i\mathbb{R}$. When $\zeta_c \in i\mathbb{R}$, $|\mathrm{Re}(\lambda)| > 0$ on S (Lemma 2.2.17) so every $T(k)\mu$ value on S corresponds to an unstable eigenvalue. Since $\mu \neq 0 \mod 2\pi$ on S (Lemma 2.2.8), $M(\zeta)$ is increasing from ζ_2 to $\hat{\zeta}$ [27, Lemma 9.2], and $\partial S = \{0, \pi\}$ (Lemmas 2.2.15 and 2.2.16), $M(\zeta) \in (0, \pi)$ on the interior of S. Therefore every $T(k)\mu \in (0, \pi)$ corresponds to an unstable eigenvalue. By the symmetry of the Lax spectrum in each quadrant, the analysis beginning at any of the roots ζ_j gives the same result, except perhaps with $(0, \pi)$ replaced with $(\pi, 2\pi)$, which yields the same stability results. Since $\mathrm{Re}(\lambda(\zeta)) = 0$ only at $T(k)\mu = 0$, or $T(k)\mu = \pi$, if $2E(k) - K(k) < 0$, the cn solutions are spectrally stable with respect to coperiodic and 2-subharmonic perturbations, but no other subharmonic perturbations.

If $2E(k) - K(k) \geq 0$, the band emanating from ζ_2 intersects the real axis at $-\zeta_c$ (Lemma 2.2.5). Then $M(\zeta) \in (0, T(k)\mu(-\zeta_c))$ along the interior of this band and $M(\zeta) = 0$ and $M(\zeta) = T(k)\mu(-\zeta_c)$ at the respective endpoints (Lemma 2.2.16). Since $|\mathrm{Re}(\lambda)| > 0$ on the interior of this band (Lemma 2.2.17), every $T(k)\mu$ value along this band corresponds to an unstable eigenvalue. By Lemma 2.2.8, $M(-\zeta_c) < 2\pi$. Therefore, in order to have spectral stability with respect to P-subharmonic perturbations, it must be that $M(-\zeta_c)$ is at least as small as the smallest nonzero μ value obtained in (2.16) for this P. The smallest nonzero μ value corresponds to $m = 1$ or $m = P - 1$, so if

$$M(-\zeta_c) \leq \frac{2\pi}{P}, \tag{2.71}$$

then solutions are spectrally stable with respect to perturbations of period $PT(k)$. Since the Lax spectrum is symmetric about the real and imaginary axes for the cn solutions (see Figure 2.3(i)), the same bound is found by starting the analysis at each ζ_j. Since the preimage of all eigenvalues with $\mathrm{Re}(\Omega(\zeta)) > 0$ is the interior of the bands (Lemma 2.2.17), (2.71) is also a necessary condition for spectral stability. Since the bound holds for each $Q \leq P,\ Q \in \mathbb{N}$, spectral stability with respect to P-subharmonic perturbations also implies spectral stability with respect to Q-subharmonic perturbations. □

Remark 2.2.19. The calculations throughout this chapter use the period of the modulus of the solution, $T(k) = 2K(k)$. However, the cn solution itself (not its modulus) is periodic with period $4K(k)$. When taking this into account, $I(\zeta)$ gets replaced by $2I(\zeta)$, and

$$T(k)\mu(\zeta) = 4iI(\zeta) + 2\pi n. \tag{2.72}$$

Using (2.72) for $M(\zeta)$, Theorem 2.2.18 can be updated to cover subharmonic perturbations with respect to the period $4K(k)$ of the cn solutions. This gives that when $2E(k) - K(k) < 0$, the solutions are spectrally stable with respect to perturbations of period $4K(k)$. The bound (2.71) may also be updated using (2.72) and upon letting $T(k) = 4K(k)$. In particular, I recover the cn solution stability results found in [42, 45].

Nontrivial-phase solutions

For the nontrivial-phase solutions, $c \neq 0$ and Ω is defined by (2.35). The statement for the stability of nontrivial-phase solutions is very similar to that for the stability of cn solutions. I begin with a lemma whose proof can be found in Appendix A.2.

Lemma 2.2.20. *$M_j := M(\zeta_j) = T(k)\mu(\zeta_j) = 0 \mod 2\pi$ for each root $\{\zeta_j\}_{j=1}^4$ of $\Omega(\zeta)$.*

With this lemma, the following sufficient condition for spectral stability of nontrivial-phase solutions holds.

Theorem 2.2.21. *Consider a solution with parameters k and $b \leq B(k)$ (2.55). The solution is spectrally stable with respect to perturbations of period $QT(k)$ for all $Q \in \mathbb{N}$, $Q \leq P \in \mathbb{N}$ if*

$$M(-\zeta_c) \leq \frac{2\pi}{P}, \tag{2.73}$$

defined in the 2π interval in which $M(\zeta_j) = 0$.

Proof. The proof here, much like the statement of the theorem, is similar to the proof of Theorem 2.2.18.

Choose a solution by fixing k and $b \leq B(k)$ so that ζ_c is real. Choose a P-subharmonic perturbation. Consider the band of the spectrum with endpoint ζ_2 (see Figure 2.3 (iii, iv)) , at which $M(\zeta_2) = 0$ (Lemma 2.2.20), and which intersects the real line at $-\zeta_c$ (Lemmas 2.2.6 and 2.2.10). Since $M(\zeta)$ is increasing along the band (Lemma 2.2.4), $0 < M(\zeta) < T(k)\mu(-\zeta_c)$ along the interior of the band with $M(\zeta) = 0$ and $M(\zeta) = T(k)\mu(-\zeta_c) < 2\pi$ (Lemma 2.2.8) at the respective endpoints.

Since the tangent lines of σ_L are non vertical at the origin for $b < B(k)$ and $|\mathrm{Re}(\lambda(-\zeta_c \pm i\epsilon))| > 0$ [27], there exist ζ on the bands in a neighborhood of $-\zeta_c$ and a neighborhood of ζ_2 which correspond to eigenvalues λ with $\lambda_r > 0$, *i.e.*, unstable eigenvalues. Since there exist unstable eigenvalues on this band, in order to have spectral stability with respect to P-subharmonic perturbations, it must be that $M(-\zeta_c)$ is at least as small as the smallest nonzero μ obtained in (2.16) for this P. The smallest nonzero μ value corresponds to $m = 1$ or $m = P - 1$, so if

$$M(-\zeta_c) \leq \frac{2\pi}{P}, \tag{2.74}$$

then solutions are spectrally stable with respect to perturbations of period $PT(k)$.

By Lemma 2.2.4, the same bound is found for the starting point ζ_3. Starting at ζ_1 or ζ_4 gives the bound

$$M(\zeta_c) \leq \frac{2\pi}{P}. \tag{2.75}$$

However, since

$$M(-\zeta_c) > M(\zeta_c), \tag{2.76}$$

as shown in [27], the tighter bound is found with $M(-\zeta_c)$. This is the sufficient condition for spectral stability. As for the cn case, if the bound is satisfied for P, then it is also satisfied for all $Q \leq P$. □

Remark 2.2.22. Determining whether or not the bound (2.73) is also a necessary condition for spectral stability is a significant challenge. Work in this direction is presented in Appendix A.3.1.

Remark 2.2.23. Note that Lemma 2.2.4 implies that near $-\zeta_c \in \mathbb{R}$, two eigenvalues with the same $|T(k)\mu|$ value are found equidistant from $-\zeta_c$ along the band above and below the real axis. Since

two eigenvalues with the same $|T(k)\mu| \mod 2\pi$ value represent the same perturbation of period $PT(k)$, the eigenvalues associated with a perturbation of period $PT(k)$ straddle $-\zeta_c$ on either of the arcs and come together or separate as the solution parameters vary, see Figure 2.4.

Theorem 2.2.24. *If $b > B(k)$ (2.55), solutions are spectrally stable with respect to coperiodic perturbations. Additionally, they can be spectrally stable with respect to perturbations of twice the period, but they are not stable with respect to any other subharmonic perturbations.*

Proof. See Appendix A.3.2. □

Remark 2.2.25. Numerical evidence suggests that when $b > B(k)$, NTP solutions are spectrally stable with respect to coperiodic perturbations and no other subharmonic perturbations. However, there are some parameter values for which the stability spectrum intersects the imaginary axis at a point. I cannot rule out the possibility of this point corresponding to 2-subharmonic perturbations. For the cn solutions, this intersection point corresponds to $M(\zeta) = \pi$, which gives rise to spectral stability with respect to 2-subharmonic perturbations. Because of this, a cn solution and a NTP solution with $b > B(k)$ can be arbitrarily close to each other but have different stability properties. One way to rule out this spurious stability for NTP solutions with $b > B(k)$ is to show that the point $M(\zeta) = \pi$, which is known to occur exactly once on the band of Lax spectrum in the upper half plane, remains in the left half plane (see Lemma A.3.6) for all parameter values.

Having put the subharmonic stability results from [27] on a rigorous footing, the findings are summarized in Figure 2.5. Equality in condition (2.73) defines a family of "stability curves", for $P \in \mathbb{N}$, in the parameter space which split up the parameter space into regions bounded by these different curves. The dashed curve shows where $\zeta_c = 0$. Below (above) the dashed curve, ζ_c is real (imaginary). The lightest shading represents spectral stability with respect to coperiodic perturbations: all solutions are spectrally stable with respect to such perturbations [36]. Darker shaded regions represent where solutions additionally are spectrally stable with respect to perturbations of higher multiples of the fundamental period. The P labels inside of the parameter space indicate which solutions are spectrally stable with respect to P-subharmonic perturbations in the given region.

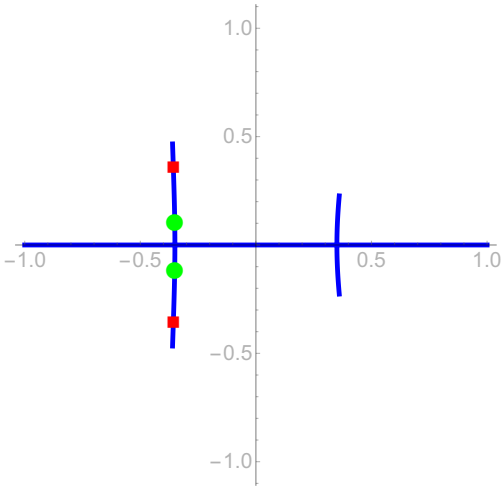

Figure 2.4: The Lax spectrum for $(k, b) = (0.65, 0.48)$. Green circles map to eigenvalues of $\mathcal{L}_\pi$ (elements of σ_π (2.18)) through $\Omega(\zeta)$ (2.35). In other words, $P = 2$ and $T(k)\mu = \pi$. Red squares map to eigenvalues of $\mathcal{L}_{2\pi/3}$: $P = 3$ and $T(k)\mu = 2\pi/3$. See Remark 2.2.23.

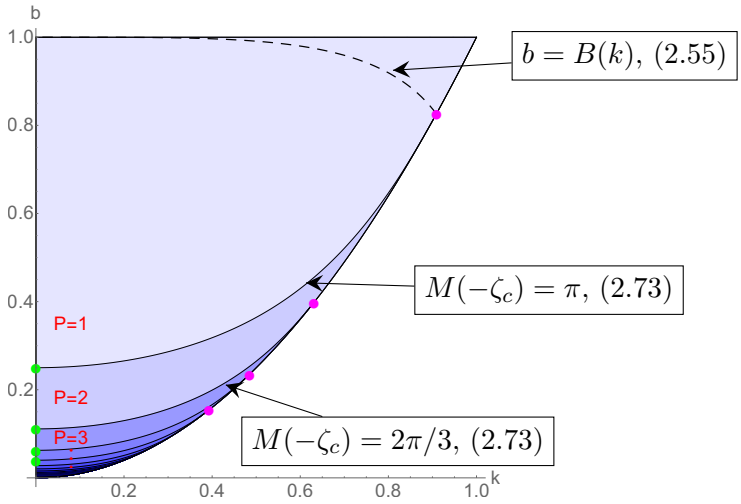

Figure 2.5: The parameter space split up into different regions of subharmonic spectral stability. Each solid curve separating regions of different color corresponds to equality in (2.73) for different values of P. Curves end at $b = 1/P^2$ (green), the stability bound (2.28) for Stokes waves. The magenta dots, along the curve $b = k^2$, show where the stability curves, which are the boundary of different stability regions, intersect the cn solution regime. The dashed line corresponds to (2.55). Below it, $\zeta_c \in \mathbb{R} \setminus \{0\}$ and above it $\zeta_c \in i\mathbb{R} \setminus \{0\}$.

2.3 The advent of instability

Many results on the spectral stability of the elliptic solutions with respect to subharmonic perturbations were shown in [27]. However, no explanation is given there as to how a solution which is spectrally stable with respect to subharmonic perturbations loses stability as its parameters are varied. I show here that as the amplitude increases, the instabilities of elliptic solutions arise in the same manner as was demonstrated for the Stokes waves (Section 2.2.2). I begin by using the Floquet-Fourier-Hill-Method [23] to compute the point spectrum for a single subharmonic perturbation (2.18) (Figure 2.6). I show that two eigenvalues collide on the imaginary axis and leave it at the intersection of the figure 8 spectrum and the imaginary axis.

Consider a point (k_Q, b_Q) in the parameter space lying below a stability curve labeled $P = Q$ ($Q = 1, 2, 3, \ldots$), *i.e.*, $M(-\zeta_c(k_Q, b_Q)) < 2\pi/Q$ (see Figure 2.5). This solution is spectrally stable with respect to perturbations of period $QT(k)$ and the Lax eigenvalues corresponding to Q-periodic perturbations lie on the real axis. Two Lax eigenvalues, $\hat{\zeta}_R$ and $\tilde{\zeta}_R = \hat{\zeta}_R^*$, corresponding to $R > Q$ perturbations lie equidistant from $-\zeta_c(k_Q, b_Q) \in \mathbb{R}$ on the bands connecting to $-\zeta_c(k_Q, b_Q)$ (see Remark 2.2.23 and Figure 2.5). The value $-\zeta_c(k_Q, b_Q)$ lies at the intersection of $\overline{\sigma_L \setminus \mathbb{R}}$ and $\sigma_L \cap \mathbb{R}$ which maps to the intersection of the figure 8 and the imaginary axis in the $\sigma_{\mathcal{L}}$ plane [27]. The stability spectrum eigenvalues, $\hat{\lambda}_R = 2\Omega(\hat{\zeta}_R)$ and $\tilde{\lambda}_R = 2\Omega(\tilde{\zeta}_R)$, corresponding to R-subharmonic perturbations, are on the figure 8 to the left and right of the intersection with the imaginary axis. As the solution parameters are monotonically varied approaching the stability curve which is the boundary of the stability region for R-subharmonic perturbations, where $M(-\zeta_c(k_R, b_R)) = 2\pi/R$, $\tilde{\zeta}_R$ and $\hat{\zeta}_R$ move to $-\zeta_c(k_R, b_R)$, and $\hat{\lambda}_R$ and $\tilde{\lambda}_R$ converge to the top of the figure 8. When this happens, the solution gains spectral stability with respect to perturbations of period $RT(k)$. Spectral Stability is gained through a Hamiltonian Hopf bifurcation in which two complex conjugate pairs of eigenvalues come together onto the imaginary axis in the upper and lower half planes.

I am interested in the transition from spectrally stable to unstable solutions. For fixed μ, consider two eigenvalues $\hat{\lambda} = 2\Omega(\hat{\zeta}) \in i\mathbb{R}$ and $\tilde{\lambda} = 2\Omega(\tilde{\zeta}) \in i\mathbb{R}$ spectrally stable). Stability is lost as the solution parameters are varied to cross a stability curve, $\hat{\zeta} \to -\zeta_c$ and $\tilde{\zeta} \to -\zeta_c$, entering a new stability region. The Krein signature [54] gives a necessary condition for two colliding eigenvalues to leave the imaginary axis, leading to instability. For a given eigenvalue λ of the operator $\mathcal{L}_\mu$ associated with a perturbation of period $PT(k)$ and eigenfunction $W = (W_1, W_2)$, the

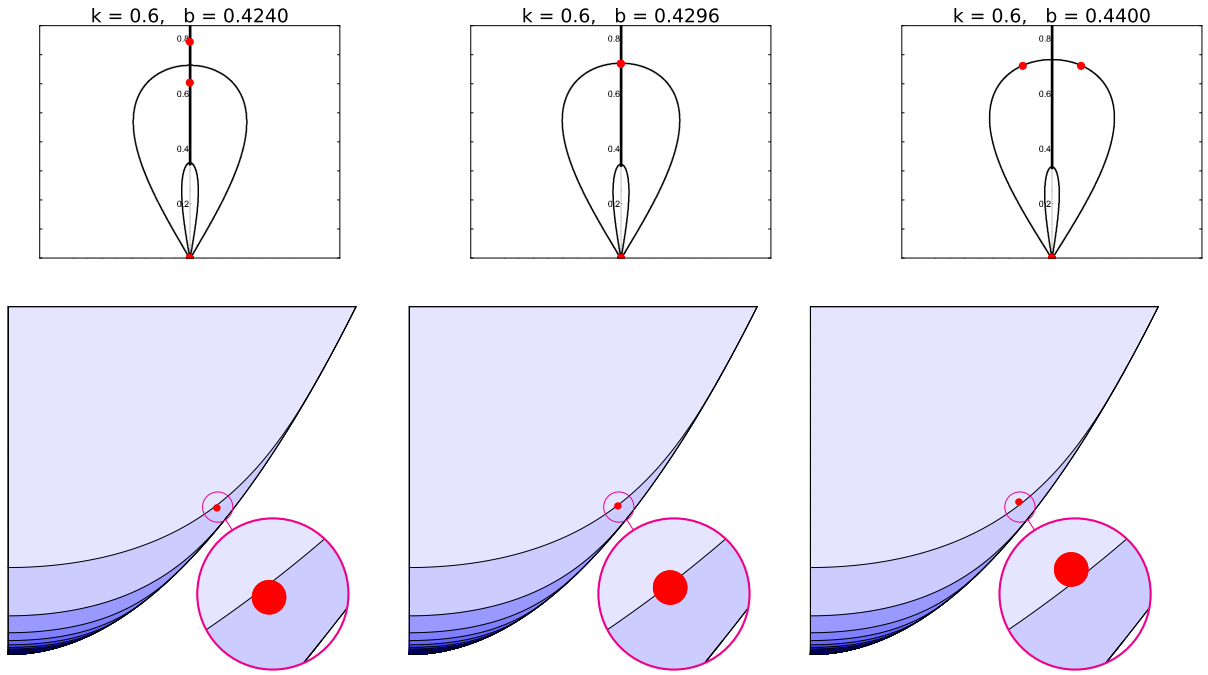

Figure 2.6: For $k = 0.6$ and $P = 2$ (perturbations of twice the period) I vary b to go from spectrally stable to unstable solutions. Top: the top half of the continuous spectrum of $\mathcal{L}$ (black, Re λ *vs.* Im λ, plotted using the analytic expression (2.43) and (2.35)) and two eigenvalues with $P = 2$ highlighted with red dots computed using the FFHM. Bottom: Location in parameter space (k *vs.* b)

Krein signature is the sign of

$$K_2(\zeta) := \langle W, \mathscr{L}_2 W\rangle = \left\langle W, \hat{H}''(\tilde{r},\tilde{\ell})W\right\rangle = \int_{-PT(k)/2}^{PT(k)/2} W^*\hat{H}''(\tilde{r},\tilde{\ell})W \ \mathrm{d}x, \tag{2.77}$$

where $\mathscr{L}_2 = \hat{H}''(\tilde{r},\tilde{\ell})$ is the Hessian of the Hamiltonian of the fNLS equation, $\hat{H}(r,\ell)$ (defined in Appendix A.1), evaluated at the elliptic solution.

To relate the eigenfunctions of $J\mathscr{L}_2$ to those of $\mathcal{L}$, I use (A.12) in Appendix A.1. Linearizing (A.12) about the elliptic solution,

$$\begin{pmatrix} r(x,t) \\ \ell(x,t)\end{pmatrix} = \begin{pmatrix} \tilde{r}(x) \\ \tilde{\ell}(x)\end{pmatrix} + \epsilon \begin{pmatrix} w_1(x,t) \\ w_2(x,t)\end{pmatrix} + \mathcal{O}\left(\epsilon^2\right), \tag{2.78}$$

gives

$$\begin{aligned} \frac{\partial}{\partial t}\begin{pmatrix} w_1 \\ w_2\end{pmatrix} &= \begin{pmatrix} -\tilde{r}\tilde{\ell} & -\frac{1}{2}\partial_x^2 - \frac{1}{2}(\tilde{r}^2+3\tilde{\ell}^2) - \omega \\ \frac{1}{2}\partial_x^2 + \frac{1}{2}(3\tilde{r}^2+\tilde{\ell}^2) + \omega & \tilde{r}\tilde{\ell}\end{pmatrix}\begin{pmatrix} w_1 \\ w_2\end{pmatrix} \\ &= J\hat{H}''(\tilde{r},\tilde{\ell})\begin{pmatrix} w_1 \\ w_2\end{pmatrix} = J\mathscr{L}_2\begin{pmatrix} w_1 \\ w_2\end{pmatrix}. \end{aligned} \tag{2.79}$$

Separation of variables, $(w_1,w_2)^\intercal = e^{\lambda t}(W_1,W_2)^\intercal$, and the squared-eigenfunction give $\lambda = 2\Omega(\zeta)$ and

$$W = \begin{pmatrix} W_1 \\ W_2\end{pmatrix} = \begin{pmatrix} \varphi_1^2 + \varphi_2^2 \\ -i\varphi_1^2 + i\varphi_2^2\end{pmatrix}. \tag{2.80}$$

From the expressions for the eigenfunctions (2.47) and (2.80) it is clear that if an eigenfunction $(U,V)^\intercal$ of $\mathcal{L}$ corresponds to a spectral element λ, then there is a corresponding eigenfunction $(W_1,W_2)^\intercal$ of $J\mathscr{L}_2$ with the same spectral element $\lambda = 2\Omega(\zeta)$.

Since $2\Omega W = J\mathscr{L}_2 W$ and since J is invertible, (2.80) gives

$$W^*\mathscr{L}_2 W = 2\Omega W^* J^{-1} W = 2\Omega(W_1W_2^* - W_2W_1^*) = 4i\Omega(|\varphi_1|^4 - |\varphi_2|^4), \tag{2.81}$$

with $\varphi_1 = -y(x)B(x)$, and $\varphi_2 = y(x)(A(x)-\Omega)$. For a fixed μ and a corresponding spectrally stable solution, $\Omega(\zeta) \in i\mathbb{R}$ for $\zeta \in \mathbb{R}$. When $\zeta \in \mathbb{R}$, the preimage of $\lambda(\zeta) \in i\mathbb{R}$ is only one point (2.57) so that by Theorem 2.2.2, $\lambda(\zeta)$ is a simple eigenvalue. Therefore, I compute the Krein signature only for $\zeta \in \mathbb{R}$. From (2.36),

$$y(x) = \frac{y_0}{B}\exp(\mathrm{imag})\exp\left(-\int \frac{(A-\Omega)\phi}{B}\ \mathrm{d}x\right), \tag{2.82}$$

where "imag" represents imaginary terms which are not important for the magnitude of $y(x)$. The magnitude of $y(x)$ depends critically on

$$\begin{aligned} -\frac{(A-\Omega)\phi}{B} = \frac{C\phi}{(A+\Omega)} &= \frac{-i\zeta|\phi|^2 - (\tilde{r}\tilde{r}_x + \tilde{\ell}\tilde{\ell}_x + i\tilde{\ell}\tilde{r}_x - i\tilde{r}\tilde{\ell}_x)/2}{\zeta^2 - |\phi|^2/2 - \omega/2 + i\Omega} \\ &= \text{imag} + \frac{1}{2}\frac{\mathrm{d}}{\mathrm{d}x}\ln\left|i(A(x)+\Omega)\right|, \end{aligned} \tag{2.83}$$

where $\phi = \tilde{r} + i\tilde{\ell}$ is the elliptic solution whose stability is being investigated. Since $A(x) - \Omega \in i\mathbb{R}$, it follows that

$$y(x) = \frac{y_0}{B}\exp\left(\text{imag}\right)\left|i(A(x)+\Omega)\right|^{1/2}. \tag{2.84}$$

Equating $|y_0| = 1$,

$$|y(x)|^2 = \frac{|A+\Omega|}{|B|^2} = \frac{1}{|A-\Omega|}, \tag{2.85}$$

so that

$$|\varphi_1|^4 = |y|^4|B|^4 = |A+\Omega|^2, \qquad |\varphi_2|^4 = |y|^4|A-\Omega|^4 = |A-\Omega|^2. \tag{2.86}$$

Further,

$$W^*\mathscr{L}_2 W = 4i\Omega\left(|A+\Omega|^2 - |A-\Omega|^2\right) = -16\Omega^2 iA, \tag{2.87}$$

implies

$$K_2(\zeta) = -16\Omega^2(\zeta)\int_{-PT(k)/2}^{PT(k)/2}\left(\zeta^2 - \frac{1}{2}|\phi|^2 - \frac{\omega}{2}\right)\,\mathrm{d}x, \tag{2.88}$$

which is the same K_2 found in [11] with appropriate modifications for the focusing case. This integral can be computed directly using elliptic functions [13, equation (310.01)]:

$$\begin{aligned} K_2(\zeta) &= -32\Omega^2(\zeta)PT(k)\left(\zeta^2 + \frac{b}{4} + \frac{1}{4}\left(1 - k^2 - 2\frac{E(k)}{K(k)}\right)\right) \\ &= -32\Omega(\zeta)^2 PT(k)(\zeta^2 - \zeta_c^2). \end{aligned} \tag{2.89}$$

Note that since $\Omega^2 < 0$ for stable eigenvalues, $K_2(\zeta) < 0$ for $\zeta \in (-\zeta_c, \zeta_c)$ changing sign at $\zeta = \pm\zeta_c$. Therefore the two eigenvalues which collide at $-\zeta_c$ have opposite Krein signatures, a necessary condition for instability.

For the trivial-phase solution, $\Omega(\zeta) = \Omega(-\zeta)$, so the Krein signature calculation here might not be sufficient, since the colliding eigenvalues, $\hat{\lambda}$ and $\tilde{\lambda}$, might not be simple. The remaining stability results do not rely on this fact. Computing the Krein signature for Stokes waves (Section 2.2.2) is simpler than the calculation here, but it is omitted for brevity.

2.4 Orbital stability

The results on spectral stability may be strengthened to orbital stability (Definition 1.1.4) by constructing a Lyapunov functional in conjunction with the results of [40, 61]. In Theorem 2.2.21, I have established spectral stability for solutions below the curve (2.73) (see Figure 2.5). In this section I show that those solutions are also orbitally stable. To this end, I use the higher-order conserved quantities of the fNLS equation (see Appendix A.1).

To prove nonlinear stability, I construct a Lyapunov function, *i.e.*, a constant of the motion $\mathcal{K}(r,\ell)$ for which the solution $(\tilde{r},\tilde{\ell})$ is an unconstrained minimizer:

$$\mathcal{K}'(\tilde{r},\tilde{\ell})=0, \quad \frac{\mathrm{d}}{\mathrm{d}t}\mathcal{K}(\tilde{r},\tilde{\ell})=0, \quad \left\langle v,\mathcal{K}''(\tilde{r},\tilde{\ell})v\right\rangle>0, \quad \forall v\in\mathbb{V}, v\neq 0. \tag{2.90}$$

In Section 2.3 it is shown that the energy $\hat{H}$ satisfies the first two conditions in (2.90) but not the third since K_2 is not of definite sign. When evaluated at stationary solutions, each equation defined in (A.10) satisfies the first and second conditions. Following the work of [11, 26, 61, 64] I choose one member of (A.10) to satisfy the third condition by choosing the constants $c_{n,j}$ in a particular manner. A different approach to finding a Lyapunov function is used in [37] for the defocusing NLS (dNLS) equation.

Linearizing the n-th fNLS equation about the elliptic solution results in

$$w_{t_n}=J\mathscr{L}_n w, \qquad \mathscr{L}_n=\hat{H}_n''(\tilde{r},\tilde{\ell}).$$

The squared-eigenfunction connection and separation of variables gives

$$2\Omega_n W(x)=J\mathscr{L}_n W(x), \tag{2.91}$$

where Ω_n is defined by

$$w(x,t_n)=e^{\Omega_n t_n}\begin{pmatrix}W_1(x)\\ W_2(x)\end{pmatrix}=e^{\Omega_n t_n}W(x), \tag{2.92}$$

and where $W(x)$ is any eigenfunction of $\mathcal{L}_2$. The relation

$$\Omega_n^2(\zeta)=p_n^2(\zeta)\Omega^2(\zeta), \qquad n\geq 2, \tag{2.93}$$

where p_n is a polynomial of degree $n-2$, is found in [11] and applies in the focusing case as well. When $n=2$, $p_2=1$ so that $\Omega_2=\Omega$ and (2.91) implies

$$2J^{-1}W=\frac{1}{\Omega}\mathscr{L}_2 W=\frac{1}{\Omega}\mathscr{L}W, \tag{2.94}$$

for any eigenfunction W of $\mathcal{L}_2$. The definition of K_2 (2.77) and (2.93) imply

$$K_n(\zeta) := \langle W, \mathscr{L}_n W\rangle = \left\langle W, \hat{H}_n''(\tilde{r},\tilde{\ell})W\right\rangle = \frac{\Omega_n}{\Omega}\int_{-PT(k)/2}^{PT(k)/2} W^*\mathscr{L}_2 W \,\mathrm{d}x = p_n(\zeta)K_2(\zeta). \tag{2.95}$$

$K_2(\zeta)$ takes the sign $+,-,+$ for $\zeta\in(-\infty,-\zeta_c)$, $\zeta\in(-\zeta_c,\zeta_c)$, and $\zeta\in(\zeta_c,\infty)$ respectively. Since $p_4(\zeta)$ is quadratic, I use $K_4(\zeta) = p_4(\zeta)K_2(\zeta)$, where $p_4(\zeta)$ is defined by (2.93). Adjusting the constants of p_4 so that it has the same sign as K_2 with zeros at $\zeta=\pm\zeta_c$ makes K_4 non negative. In order to calculate $\Omega_4(\zeta)$, I need

$$\hat{T}_4 = T_4 + c_{4,3}T_3 + c_{4,2}T_2 + c_{4,1}T_1 + c_{4,0}T_0, \tag{2.96}$$

since Ω_4 is defined by $\hat{T}_4\Phi = \Omega_4\Phi$ by separation of variables in (A.7e). The $c_{4,k}$ are not entirely arbitrary. They are determined by requiring that the stationary elliptic solutions are stationary with respect to t_4, or

$$\frac{\partial}{\partial t_4}\begin{pmatrix} r \\ \ell\end{pmatrix} = J\hat{H}_4' = J\left(H_4' + c_{4,3}H_3' + c_{4,2}H_2' + c_{4,1}H_1' + c_{4,0}H_0'\right) = 0. \tag{2.97}$$

Since J is invertible,

$$\hat{H}_4' = H_4' + c_{4,3}H_3' + c_{4,2}H_2' + c_{4,1}H_1' + c_{4,0}H_0' = 0, \tag{2.98}$$

when evaluated at the stationary solution. Equating

$$0 = \Psi_{\tau_4} + c_{4,3}\Psi_{\tau_3} + c_{4,2}\Psi_{\tau_2} + c_{4,1}\Psi_{\tau_1} + c_{4,0}\Psi_{\tau_0}, \tag{2.99}$$

and using (A.7) with Ψ defined in (2.4) gives

$$c_{4,0} = \omega c_{4,2} - cc_{4,3} + \frac{1}{8}\left(1 + 15b^2 + 4k^2 + k^4 + 10b + 10bk^2\right), \tag{2.100a}$$

$$c_{4,1} = \frac{1}{2}c - \frac{1}{2}\omega c_{4,3}, \tag{2.100b}$$

with $c_{4,2}$ and $c_{4,3}$ arbitrary. Then

$$\Omega_4^2 = \frac{1}{16}\left(2\omega + 4\zeta^2 + 4c_{4,2} + 4\zeta c_{4,3}\right)^2\Omega_2^2, \tag{2.101}$$

so that

$$p_4(\zeta) = \zeta^2 + \zeta c_{4,3} + \frac{1}{2}\omega + c_{4,2}. \tag{2.102}$$

The constants $c_{4,2}$ and $c_{4,3}$ are chosen so that $K_4(\zeta) = p_4(\zeta)K_2(\zeta) \geq 0$. Setting

$$c_{4,3} = 0, \tag{2.103a}$$

$$c_{4,2} = -\frac{\omega}{2} + \frac{b}{4} + \frac{1}{4}\left(1 - k^2 - 2\frac{E(k)}{K(k)}\right), \tag{2.103b}$$

gives

$$K_4(\zeta) = -32\Omega^2(\zeta)PT(k)\left(\zeta^2 - \zeta_c^2\right)^2 \geq 0, \tag{2.104}$$

for $\zeta \in \mathbb{R}$ and equality only at $\zeta = \pm\zeta_c$ and the roots of Ω. The result (2.104) has only been proven for eigenfunctions of $\mathcal{L}_2$. However since the eigenfunctions of $\mathcal{L}_2$ are complete in $L^2_{\text{per}}([-T(k)/2, T(k)/2])$ [44] the results apply to all functions in $L^2_{\text{per}}([-T(k)/2, T(k)/2])$. This result implies that H_4, with the constants chosen above, acts as a Lyapunov functional for the spectrally stable elliptic solutions with respect to the t_4 dynamics. However since all flows of the fNLS equation hierarchy commute, H_4 is a conserved quantity with respect to the t dynamics as well. Therefore whenever solutions are spectrally stable with respect to a given subharmonic perturbation, they are also formally stable [61].

To go from formal to orbital stability, the conditions of [40] must be satisfied. The kernel of the functional $\hat{H}_4''(\tilde{r}, \tilde{\ell})$ must consist only of the infinitesimal generators of the symmetries of the solution $(\tilde{r}, \tilde{\ell})$. The infinitesimal generators of the Lie point symmetries correspond to the values of ζ for which $\Omega(\zeta) = 0$, so the kernel of $\hat{H}_4''(\tilde{r}, \tilde{\ell})$ contains the infinitesimal generators of the Lie point symmetries. In order for the kernel to consist only of this set, I need strict inequality in (2.73). This comes from the following lemma.

Lemma 2.4.1. *Let b, k and P be such that* (2.73) *holds with a strict inequality. Then the set*

$$S := \{\zeta \in \sigma_L : M(\zeta) = m2\pi/P, \quad m = 0, \ldots, P-1\} \tag{2.105}$$

does not contain $\pm\zeta_c$.

Proof. Since $M(-\zeta_c) < 2\pi/P$, the only possibility for $-\zeta_c$ to be in S is that $M(-\zeta_c) = 0 \mod 2\pi$. But since $-\zeta_c$ represents the intersection of the branch of spectra and the real line, Lemma 2.2.8 applies and $M(-\zeta_c) \neq 0 \mod 2\pi$. Since $M(\zeta_c) < M(-\zeta_c)$, it is also the case that ζ_c is not in S $\square$

The above lemma implies that if $M(-\zeta_c) < 2\pi/P$, the kernel of $\hat{H}_4''(\tilde{r}, \tilde{\ell})$ consists only of the roots of $\Omega(\zeta)$. **It follows that, for a fixed perturbation with period $PT(k)$, all solutions**

which are spectrally stable with respect to that perturbation and whose parameters do not lie *on* stability curves (the boundary of subharmonic stability regions, at which $M(-\zeta_c) = 2\pi/P$) are also orbitally stable.

Conclusion

I have proven the orbital stability with respect to subharmonic perturbations for the elliptic solutions of the focusing nonlinear Schrödinger equation. The necessary condition for stability (2.73) is shown to also be a sufficient condition with the help of a numerical check. I see three main remaining tasks to be completed for this problem: (i) remove the numerical check for sufficiency of Theorem 2.2.21; (ii) determine whether or not solutions lying on stability curves, $M(-\zeta_c) = 2\pi/P$, are orbitally stable; and (iii) prove that the solutions satisfying $b > B(k)$ in Theorem 2.2.24 are not stable with respect to 2-subharmonic perturbations.

The main difficulty in establishing the results presented in this chapter is that the Lax pair does not define a self-adjoint spectral problem. In the next two chapters, I give a general method for determining important parts of the Lax spectrum, namely those that map to stable elements of the Lax spectrum.

Chapter 3

THE LAX SPECTRUM AND SPECTRAL STABILITY FOR THE AKNS HIERARCHY

While working on the problem in Chapter 2, I noticed a common theme shared by all the problems that have been studied using techniques used in this dissertation (see *e.g.,* [10, 11, 22, 24, 26, 27, 64]): the real line, as a subset of the Lax spectrum, always makes the spectral problem defining Ω (2.34) skew adjoint (see Remark 2.2.11). If true, this implies that real elements of the Lax spectrum map to imaginary (and hence stable) elements of the stability spectrum, as long as the squared eigenfunction connection gives $\lambda = 2\Omega(\zeta)$. In this chapter I show that this feature generally holds for members of the AKNS hierarchy admitting a common reduction. I also give examples for which my results apply directly and examples which indicate that these results may be more general. In Chapter 4 I generalize these results to integrable equations outside of the AKNS hierarchy. Throughout this chapter and the next, *stability* refers to spectral stability (Definition 1.1.3).

3.1 The Lax pair, the Lax spectrum, and the Squared-eigenfunction connection

The AKNS hierarchy [7] is a special class of integrable equations (Section 1.2) containing a variety of physically important nonlinear evolution equations. The Lax pair for members of the AKNS hierarchy is

$$\Phi_x(x,t;\zeta) = \begin{pmatrix} -i\zeta & q(x,t) \\ r(x,t) & i\zeta \end{pmatrix} \Phi(x,t;\zeta) = X\Phi, \tag{3.1a}$$

$$\Phi_t(x,t;\zeta) = \begin{pmatrix} A(x,t;\zeta) & B(x,t;\zeta) \\ C(x,t;\zeta) & -A(x,t;\zeta) \end{pmatrix} \Phi(x,t;\zeta) = T\Phi. \tag{3.1b}$$

Here $\zeta \in \mathbb{C}$ is called the *Lax parameter*, assumed to be independent of x and t, and $r,\ q,\ A,\ B$, and C are complex-valued functions chosen such that the compatibility of mixed derivatives, $\partial_t\Phi_x = \partial_x\Phi_t$

holds if and only if (1.1) holds. The compatibility condition defines the evolution equations [7]

$$q_t = B_x + 2i\zeta B + 2Aq, \tag{3.2a}$$

$$r_t = C_x - 2i\zeta C - 2Ar, \tag{3.2b}$$

as well as the condition

$$A_x = qC - rB. \tag{3.3}$$

I am interested in studying the stability of stationary and periodic or quasiperiodic solutions of members of the AKNS hierarchy with

$$r = \kappa q^*, \tag{3.4}$$

where $\kappa = \pm 1$. I make the following assumption.

Assumption 3.1.1. The functions q and r are related by (3.4), are t-independent, and have the form

$$q(x) = e^{i\theta(x)}Q(x), \quad \text{and} \quad r(x) = \kappa e^{-i\theta(x)}Q(x), \tag{3.5}$$

where Q and θ are real-valued functions and $Q \geq 0$ is P-periodic.

With this assumption, (3.2) gives

$$B_x = -2i\zeta B - 2Aq, \tag{3.6a}$$

$$C_x = 2i\zeta C + 2Ar. \tag{3.6b}$$

Remark 3.1.2. Many evolution equations are found by assuming $A,\ B$, and C can be written as a ζ-power series [8]. In such cases, a recursion operator is used to find $A,\ B$, and C [8, 3] and [39, Chapter 2]. Using the recursion operator, A is a function of products of $q_{nx}^j r_{nx}^j$, where $n,\ j \in \mathbb{N}$. Similarly, B is a function of products of the form $q_{nx}^{j+1} r_{mx}^j$ and C is a function of products of the form $q_{nx}^j r_{mx}^{j+1}$. Therefore, when Assumption 3.1.1 holds, $A,\ B$, and C are t-independent, bounded for $x \in \mathbb{R}$, including ∞, and A is P-periodic. Each of these statements are assumed to be true in what follows.

Remark 3.1.3. The x-equation of the Lax pair (3.1) may be written in terms of a problem with spectral parameter ζ,

$$\zeta\Phi = \begin{pmatrix} i\partial_x & -iq \\ ir & -i\partial_x \end{pmatrix} \Phi = L\Phi. \tag{3.7}$$

This formulation is the original basis for the term "Lax *spectrum*." L is self adjoint if and only if $r = q^*$. Any reference to the equation or the Lax pair being self adjoint refers to the case $r = q^*$. When L is self adjoint, the Lax spectrum (Definition 1.2.1) is a subset of the real line, $\sigma_L \subset \mathbb{R}$.

Although finding the Lax spectrum (Definition 1.2.1) is an interesting and important problem in its own right, I am primarily interested in using the Lax spectrum to determine the stability of stationary solutions to integrable equations. The connection between the Lax spectrum and stability is through the squared-eigenfunction connection. For AKNS systems, the squared-eigenfunction connection (sometimes referred to as quadratic eigenfunctions) gives a connection involving quadratic combinations of the eigenfunctions of (3.1) between eigenfunctions of the stability problem (1.4) and eigenfunctions of the Lax problem (3.1) [7, 39]. In order to connect the Lax spectrum with the stability spectrum, I make the following observation (originally used in [10]). When A, B, and C are t-independent (see Remark 3.1.2), (3.1b) may be solved by separation of variables. Equating

$$\Phi(x,t) = e^{\Omega t}\varphi(x), \tag{3.8}$$

where Ω is complex valued and $\varphi(x)$ is a complex vector-valued function, (3.1b) becomes a 2×2 eigenvalue equation for Ω:

$$\Omega\varphi = T\varphi. \tag{3.9}$$

Using the expression (3.1b) for T,

$$\Omega^2 = A^2 + BC. \tag{3.10}$$

The following lemma establishes that Ω is not a function of x, in addition to the obvious fact that it is not a function of t.

Lemma 3.1.4. *Under Assumption 3.1.1, Ω is independent of x and t.*

Proof. Independence of t is immediate since A, B and C are independent of t for stationary solutions (Remark 3.1.2). Multiplying (3.6a) by C and (3.6b) by B and adding the resulting equations yields

$$0 = \partial_x(BC) + 2A(qC - rB). \tag{3.11}$$

Using (3.3),

$$0 = \partial_x(BC + A^2) = \partial_x(\Omega^2), \tag{3.12}$$

so Ω^2 is independent of x. □

Thus $\Omega = \Omega(\zeta)$ is a function only of ζ and the solution parameters. The connection between the Lax spectrum and the stability spectrum is through Ω. For members of the AKNS hierarchy [8, 3], comparing the exponential component of quadratic combinations of the two components of ϕ with v from (1.3) yields

$$\lambda = 2\Omega(\zeta). \tag{3.13}$$

For the AKNS hierarchy, the squared-eigenfunction connection is known to be complete on the whole line [39], but this has not yet been shown in other settings. It has been shown to e complete in every example that has been studied in depth [10, 11, 22, 26, 28, 64]. In such cases, (3.13) gives the entire stability spectrum if the set σ_L is known. In other words, the map $\Omega : \sigma_L \mapsto \sigma_{\mathcal{L}}$ is surjective. This gives a connection between the function spaces defining the stability and the Lax spectrum: both are defined by the spatial boundedness of the eigenfunctions in question. The next step for studying stability is to find the Lax spectrum. Before doing so, I provide an example of how the steps in this section work for a well-known equation, studied in depth in Chapter 2.

Example (The nonlinear Schrödinger (NLS) equation)**.**
The nonlinear Schrödinger (NLS) equation is

$$i\Psi_t + \frac{1}{2}\Psi_{xx} - \kappa\Psi\left|\Psi\right|^2 = 0, \tag{3.14}$$

where $\Psi(x,t)$ is a complex-valued function and $\kappa = -1$ and $\kappa = 1$ correspond to the focusing and defocusing equations respectively. The Lax pair for the NLS equation [77] is given by (3.1) with

$$q = \Psi, \quad r = \kappa\Psi^*, \quad A = -i\zeta^2 - i\kappa\left|\Psi\right|^2/2, \quad B = \zeta\Psi + i\Psi_x/2, \quad C = \zeta\kappa\Psi^* - i\kappa\Psi_x^*/2. \tag{3.15a}$$

Note that A, B, and C satisfy the properties in Remark 3.1.2. Equating $\Psi(x,t) = e^{-i\omega t}\psi(x,t)$, where $\omega \in \mathbb{R}$ is constant, gives the NLS equation in a frame rotating with constant phase speed ω,

$$i\psi_t + \omega\psi + \frac{1}{2}\psi_{xx} - \kappa\psi\left|\psi\right|^2 = 0. \tag{3.16}$$

Equation (3.16) can be obtained from the compatibility of the new t-equation,

$$\phi_t = \begin{pmatrix} -i\zeta^2 - i\kappa\left|\psi\right|^2/2 + i\omega/2 & \zeta\psi + i\psi_x/2 \\ \zeta\kappa\psi^* - i\kappa\psi_x^*/2 & i\zeta^2 + i\kappa\left|\psi\right|^2/2 - i\omega/2 \end{pmatrix}\phi, \tag{3.17}$$

and the x equation (3.1a), which is unchanged.

The (quasi)periodic stationary solutions of (3.16) are called the *elliptic solutions*. The stability of the elliptic solutions of the fNLS equation is covered extensively in Chapter 2. The stability of the elliptic solutions of the dNLS equation is studied in [11]. To do so, linearize (3.16) about a stationary solution $\tilde{\psi}(x)$ by letting $\psi(x,t) = \tilde{\psi}(x) + \epsilon u(x,t) + \mathcal{O}(\epsilon^2)$. This results in

$$U_t = \begin{pmatrix} u \\ \kappa u^* \end{pmatrix}_t = \begin{pmatrix} \frac{i}{2}\partial_x^2 - 2i\kappa|\tilde{\psi}|^2 + i\omega & -i\tilde{\psi}^2 \\ i\tilde{\psi}^{*2} & -\frac{i}{2}\partial_x^2 + 2i\kappa|\tilde{\psi}|^2 - i\omega \end{pmatrix}\begin{pmatrix} u \\ \kappa u^* \end{pmatrix} = \mathcal{L}_{\mathrm{NLS}}U. \tag{3.18}$$

Since $\mathcal{L}_{\mathrm{NLS}}$ does not depend explicitly on t, separating variables with

$$U(x,t) = \begin{pmatrix} u(x,t) \\ \kappa u^*(x,t) \end{pmatrix} = e^{\lambda t}\begin{pmatrix} v(x) \\ \kappa v^*(x) \end{pmatrix} = e^{\lambda t}V(x), \tag{3.19}$$

results in the spectral problem

$$\lambda V = \mathcal{L}_{\mathrm{NLS}}V. \tag{3.20}$$

The squared-eigenfunction connection for the NLS equation [11] gives

$$U(x,t) = \begin{pmatrix} \phi_1^2 \\ \\ \phi_2^2 \end{pmatrix}, \tag{3.21}$$

where $\phi = (\phi_1,\ \phi_2)^\intercal$ is an eigenfunction of (3.17). Using (3.8), the eigenfunctions of $\mathcal{L}_{\mathrm{NLS}}$ are given by

$$U(x,t) = e^{\lambda t}V(x) = \begin{pmatrix} \phi_1^2 \\ \\ \phi_2^2 \end{pmatrix} = e^{2\Omega t}\begin{pmatrix} \varphi_1^2(x) \\ \\ \varphi_2^2(x) \end{pmatrix}, \tag{3.22}$$

hence $\lambda = 2\Omega(\zeta)$ (3.13). The map $\Omega : \sigma_L \to \sigma_{\mathcal{L}_{\mathrm{NLS}}}$ is shown to be surjective in [11, 28] and Chapter 2.

3.2 Finding the Lax spectrum

I begin by introducing the isospectral transformation

$$\tilde{\Phi}(x,t) = \begin{pmatrix} \tilde{\Phi}_1 \\ \tilde{\Phi}_2 \end{pmatrix} = \begin{pmatrix} e^{-i\theta/2}\Phi_1 \\ e^{i\theta/2}\Phi_2 \end{pmatrix}, \tag{3.23}$$

where θ is defined in (3.5). Under (3.23), the Lax pair (3.1) becomes

$$\tilde{\Phi}_x = \begin{pmatrix} \alpha & Q(x) \\ \kappa Q(x) & -\alpha \end{pmatrix} \tilde{\Phi}, \tag{3.24a}$$

$$\tilde{\Phi}_t = \begin{pmatrix} A & e^{-i\theta}B \\ e^{i\theta}C & -A \end{pmatrix} \tilde{\Phi} = \begin{pmatrix} A & \hat{B} \\ \hat{C} & -A \end{pmatrix} \tilde{\Phi}, \tag{3.24b}$$

where

$$\alpha = -i\zeta - i\theta_x/2, \qquad \hat{B} = e^{-i\theta}B, \qquad \hat{C} = e^{i\theta}C. \tag{3.25}$$

This form is helpful since, by Remark 3.1.2, $\hat{B}$ and $\hat{C}$ are P-periodic along with A. The compatibility conditions (3.3) and (3.6) become

$$A_x = Q\hat{C} - \kappa Q\hat{B}, \qquad \hat{B}_x = 2(\alpha\hat{B} - AQ), \qquad \hat{C}_x = -2(\alpha\hat{C} - \kappa AQ). \tag{3.26}$$

To find σ_L, the eigenfunctions of (3.1) are found using a technique first used in [11]. The eigenfunctions can be found using other techniques, see *e.g.,* [17, 18, 19]. From (3.24b), the eigenfunctions are of the form

$$\tilde{\Phi}(x,t) = e^{\Omega t}y_1(x)\begin{pmatrix} -\hat{B}(x) \\ A(x) - \Omega \end{pmatrix}, \qquad \text{or} \qquad \tilde{\Phi}(x,t) = e^{\Omega t}y_2(x)\begin{pmatrix} A(x) + \Omega \\ \hat{C}(x) \end{pmatrix}. \tag{3.27}$$

Here the scalar functions $y_1(x)$ and $y_2(x)$ are determined by the requirement that $\tilde{\Phi}(x,t)$ not only solves (3.24b), but also (3.24a), since (3.24a-b) have a common set of eigenfunctions. The first equation of (3.27) is used here, but both representations can be helpful (see Section 4.2 for more on this). Substitution in (3.24a) gives

$$-\hat{B}y_1' - \hat{B}_x y_1 = (-\alpha\hat{B} + Q(A - \Omega))y_1, \quad (A - \Omega)y_1' + A_x y_1' = (-\kappa Q\hat{B} - \alpha(A - \Omega))y_1, \tag{3.28}$$

so that different (but equivalent) representations for $y_1(x)$ are obtained from the first or second equation of (3.1a):

$$y_1 = \hat{y}_1 \exp\left(\int \frac{\alpha\hat{B} - Q(A-\Omega) - \hat{B}_x}{\hat{B}} \, \mathrm{d}x \right), \tag{3.29a}$$

$$y_1 = \tilde{y}_1 \exp\left(- \int \frac{\kappa Q\hat{B} + \alpha(A-\Omega) + A_x}{A-\Omega} \, \mathrm{d}x \right), \tag{3.29b}$$

where $\hat{y}_1$ and $\tilde{y}_1$ are constants of integration. At this point I define S_L, the function space that defines σ_L. Physically, the eigenfunctions Φ should be bounded for $\overline{\mathbb{R}}$. Therefore I define S_L to be the space where Φ are bounded for $x \in \overline{\mathbb{R}}$. Since A and B are bounded for $x \in \overline{\mathbb{R}}$ (Remark 3.1.2), $y_1(x)$ must be bounded for $x \in \overline{\mathbb{R}}$ in order for $\Phi(x,t)$ to be an eigenfunction. I use the second expression of (3.29). Similar work is done for the first expression of (3.29) in Section 4.2. To bound the exponential growth, I consider the real part of the exponential. Therefore I need the indefinite integral

$$I = \mathrm{Re} \int \left(\frac{\kappa Q\hat{B}}{A-\Omega} + \alpha + \frac{\mathrm{d}}{\mathrm{d}x} \log(A-\Omega) \right) \, \mathrm{d}x, \tag{3.30}$$

to be bounded for $x \in \overline{\mathbb{R}}$. By Remark 3.1.2 the integrand in I is P-periodic, so it suffices to examine the average over one period. Therefore I need

$$J = \mathrm{Re} \left\langle \alpha + \frac{\kappa Q\hat{B}}{A-\Omega} + \frac{\mathrm{d}}{\mathrm{d}x} \log(A-\Omega) \right\rangle = 0, \tag{3.31}$$

where $\langle \cdot \rangle = \frac{1}{P} \int_0^P \cdot \, \mathrm{d}x$ is the average over a period. Since $A - \Omega$ is P-periodic, the logarithmic derivative has no contribution to J. Further, when $\zeta \in \mathbb{R}$, $\alpha \in i\mathbb{R}$ so it also has no contribution to J. Therefore when $\zeta \in \mathbb{R}$,

$$\mathrm{Re} \left\langle \frac{\kappa Q\hat{B}}{A-\Omega} \right\rangle = 0, \tag{3.32}$$

implies $\zeta \in \sigma_L$.

Remark 3.2.1. Using the two expressions for the eigenfunctions (3.29) and (3.10) gives seven other conditions for $\zeta \in \sigma_L$. These are omitted here but given in (4.7) with $\alpha = -i\zeta$, $\beta = q$, and $\gamma = r$.

When using the recursion operator, $A(\mathbb{R}) \subset i\mathbb{R}$ since $A(\zeta)$ is defined by a power series in ζ with imaginary coefficients (see Remark 3.1.2). The following lemma applies when $\zeta \in \mathbb{R}$.

Lemma 3.2.2. *Consider a member of the AKNS hierarchy with $r = \kappa q^*$, where $\kappa = \pm 1$, and $q_t = r_t = 0$. Then $C = \kappa B^*$ when $\zeta \in \mathbb{R}$ and $A(\zeta) \in i\mathbb{R}$, where A, B, and C are defined in* (3.1b)*.*

Proof. I first establish that $\hat{C} = \kappa \hat{B}^*$ (3.25) from which it follows that $C = \kappa B^*$. From (3.26),

$$0 = \operatorname{Re}(A_x) = Q \operatorname{Re}(\hat{C} - \kappa \hat{B}), \tag{3.33}$$

and

$$0 = \operatorname{Re}(\hat{C}_x - \kappa \hat{B}_x) = \operatorname{Re}[-2\alpha(\hat{C} + \kappa \hat{B}) + 4\kappa Q A] = \operatorname{Re}[-2\alpha(\hat{C} + \kappa \hat{B})], \tag{3.34}$$

since $\kappa Q A \in i\mathbb{R}$ when $\zeta \in \mathbb{R}$, by assumption. If $\alpha(\zeta) \neq 0$, $\operatorname{Im}(\hat{C}) = -\kappa \operatorname{Im}(\hat{B})$ and (3.33) implies that $\hat{C} = \kappa \hat{B}^*$. If $\alpha = 0$,

$$\partial_x(\hat{C} + \kappa \hat{B}) = \hat{C}_x + \kappa \hat{B}_x = 0. \tag{3.35}$$

Since $\operatorname{Im}(\hat{C} + \kappa \hat{B}) = 0$ at x with $\alpha \neq 0$, it must be zero for all x. Therefore $\hat{C} = \kappa \hat{B}^*$ for all x. □

Part of the Lax spectrum with imaginary (stable) elements of the stability spectrum can now be determined.

Theorem 3.2.3. *Consider a member of the AKNS hierarchy* (3.1) *satisfying Assumption 3.1.1 and Remark 3.1.2. Assume further that A, $\hat{B}$, and $\hat{C}$ from* (3.24) *are P-periodic. Let $\mathcal{Q} = \{\zeta \in \mathbb{R} : A(\zeta) \in i\mathbb{R}\}$, $\Omega_i = \{\zeta \in \mathbb{R} : \Omega(\zeta) \in i\mathbb{R}\}$ and $\Omega_r = \{\zeta \in \mathbb{R} : \Omega(\zeta) \in \mathbb{R}\}$.*

When $\kappa = -1$, $\mathcal{Q} \subset \Omega_i$. When $\kappa = 1$, $\mathcal{Q} \subset \Omega_i \cup \Omega_r$. Also, $\mathcal{Q} \cap \Omega_i \subset \sigma_L$, and if Ω is shown to be surjective, $\Omega(\mathcal{Q} \cap \Omega_i) \subset \sigma_{\mathcal{L}} \cap i\mathbb{R}$ for $\kappa = \pm 1$. In other words, all real ζ for which $\Omega(\zeta), A(\zeta) \in i\mathbb{R}$ are part of the Lax spectrum and map to stable elements of the stability spectrum.

Proof. Let $\zeta \in \mathcal{Q}$. By Lemma 3.2.2

$$\Omega^2(\zeta) = A^2 + \kappa |B|^2 \in \mathbb{R}, \tag{3.36}$$

so $\mathcal{Q} \subset \Omega_i \cup \Omega_r$. When $\kappa = -1$, $\Omega^2(\zeta) < 0$ so $\mathcal{Q} \subset \Omega_i$. At this point, I am not assuming that $\zeta \in \sigma_L$. I show that this is the case by showing that $\tilde{I}_1 = 0$ (3.32). If $\Omega(\zeta) \in i\mathbb{R}$, then

$$\operatorname{Re} \frac{Q\hat{B}}{A - \Omega} = \frac{1}{2}\left(\frac{Q\hat{B}}{A - \Omega} + \frac{Q\hat{B}^*}{A^* - \Omega^*}\right) \tag{3.37}$$

$$= \frac{1}{2}\left(\frac{Q\hat{B} - \kappa\hat{C}}{A - \Omega}\right) = -\frac{A_x}{2(A - \Omega)} = -\frac{1}{2}\frac{\mathrm{d}}{\mathrm{d}x}\log(A - \Omega). \tag{3.38}$$

Since A is assumed to be periodic, $\operatorname{Re}\tilde{I}_1 = 0$, establishing that $\zeta \in \sigma_L$ and that $\mathcal{Q} \cap \Omega_i \subset \sigma_L$. By definition, $\Omega(\mathcal{Q} \cap \Omega_i) \subset \sigma_{\mathcal{L}} \cap i\mathbb{R}$ when Ω is surjective onto $\sigma_{\mathcal{L}}$. □

Remark 3.2.4. When using the recursion operator, $A(\mathbb{R}) \subset i\mathbb{R}$ (see statement just before Lemma 3.2.2). Therefore when $\kappa = -1$, Theorem 3.2.3 implies that $\mathbb{R} \subset \sigma_L$ and $\Omega(\mathbb{R}) \subset i\mathbb{R}$ for all members of the AKNS hierarchy satisfying Assumption 3.1.1 and where Remark 3.1.2 applies.

When $\kappa = 1$, the spectral problem (3.1) is self adjoint so $\sigma_L \subset \mathbb{R}$. Therefore the assumption that $\zeta \in \mathbb{R}$ is not actually an assumption for such problems. Theorem 3.2.3 establishes that all $\{\zeta \in \mathbb{R} : \Omega(\zeta) \in i\mathbb{R}\} \subset \sigma_L$. If one can establish that $\{\zeta \in \mathbb{R} : \Omega(\zeta) \in \mathbb{R} \setminus \{0\}\} \not\subset \sigma_L$ for a specific problem, then one has shown that the underlying solution is stable.

Example (The NLS equation, continued)**.**
The dNLS equation has $q = r^*$ so the Lax pair is self-adjoint and $\sigma_L \subset \mathbb{R}$. In [11] the authors establish that $\{\zeta \in \mathbb{R} : \Omega(\zeta) \in \mathbb{R} \setminus \{0\}\} \not\subset \sigma_L$ by working with (3.32) directly. Since $\sigma_L = \{\zeta \in \mathbb{R} : \Omega(\zeta) \in i\mathbb{R}\}$ and $\Omega : \sigma_L \to \sigma_{\mathcal{L}_{\text{NLS}}}$ is surjective, the elliptic solutions are stable (see Figure 3.1a).

The situation for the elliptic solutions of the fNLS equation is more complicated since the Lax pair is not self adjoint and σ_L is not a subset of the real line. The rest of σ_L is found in Chapter 2 by computing the integral (3.31) in terms of elliptic functions and working with the result, but it may also be found using the Floquet Discriminant (see Appendix B). It was originally shown in [27] that $\mathbb{R} \subset \sigma_L$ by working with the complicated expression for (3.31) directly. In [28] and Chapter 2, I establish that the set $\mathcal{E} = \mathbb{R} \cup \{\zeta \in \mathbb{C} : \Omega(\zeta) = 0\}$ are the only elements in σ_L that map to $i\mathbb{R} \subset \sigma_{\mathcal{L}}$ under Ω. Everything else in the spectrum maps to unstable modes, hence the solutions are, in general, unstable. Special classes of perturbations exist, the *subharmonic perturbations*, for which only members of $\mathcal{E}$ are excited. Some of the elliptic solutions are stable with respect to this class of perturbations (see [28] and Chapter 2). This demonstrates the power of what is established here: since it is now known what maps to stable elements of the stability spectrum, one only needs to find the class of perturbations for which the solution is stable. See Figure 3.1b for an example.

3.3 AKNS Examples

In this section I apply the results of Sections 3.1 and 3.2 to several equations in the AKNS hierarchy. The first set of examples are found via the reduction (3.4) and thus Theorem 3.2.3 applied directly. The next set of equations are in the AKNS hierarchy but are found via a reduction other than 3.4. For these equations, I show that similar results still apply, implying that the results in Section 3.2 are generalizable. This leads to a generalization of Theorem 3.2.3 in Chapter 4.

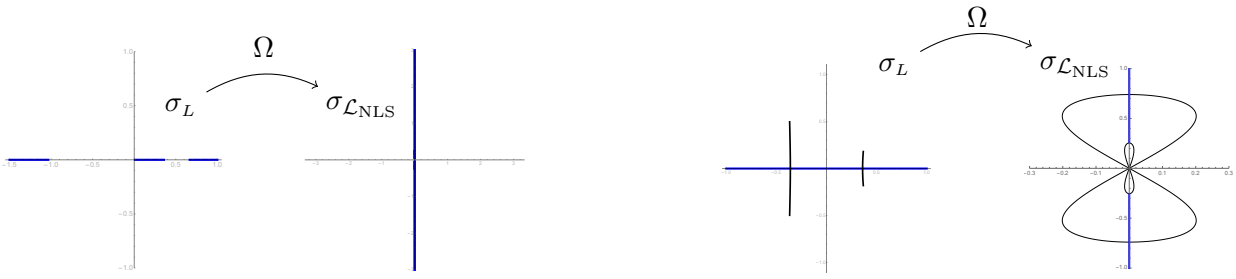

(a) (b)

Figure 3.1: The real *vs.* imaginary part of the Lax and stability spectrum (left and right of each panel, respectively) for an elliptic solution of (a) the dNLS equation and (b) the fNLS equation. The real component of σ_L and its image under Ω is colored blue. The rest of σ_L is in black. The Lax spectrum is computed analytically using (3.32) [11, 27] and the stability spectrum is the image under Ω.

3.3.1 Members of the AKNS hierarchy satisfying (3.4)

The modified Korteweg-de Vries equation

The modified Korteweg-de Vries (mKdV) equation is given by

$$u_t - 6\kappa u^2 u_x + u_{xxx} = 0, \tag{3.39}$$

where u is a real-valued function and $\kappa = -1$ and $\kappa = 1$ correspond to the focusing and defocusing cases respectively. Equation (3.39) is a member of the AKNS hierarchy (Section 3.1) with the Lax pair [7]

$$A = -4i\zeta^3 - 2i\zeta qr, \quad B = 4\zeta^2 q + 2q^2 r + 2i\zeta q_x - q_{xx}, \quad C = 4\zeta^2 r + 2qr^2 - 2i\zeta r_x - r_{xx}, \tag{3.40}$$

and $r = \kappa q = \kappa u$. Letting $(y, \tau) = (x - ct, t)$, where $c \in \mathbb{R}$ is constant, gives the mKdV equation in the traveling frame,

$$u_\tau - cu_y - 6\kappa u^2 u_y + u_{yyy} = 0. \tag{3.41}$$

The Lax pair for (3.41) changes accordingly:

$$\Phi_y = X\Phi, \qquad \Phi_\tau = (T + cX)\Phi. \tag{3.42}$$

The elliptic solutions of the mKdV equation are found upon equating $u_\tau = 0$ [26]. The Lax pair can be found by using the recursion operator as mentioned in Remark 3.1.2, so the remarks there holds and Assumption 3.1.1 applies. The squared-eigenfunction connection gives $\lambda = 2\Omega(\zeta)$ [26] so $\Omega(\zeta) \in i\mathbb{R}$ implies $\lambda \in i\mathbb{R}$.

Theorem 3.2.3 applies with $\mathcal{Q} = \mathbb{R}$ since $A(\mathbb{R}) \subset i\mathbb{R}$. When $\kappa = -1$, $\mathbb{R} \subset \sigma_L$ and $\Omega(\mathbb{R}) \subset \sigma_{\mathcal{L}} \cap i\mathbb{R}$. This result is new: it can be used as a first step for studying the stability of the elliptic solutions of the focusing mKdV equation. Solutions are stable with respect to perturbations that excite only real elements of the Lax spectrum. Determining the class of perturbations that this set belongs to is ongoing work. When $\kappa = 1$, $\Omega_i = \{\zeta \in \mathbb{R} : \Omega(\zeta) \in i\mathbb{R}\} \subset \sigma_L$ and $\Omega(\Omega_i) \subset \sigma_{\mathcal{L}} \cap i\mathbb{R}$. Since this is the self-adjoint case, $\sigma_L \subset \mathbb{R}$. In order to establish stability, one must show that $\{\zeta \in \mathbb{R} : \Omega(\zeta) \notin i\mathbb{R} \setminus \{0\}\} \not\subset \sigma_L$. This is proven in [26] to show that the elliptic solutions for the defocusing mKdV equation are stable.

The mixed generalized NLS-generalized mKdV equation (GNLS-GmKdV)

The mixed generalized NLS-generalized mKdV equation (GNLS-GmKdV, or Hirota's equation) [39, 34, 53] is given by

$$iu_t + u_{xx} + 2\kappa |u|^2 u + ic_3(u_{xxx} + 6\kappa |u|^2 u_x) = 0, \tag{3.43}$$

where $\kappa = \pm 1$, c_3 is an arbitrary real constant, and u is a complex-valued function. Equation (3.43) has applications in nonlinear optics [53] and is a member of the AKNS hierarchy with

$$A = -4ic_3\zeta^3 - 2i\zeta^2 - 2ic_3qr\zeta - iqr + c_3(rq_x - qr_x), \tag{3.44a}$$

$$B = 4c_3q\zeta^2 + 2\zeta(q + ic_3q_x) + iq_x + c_3(2q^2r - q_{xx}), \tag{3.44b}$$

$$C = 4c_3r\zeta^2 + 2\zeta(r - ic_3r_x) - ir_x + c_3(2qr^2 - r_{xx}), \tag{3.44c}$$

under the reduction $q = \kappa r^* = u$. Periodic stationary solutions of (3.43) have not been studied, to the best of my knowledge. When they are studied, the first step for establishing stability will be applying Theorem 3.2.3 which applies directly with $\mathcal{Q} = \mathbb{R}$ since $A(\mathbb{R}) \subset i\mathbb{R}$ when $q = \kappa r^*$. When $\kappa = -1$, $\mathbb{R} \subset \sigma_L$ and $\Omega(\mathbb{R}) \subset \sigma_{\mathcal{L}} \cap i\mathbb{R}$. When $\kappa = 1$, $\Omega_i = \{\zeta \in \mathbb{R} : \Omega(\zeta) \in i\mathbb{R}\} \subset \sigma_L$ and $\Omega(\Omega_i) \subset \sigma_{\mathcal{L}} \cap i\mathbb{R}$. Since the squared-eigenfunction connection for this equation is given by

$$(\delta u,\ \delta u^*)^\intercal = \left(\Phi_1^2,\ -\Phi_2^2\right)^\intercal, \tag{3.45}$$

where $(\delta u,\ \delta u^*)$ is the linearization of u, $\lambda = 2\Omega(\zeta)$. Therefore solutions are stable when $\Omega(\zeta) \in i\mathbb{R}$. When $\kappa = 1$, $\sigma_L \subset \mathbb{R}$ so establishing that $\{\zeta \in \mathbb{R} : \Omega(\zeta) \notin i\mathbb{R} \setminus \{0\}\} \not\subset \sigma_L$ establishes stability.

The sine- and sinh-Gordon equations

The sine-Gordon (s-G) equation in light-cone coordinates is given by

$$u_{\xi\eta} = \sin u, \tag{3.46}$$

where $u(\xi, \eta)$ is real valued. Equation (3.46) is a member of the AKNS hierarchy (Section 3.1) with Lax pair [7]

$$A = \frac{i}{4\zeta}\cos(u), \qquad B = \frac{i}{4\zeta}\sin(u), \qquad C = \frac{i}{4\zeta}\sin(u). \tag{3.47}$$

Here I use (ξ, η) instead of (x, t) to distinguish between the light-cone coordinates (ξ, η) and the space-time coordinates (x, t). Equation (3.46) is equivalent to the compatibility of mixed derivatives, $\partial_\eta v_\xi = \partial_\xi v_\eta$, by requiring that $r = -q = u_\xi/2$. Since $r = -q$, (3.46) is not self adjoint. A self-adjoint variant of the s-G equation is the sinh-Gordon (sh-G) equation,

$$u_{\xi\eta} = \sinh u. \tag{3.48}$$

Equation (3.48) is a member of the AKNS hierarchy (Section 3.1) with Lax pair [7]

$$A = \frac{i}{4\zeta}\cosh(u), \qquad B = -\frac{i}{4\zeta}\sinh(u), \qquad C = \frac{i}{4\zeta}\sinh(u), \tag{3.49}$$

and is equivalent to the compatibility of mixed derivatives under the reduction $r = q = u_\xi/2$.

The Lax par for both the s-G and the sh-G equations can be found by using the recursion operator as mentioned in Remark 3.1.2, so the remarks there and Assumption 3.1.1 apply. Theorem 3.2.3 applies to the s-G and sh-G equations with $\mathcal{Q} = \mathbb{R}$ since $A(\mathbb{R}) \subset i\mathbb{R}$ for both. For the s-G equation, $\mathbb{R} \subset \sigma_L$ and $\Omega(\mathbb{R}) \subset \sigma_{\mathcal{L}} \cap i\mathbb{R}$. For the sh-G equation, $\Omega_i = \{\zeta \in \mathbb{R} : \Omega(\zeta) \in i\mathbb{R}\} \subset \sigma_L$ and $\Omega(\mathcal{L}) \subset \sigma_{\mathcal{L}} \cap i\mathbb{R}$. However since η is not a timelike variable, stability results mean little for this equation in these variables. A timelike variable appears in laboratory coordinates, for which stability results are meaningful.

To transform (3.46) from light-cone to laboratory coordinates, let $(x, t) = (\eta+\xi, \eta-\xi)$ to obtain

$$u_{tt} - u_{xx} + \sin(u) = 0. \tag{3.50}$$

The same coordinate transformation on (3.48) gives

$$u_{tt} - u_{xx} + \sinh(u) = 0. \tag{3.51}$$

The Lax pair for both systems is

$$\Phi_x = \frac{1}{2}(T + X)\Phi = \hat{X}\Phi, \qquad \Phi_t = \frac{1}{2}(T - X)\Phi = \hat{T}\Phi. \tag{3.52}$$

Note that (3.50) and (3.51) are not members of the AKNS hierarchy. Nonetheless I show that statements very similar to those made in Theorem 3.2.3 hold for this equation. This gives a bridge from the AKNS framework to generalizations.

I move the s-G equation (3.50) and the sh-G equation (3.51) to a traveling frame by letting $(z, \tau) = (x - Vt, t)$ for constant $V \in \mathbb{R}$ and find

$$(V^2 - 1)u_{zz} - 2Vu_{z\tau} + u_{\tau\tau} + \sin(u) = 0, \tag{3.53}$$

and

$$(V^2 - 1)u_{zz} - 2Vu_{z\tau} + u_{\tau\tau} + \sinh(u) = 0, \tag{3.54}$$

respectively. The new Lax pair is given by

$$\Phi_z = \hat{X}\Phi, \qquad \Phi_\tau = (\hat{T} + V\hat{X})\Phi = \tilde{T}\Phi. \tag{3.55}$$

Periodic stationary solutions are found by letting $u_\tau = 0$ and assuming u is periodic in x. Assumption 3.1.1 holds and the Lax pair is of the form mentioned in Remark 3.1.2. Since the transformation to lab coordinates is isospectral, the spectrum σ_L does not change and the results on the spectrum mentioned above still hold. Since the squared-eigenfunction connection gives $\lambda = 2\Omega(\zeta)$ [24], these results are the first step for studying stability. For the s-G equation, $\mathbb{R} \subset \sigma_L$ and $\Omega(\mathbb{R}) \subset \sigma_{\mathcal{L}} \cap i\mathbb{R}$ so solutions are stable with respect to perturbations that excite only real elements of the Lax spectrum. These results are known and have been shown in [24] (whose results agree with [46] where the Lax spectrum is not used). For the sh-G equation, $\Omega_i = \{\zeta \in \mathbb{R} : \Omega(\zeta) \in i\mathbb{R}\} \subset \sigma_L$ and $\Omega(\Omega_i) \subset \sigma_{\mathcal{L}} \cap i\mathbb{R}$. Since $\sigma_L \subset \mathbb{R}$, one must establish that $\mathcal{U} = \{\zeta \in \mathbb{R} : \Omega(\zeta) \notin i\mathbb{R} \setminus \{0\}\} \not\subset \sigma_L$ to establish stability. This result is new and $\mathcal{U} \not\subset \sigma_L$ has not yet been shown.

The above results show that Theorem 3.2.3 may be applicable to some non-AKNS integrable equations. This is explored in Chapter 4 and a theorem to this effect is proven. Before continuing on I continue to study the spectral problem for (3.50) and (3.51) for exposition purposes.

The Lax pair of integrable equations not in the AKNS hierarchy generally define a generalized eigenvalue problem. The Lax pair (3.52) defines a quadratic eigenvalue problem (QEP),

$$Q(\zeta)\Phi = (M\zeta^2 + N\zeta + K)\Phi = 0. \tag{3.56}$$

There are two choices for $M,\ N$, and K:

$$M_1 = \begin{pmatrix} 1 & 0 \\ 0 & 1 \end{pmatrix}, \qquad N_1 = \begin{pmatrix} -2i\partial_x & iq \\ -ir & 2i\partial_x \end{pmatrix}, \qquad K_1 = \begin{pmatrix} ia & ib \\ ic & -ia \end{pmatrix}, \tag{3.57a}$$

$$M_2 = \begin{pmatrix} 1 & 0 \\ 0 & -1 \end{pmatrix}, \qquad N_2 = \begin{pmatrix} -2i\partial_x & iq \\ ir & -2i\partial_x \end{pmatrix}, \qquad K_2 = \begin{pmatrix} ia & ib \\ -ic & ia \end{pmatrix}, \tag{3.57b}$$

where

$$a = \zeta A, \quad b = \zeta B, \quad c = \zeta C. \tag{3.58}$$

Then $\zeta \in \mathbb{C}$ is an eigenvalue of Q if and only if $Q(\zeta)\Phi = 0$ for all bounded Φ. A QEP is classified as self adjoint if $M,\ N$, and K are self adjoint [70]. The eigenvalues for self-adjoint QEPs are either real or come in complex-conjugate pairs [70, 63]. If $M_1,\ N_1$, and K_1 are chosen, then $Q(\zeta)$ is self adjoint if $r = q^*$, $a^* = -a$, and $c^* = b$, which is the case for the sh-G equation. If $M_2,\ N_2$, and K_2 are chosen, then $Q(\zeta)$ is self adjoint if $r = -q^*$, $a^* = -a$, and $c^* = -b$, which is the case for the s-G equation. It follows that for either equation, the Lax spectrum consists of real or complex-conjugate spectral elements. This confirms what is known from the isospectral transform to light-cone coordinates. The whole real line is part of the Lax spectrum for the s-G equation and the Lax spectrum for the sh-G equation is a subset of the real line. To determine the subset of σ_L off the real line, one may use the integral condition (3.31) (used in [24] to find σ_L) or the Floquet discriminant (Appendix B).

3.3.2 Members of the AKNS hierarchy not satisfying (3.4)

The s-G and sh-G equation examples indicate that the results of Section 3.2 may be applied to integrable equations not in the AKNS hierarchy. Before examining that case, I show how the results can be applied to members of the AKNS hierarchy that do not have the common reduction (3.4).

The Korteweg-de Vries equation

Perhaps the best-known integrable equation is the Korteweg-de Vries (KdV) equation [8],

$$u_t + 6uu_x + u_{xxx} = 0, \tag{3.59}$$

where u is a real-valued function of x and t. The KdV equation is a singular member of the AKNS hierarchy: it is obtained using the AKNS Lax pair (3.1) with $r = -1$ [7]. When r is constant, the

Lax pair can be rewritten as an eigenvalue problem with spectral parameter ζ^2. With $r = -1$,

$$\zeta^2 v = -(q + \partial_x^2)v = L_{\mathrm{KdV}}\, v. \tag{3.60}$$

The operator L_{KdV} is self adjoint, so the KdV equation is said to have a self-adjoint Lax pair even though the Lax operator L (3.7) is not. Since L_{KdV} is self adjoint, $\zeta^2 \in \mathbb{R}$.

Defining $(y, \tau) = (x - ct, t)$ gives the KdV equation in the traveling frame,

$$u_\tau - cu_y + 6uu_y + u_{yyy} = 0. \tag{3.61}$$

The periodic stationary solutions of (3.61) are the cnoidal waves which are defined in terms of Jacobi elliptic functions [1, 22]. In the traveling frame, the Lax pair is given by (3.1) with

$$A = -4i\zeta^3 + 2iu\zeta - u_x - ic\zeta, \quad B = 4u\zeta^2 + 2i\zeta u_x - 2u^2 - u_{xx} + cu, \quad C = -4\zeta^2 + 2u - c, \tag{3.62a}$$

$q = u$ and $r = -1$. Using (3.10) and (3.61) with $u_\tau = 0$,

$$\Omega^2 = 2a - (c + 4\zeta^2)(-k + c\zeta^2 + 4\zeta^4), \tag{3.63}$$

where

$$k = 3u^2 - cu + u_{xx} \quad \text{and} \quad 2a = u_x - 2ku + 2u^3 - cu^2 \tag{3.64}$$

are constants found from integrating (3.61) with $u_\tau = 0$. A condition, analogous to (3.32) and found in Section 4.2, for $\zeta \in \sigma_L \cap \mathbb{R}$ is

$$\mathrm{Re}\left\langle \frac{q\Omega}{C} \right\rangle = 0. \tag{3.65}$$

Since q and C are real-valued functions for $\zeta \in \mathbb{R}$, the above condition is satisfied when $\Omega(\zeta) \in i\mathbb{R}$. This implies that $\Omega_i = \{\zeta \in \mathbb{R} : \Omega(\zeta) \in i\mathbb{R}\} \subset \sigma_L$ and $\Omega(\Omega_i) \subset \sigma_{\mathcal{L}} \cap i\mathbb{R}$. The analysis of the Lax spectrum for the cnodial waves of the KdV equation can be found in [22] including plots of the real Lax spectrum [22, Figure 4] and of the imaginary stability spectrum [22, Figure 1]. There it is shown that $\sigma_L = \Omega_i$ and that $\lambda = 2\Omega(\zeta)$ establishing that the cnoidal solutions are stable.

The PT-symmetric reverse space nonlocal NLS equation

The PT-symmetric reverse space nonlocal NLS equation is given by [5]

$$i\Psi_t(x,t) + \frac{1}{2}\Psi_{xx}(x,t) - \kappa\Psi(x,t)^2\Psi^*(-x,t) = 0, \tag{3.66}$$

where $\kappa = \pm 1$. This equation is a member of the AKNS hierarchy with the Lax pair [5]

$$A(x,t) = -i\zeta^2 - iqr/2, \qquad B = \zeta q + iq_x/2, \qquad C = \zeta r - ir_x/2, \tag{3.67}$$

and $r(x,t) = \kappa q^*(-x,t) = \kappa \Psi^*(-x,t) \in \mathbb{C}$. Solutions of (3.14) with

$$\Psi(x,t) = \Psi(-x,t), \tag{3.68}$$

are also solutions of (3.66). Thus all even solutions of (3.14) examined in [11] for $\kappa = 1$ and in [28] for $\kappa = -1$ are solutions to (3.66). These solutions, and other periodic and quasi-periodic solutions of (3.66), were first reported in [51]. Almost every solution found in [51] is even in x, except for one that is odd. For the even solutions, the Lax spectrum remains unchanged since $\Psi(x,t) = \Psi(-x,t)$: hence the stability results in [11, 28] and Chapter 2 hold for these solutions.

The Lax pair is not self adjoint for $\kappa = 1$, so σ_L is not necessarily a subset of $\mathbb{R}$. With the equation written in a uniformly rotating frame so that all components are time independent, Assumption 3.1.1 and Remark 3.1.2 apply. Upon assuming that q and r are P-periodic or quasiperiodic and $\zeta \in \mathbb{R}$, $\zeta \in \sigma_L$ if

$$\operatorname{Re}\left\langle \frac{qC}{A - \Omega} \right\rangle = 0. \tag{3.69}$$

This condition is found just as (3.32) was found and is an example of several equivalent conditions for the Lax spectrum derived in Section 4.2. For $\zeta \in \mathbb{R}$,

$$A^*(-x) = -A(x), \qquad \text{and} \qquad C^*(-x) = \kappa B(x). \tag{3.70}$$

so that

$$\begin{aligned} \Omega^2(\zeta) &= A(x)^2 + B(x)C(x) = A(-x)^2 + B(-x)C(-x) \\ &= (A^2 + BC)^* = \left(\Omega^2(\zeta)\right)^*, \end{aligned} \tag{3.71}$$

and $\Omega(\mathbb{R}) \subset \mathbb{R} \cup i\mathbb{R}$. If $\zeta \in \mathbb{R}$ and $\Omega(\zeta) \in i\mathbb{R}$,

$$\begin{aligned}
\operatorname{Re}\int_0^P \left(\frac{q(x)C(x)}{A(x)-\Omega}\right)\,\mathrm{d}x &= \frac{1}{2}\left(\int_0^P \frac{q(x)C(x)}{A(x)-\Omega}\,\mathrm{d}x + \int_0^P \frac{q^*(x)C^*(x)}{A^*(x)-\Omega^*}\,\mathrm{d}x\right)\\
&= \frac{1}{2}\left(\int_0^P \frac{q(x)C(x)}{A(x)-\Omega}\,\mathrm{d}x - \int_0^{-P} \frac{q^*(-x)C^*(-x)}{A^*(-x)-\Omega^*}\,\mathrm{d}x\right)\\
&= \frac{1}{2}\left(\int_0^P \frac{q(x)C(x)}{A(x)-\Omega}\,\mathrm{d}x + \int_{-P}^0 \frac{q^*(-x)C^*(-x)}{-A(x)+\Omega}\,\mathrm{d}x\right)\\
&= \frac{1}{2}\left(\int_0^P \frac{q(x)C(x)}{A(x)-\Omega}\,\mathrm{d}x + \int_0^P \frac{q^*(-x)C^*(-x)}{-A(x)+\Omega}\,\mathrm{d}x\right)\\
&= \frac{1}{2}\left(\int_0^P \frac{q(x)C(x)-q^*(-x)C^*(-x)}{A(x)-\Omega}\,\mathrm{d}x\right)\\
&= \frac{1}{2}\int_0^P \frac{A_x}{A(x)-\Omega}\,\mathrm{d}x = 0,
\end{aligned} \tag{3.72}$$

since A is periodic when q and r are. It follows from (3.69) that $\Omega_i = \{\zeta \in \mathbb{R} : \Omega(\zeta) \in i\mathbb{R}\} \subset \sigma_L$ for $\kappa = \pm 1$. The squared-eigenfunction connection in this case is the same as the local NLS equation, $\lambda = 2\Omega(\zeta)$. Therefore the results here can be used to understand the stability spectrum.

Reverse space-time nonlocal generalized sine-Gordon equations

The generalized sine-Gordon equations satisfy [6]

$$\partial_{xt} q(x,t) + 2s(x,t)q(x,t) = 0, \tag{3.73a}$$

$$\partial_{xt} r(x,t) + 2s(x,t)r(x,t) = 0, \tag{3.73b}$$

$$\partial_x s(x,t) + \partial_t(q(x,t)r(x,t)) = 0, \tag{3.73c}$$

where s is a prescribed complex-valued function and q and r are also complex-valued functions. These equations are members of the AKNS hierarchy with

$$A(x,t;\zeta) = \frac{s(x,t)}{2i\zeta}, \qquad B(x,t;\zeta) = \frac{q_t(x,t)}{2i\zeta}, \qquad C(x,t;\zeta) = -\frac{r_t(x,t)}{2i\zeta}. \tag{3.74}$$

Note that (3.46) is found by equating $s(x,t) = -\cos(u(x,t))/2,\ r(x,t) = -q(x,t) = u_x(x,t)/2$, and (3.48) is found by equating $s(x,t) = -\cosh(u(x,t))/2,\ r(x,t) = q(x,t) = u_x(x,t)/2$.

The reverse space-time nonlocal sine-Gordon equations [6] are found by using the reduction $r(x,t) = \sigma q^*(-x,-t)$. The equations (3.73a) and (3.73b) are compatible under this reduction if and only if

$$s^*(-x,-t) = s(x,t). \tag{3.75}$$

The evolution equation is

$$q_{xt}(x,t) + 2s(x,t)q(x,t) = 0, \qquad s^*(-x,-t) = s(x,t). \tag{3.76}$$

Assuming that the equation is in a stationary frame, $q_t = s_t = 0$, the same analysis as is completed in the above example shows that $\Omega(\mathbb{R}) \subset \mathbb{R} \cup i\mathbb{R}$ and $\Omega_i = \{\zeta \in \mathbb{R} : \Omega(\zeta) \in i\mathbb{R}\} \subset \sigma_L$ for $\sigma = \pm 1$. The squared-eigenfunction connection here is the same as for the local s-G equation, $\lambda = 2\Omega(\zeta)$. Therefore these results can be used as a starting point for determining the stability spectrum.

The complex reverse space-time nonlocal mKdV

The complex reverse space-time nonlocal mKdV equation is given by

$$u_t(x,t) - 6\kappa u(x,t)u^*(-x,-t)u_x(x,t) = 0, \tag{3.77}$$

where $\kappa = \pm 1$ and u is a complex-valued function. This equation is a member of the AKNS hierarchy with

$$A(x,t;\zeta) = -4i\zeta^3 - 2i\zeta q(x,t)r(x,t) + r(x,t)\partial_x q(x,t) - q(x,t)\partial_x r(x,t), \tag{3.78a}$$

$$B(x,t;\zeta) = 4\zeta^2 q(x,t) + 2i\zeta\partial_x q(x,t) + 2q^2(x,t)r(x,t) - \partial_x^2 q(x,t), \tag{3.78b}$$

$$C(x,t;\zeta) = 4\zeta^2 r(x,t) - 2i\zeta\partial_x r(x,t) + 2q(x,t)r^2(x,t) - \partial_x^2 r(x,t), \tag{3.78c}$$

under the reduction $r(x,t) = \kappa q^*(-x,-t) = \kappa u^*(-x,-t)$. Note that when

$$u(-x,-t) = u(x,t) \in \mathbb{R}, \tag{3.79}$$

solutions of (3.39) are solutions of (3.77). In such cases, the Lax spectrum is the same since A, B, and C inherit their properties from q and r. There may be solutions to (3.77) without the property (3.79). For these solutions, the same procedure followed in the above two examples shows that $\Omega(\mathbb{R}) \subset \mathbb{R} \cup i\mathbb{R}$ and $\{\zeta \in \mathbb{R} : \Omega(\zeta) \in i\mathbb{R}\} \subset \sigma_L$ for $\kappa = \pm 1$. The squared-eigenfunction connection here is the same as for the local mKdV equation, $\lambda = 2\Omega(\zeta)$. Therefore these results can be used as a starting point for determining the stability spectrum.

3.4 Conclusion

The stability spectrum and the Lax spectrum for solutions of many integrable equations on the whole line have been characterized for some time. The same level of understanding for the periodic

problem does not exist. One reason the whole line problem is more straightforward to study is the ability to do spatial asymptotics to find the essential spectrum that contains the unbounded components of the spectrum. In this work, **I have given a complete characterization of all unbounded components of the Lax spectrum for a number of integrable equations.**

I provided a theorem (Theorems 3.2.3) with easily verifiable assumptions that establish that real Lax spectra corresponds to stable modes of the linearization for a number of equations in the AKNS hierarchy. I demonstrated the applicability of the theorem by applying it to several examples.

Chapter 4

THE LAX SPECTRUM AND SPECTRAL STABILITY FOR OTHER INTEGRABLE EQUATIONS

In Chapter 3 I presented a method to find important parts of the Lax spectrum of members of the AKNS hierarchy admitting a common reduction. There I showed that the real line of the Lax spectrum plays an important role in stability. For the non self-adjoint members of the AKNS hierarchy (those with $\kappa = -1$), the real line is part of the Lax spectrum and maps to stable elements of the stability spectrum. For the self-adjoint members of the hierarchy (those with $\kappa = 1$), the Lax spectrum is a subset of the real line. If one can establish that $\{\zeta \in \mathbb{R} : \Omega(\zeta) \notin i\mathbb{R} \setminus \{0\}\} \not\subset \sigma_L$, then the solution of interest is stable, as long as the squared-eigenfunction connection gives $\lambda = 2\Omega(\zeta)$. The sine-Gordon and sinh-Gordon examples (Section 3.3.1) indicate that this trend holds even for integrable systems not in the AKNS hierarchy. In this chapter I extend the AKNS hierarchy results to integrable systems that are not in the AKNS hierarchy.

4.1 Setup

In this chapter I consider integrable equations (1.1) possessing a 2×2 Lax pair of the form,

$$\Phi_x(x,t;\zeta) = \begin{pmatrix} \alpha(x,t;\zeta) & \beta(x,t;\zeta) \\ \gamma(x,t;\zeta) & -\alpha(x,t;\zeta) \end{pmatrix} \Phi(x,t;\zeta) = X\Phi, \tag{4.1a}$$

$$\Phi_t(x,t;\zeta) = \begin{pmatrix} A(x,t;\zeta) & B(x,t;\zeta) \\ C(x,t;\zeta) & -A(x,t;\zeta) \end{pmatrix} \Phi(x,t;\zeta) = T\Phi, \tag{4.1b}$$

where α, β, γ, A, B, and C are complex-valued functions. As in the analysis of the AKNS hierarchy, the analysis here is restricted to Lax pairs where the elements of $\mathcal{P} = \{\alpha,\ \beta,\ \gamma,\ A,\ B,\ C\}$ are bounded for all $x \in \overline{\mathbb{R}} = \mathbb{R} \cup \{\infty\}$ and are autonomous in t. Since the interest here is in studying stationary solutions, assume that $\alpha_t = \beta_t = \gamma_t = 0$. In the stationary frame, the compatibility of

(4.1) defines the conditions

$$A_x = \beta C - \gamma B, \tag{4.2a}$$

$$B_x = 2\left(\alpha B - \beta A\right), \tag{4.2b}$$

$$C_x = -2\left(\alpha C - \gamma A\right). \tag{4.2c}$$

4.2 Computing the Lax spectrum

With A, B, and C t-independent, (4.1b) may be solved by separation of variables resulting in (3.10). Here Ω has the same properties as for the AKNS hierarchy and Lemma 3.1.4 holds with a nearly identical proof. Again I consider the special case of the reduction

$$\gamma = \kappa\beta^*, \qquad \kappa = \pm 1. \tag{4.3}$$

Using this reduction, let

$$\beta(x;\zeta) = \eta(x;\zeta)e^{i\theta(x;\zeta)}, \qquad \gamma(x;\zeta) = \kappa\eta(x;\zeta)e^{-i\theta(x;\zeta)}, \tag{4.4}$$

where η and θ are real-valued functions with $\eta(x;\zeta) \geq 0$. I also assume that η is a P-periodic function. Using the isospectral transformation (3.23), the Lax pair (4.1) becomes

$$\tilde{\Phi}_x = \begin{pmatrix} \hat{\alpha} & \hat{\beta} \\ \hat{\gamma} & -\hat{\alpha} \end{pmatrix} \tilde{\Phi}, \qquad \tilde{\Phi}_t = \begin{pmatrix} \hat{A} & \hat{B} \\ \hat{C} & -\hat{A} \end{pmatrix} \tilde{\Phi}, \tag{4.5}$$

where

$$\hat{\alpha} = \alpha - i\theta_x/2, \qquad \hat{\beta} = \beta e^{-i\theta} = \eta, \qquad \hat{\gamma} = \gamma e^{i\theta} = \kappa\eta, \tag{4.6a}$$

$$\hat{A} = A, \qquad \hat{B} = e^{-i\theta}B, \qquad \hat{C} = e^{i\theta}C. \tag{4.6b}$$

The eigenfunctions here are identical to (3.27). Similar work to what was done there gives two ODEs for y_1, but also two for y_2. This gives two expressions for y_1 and two for y_2. In each case the exponential term needs to be bounded for $x \in \overline{\mathbb{R}}$. Inspired by the results for the AKNS hierarchy, assume that $\hat{A}$, $\hat{B}$, and $\hat{C}$ are P-periodic. With these assumptions, eight boundedness conditions that define the Lax spectrum are obtain (four from y_1 and y_2, and four from rewriting those four

using (4.2)):

$$\mathrm{Re}\left\langle \hat{\alpha} - \frac{\hat{\beta}(\hat{A}-\Omega)}{\hat{B}} \right\rangle = 0, \qquad \mathrm{Re}\left\langle \hat{\alpha} + \frac{\hat{\gamma}\hat{B}}{\hat{A}-\Omega} \right\rangle = 0, \tag{4.7a}$$

$$\mathrm{Re}\left\langle \hat{\alpha} + \frac{\hat{\beta}\hat{C}}{\hat{A}+\Omega} \right\rangle = 0, \qquad \mathrm{Re}\left\langle \frac{\hat{\beta}\Omega}{\hat{B}} \right\rangle = 0, \tag{4.7b}$$

$$\mathrm{Re}\left\langle \hat{\alpha} - \frac{\hat{\gamma}(\hat{A}+\Omega)}{\hat{C}} \right\rangle = 0, \qquad \mathrm{Re}\left\langle \hat{\alpha} + \frac{\hat{\beta}\hat{C}}{\hat{A}-\Omega} \right\rangle = 0, \tag{4.7c}$$

$$\mathrm{Re}\left\langle \hat{\alpha} + \frac{\hat{\gamma}\hat{B}}{\hat{A}+\Omega} \right\rangle = 0, \qquad \mathrm{Re}\left\langle \frac{\hat{\gamma}\Omega}{\hat{C}} \right\rangle = 0, \tag{4.7d}$$

If any of these conditions are satisfied for a particular $\hat{\zeta} \in \mathbb{C}$, then $\hat{\zeta} \in \sigma_L$. Some of these conditions are new and some have been used in [10, 11, 22, 24, 26, 27, 28]. These conditions were first written down in full generality in [71]. Note that the last condition in (4.7) implies that $\{\zeta \in \mathbb{C} : \Omega(\zeta) = 0\} \subset \sigma_L$. Lemma 3.2.2 and Theorem 3.2.3 have immediate analogues here, whose proof is nearly identical.

Theorem 4.2.1. *Consider an integrable equation* (1.1) *possessing the Lax pair* (4.1) *with the reduction* (4.3)*. Assume that* $\hat{A}$*,* $\hat{B}$*, and* $\hat{C}$ *from* (4.6) *are* P*-periodic. Let*

$$\mathcal{Q}_- = \{\zeta \in \mathbb{C} : \alpha(\zeta), A(\zeta) \in i\mathbb{R} \text{ and } \beta = -\gamma^*\}, \tag{4.8a}$$

$$\mathcal{Q}_+ = \{\zeta \in \mathbb{C} : \alpha(\zeta), A(\zeta) \in i\mathbb{R} \text{ and } \beta = \gamma^*\}, \tag{4.8b}$$

$$\Omega_i = \{\zeta \in \mathbb{C} : \Omega(\zeta) \in i\mathbb{R}\}, \qquad \text{and} \qquad \Omega_r = \{\zeta \in \mathbb{C} : \Omega(\zeta) \in \mathbb{R}\}. \tag{4.8c}$$

Then $\mathcal{Q}_- \subset \Omega_i$*,* $\mathcal{Q}_+ \subset \Omega_i \cup \Omega_r$*,* $\mathcal{S} = \mathcal{Q}_- \cup (\mathcal{Q}_+ \cap \Omega_i) \subset \sigma_L$*, and* $\Omega(\mathcal{S}) \subset i\mathbb{R}$*. Further, if* $\Omega : \sigma_L \cap i\mathbb{R} \to \sigma_{\mathcal{L}} \cap i\mathbb{R}$ *,* $\Omega(\mathcal{S}) \subset \sigma_{\mathcal{L}} \cap i\mathbb{R}$*.*

In other words, assume that $\alpha(\zeta), A(\zeta) \in i\mathbb{R}$*. Then* $\Omega(\zeta) \in i\mathbb{R}$ *when* $\beta(\zeta) = -\gamma(\zeta)^*$*, (akin to the* $\kappa = -1$ *case in Theorem 3.2.3), and those* ζ *are in the Lax spectrum,* σ_L*. Further, they map to stable elements of the stability spectrum. When* $\beta(\zeta) = \gamma(\zeta)^*$*, (akin to the* $\kappa = 1$ *case in Theorem 3.2.3),* $\Omega(\zeta) \in i\mathbb{R} \cup \mathbb{R}$ *and the* ζ *such that* $\Omega(\zeta) \in i\mathbb{R}$ *are in the Lax spectrum and map to stable elements of the stability spectrum.*

The proof of this theorem is nearly identical to the proof of Theorem 3.2.3, so it is omitted here. Before moving on to examples which demonstrate the applicability of Theorem 4.2.1, note that these results do not address the intersection of σ_L with $\mathcal{Q}_\pm \cap \{\zeta \in \mathbb{C} : \Omega(\zeta) \notin i\mathbb{R} \setminus \{0\}\}$. Indeed,

establishing whether or not this intersection is trivial is important for understanding the stability of the solution in question. This difficulty is not addressed here.

4.3 Examples

In this section I provide examples for which Theorem 4.2.1 applies. Next, I provide examples for which the theorem does not apply directly, but for which similar conclusions can be drawn. I do this to demonstrate that these results can be generalized and are not necessarily limited to the special cases considered here.

4.3.1 Examples for which Theorem 4.2.1 applies directly

Derivative nonlinear Schrödinger equation

The derivative NLS equation,

$$iq_t = -q_{xx} + i\kappa(|q|^2 q)_x, \qquad \kappa = \pm 1, \tag{4.9}$$

was first solved on the whole line using the Inverse Scattering Transform in [50]. The Lax pair for (4.9) is given by (4.1) with [50]

$$\alpha = -i\zeta^2, \qquad \beta = q\zeta, \qquad \gamma = r\zeta, \tag{4.10a}$$

$$A = -2i\zeta^4 - i\zeta^2 rq, \qquad B = 2\zeta^3 q + i\zeta q_x + \zeta r q^2, \qquad C = 2\zeta^3 r - i\zeta r_x + \zeta r^2 q. \tag{4.10b}$$

where $r = \kappa q^* \in \mathbb{C}$. Using $q(x,t) \mapsto e^{-i\omega t} q(x,t)$ where ω is a real constant, (4.9) becomes

$$iq_t = -q_{xx} + i\kappa(|q|^2 q)_x - \omega q, \tag{4.11}$$

and $A \mapsto A + i\omega/2$; otherwise (4.10) remains the same. Stationary solutions satisfy

$$-q_{xx} + i\kappa(|q|^2 q)_x - \omega q = 0. \tag{4.12}$$

Quasi-periodic elliptic solutions to the stationary problem were found in [43].

The Lax pair defines a QEP (3.56). There are two choices for M, N, and K,

$$M_1 = \begin{pmatrix} 1 & 0 \\ 0 & 1 \end{pmatrix}, \qquad N_1 = \begin{pmatrix} 0 & iq \\ -ir & 0 \end{pmatrix}, \qquad K_1 = \begin{pmatrix} -i\partial_x & 0 \\ 0 & i\partial_x \end{pmatrix}, \tag{4.13a}$$

$$M_2 = \begin{pmatrix} 1 & 0 \\ 0 & -1 \end{pmatrix}, \qquad N_2 = \begin{pmatrix} 0 & iq \\ ir & 0 \end{pmatrix}, \qquad K_2 = \begin{pmatrix} -i\partial_x & 0 \\ 0 & -i\partial_x \end{pmatrix}. \tag{4.13b}$$

If $M_1,\ N_1$, and K_1 are chosen, then $Q(\zeta)$ is self adjoint if $r = q^*$. If $M_2,\ N_2$, and K_2 are chosen, then $Q(\zeta)$ is self adjoint if $r = -q^*$. It follows that eigenvalues are real or come in complex-conjugate pairs for either choice of κ.

Theorem 4.2.1 applies with different results depending on κ and ζ. When $\kappa = -1$ the theorem gives $\mathbb{R} \subset \mathcal{Q}_-$ and $i\mathbb{R} \subset \mathcal{Q}_+$. When $\kappa = 1$, the theorem gives $i\mathbb{R} \subset \mathcal{Q}_-$ and $\mathbb{R} \subset \mathcal{Q}_+$. It follows that $\mathcal{S}_- = \mathbb{R} \cup (\Omega_i \cap i\mathbb{R}) \subset \sigma_L$ and $\Omega(\mathcal{S}_-) \subset i\mathbb{R}$ for $\kappa = -1$ (see Figure 4.1a). If $\kappa = 1$, $\mathcal{S}_+ = i\mathbb{R} \cup (\Omega_i \cap \mathbb{R}) \subset \sigma_L$ and $\Omega(\mathcal{S}_+) \subset i\mathbb{R}$ (see Figure 4.1b). To compute the spectrum off of the real or imaginary axes, one must examine the integral conditions (4.7) or construct the Floquet discriminant (Appendix B).

The squared-eigenfunction connection for the derivative NLS equation is [20]

$$(\delta u,\ \delta u^*)^\intercal = \partial_x \left(\Phi_1^2,\ \Phi_2^2\right)^\intercal, \tag{4.14}$$

where δu and δu^* are the linearizations of the two independent variables. It follows that $\lambda = 2\Omega(\zeta)$, thus $\Omega(\mathcal{S}_\pm) \subset \sigma_{\mathcal{L}} \cap i\mathbb{R}$. This result can be used as the first step in studying stability of periodic or quasiperiodic solutions of the derivative NLS equation.

The derivative NLS equation is one of several equations in the Kaup-Newell hierarchy. Another example is

$$u_t = \left(u_{xx} \pm 3u^2 u_x + \frac{3}{2}u^5\right)_x, \tag{4.15}$$

which is a model for long lattice waves [50]. The method described here is applicable to all equations in the Kaup-Newell hierarchy with $q = \pm r^*$ and for which B and C satisfy the assumptions of Theorem 4.2.1.

The Massive Thirring Model (MTM)

The Massive Thirring Model in lab coordinates [48] is given by

$$i(u_x + u_t) + v + u\,|v|^2 = 0, \qquad i(-v_x + v_t) + u + v\,|u|^2 = 0, \tag{4.16}$$

where u and v are complex-valued functions of x and t. The Lax pair for this equation is given by (4.1) with

$$\alpha = \frac{i}{4}\left(|u|^2 - |v|^2 + \zeta^2 - 1/\zeta^2\right), \qquad \beta = -\frac{i}{2}\left(\zeta v^* - u^*/\zeta\right), \quad \gamma = -\frac{i}{2}\left(\zeta v - u/\zeta\right), \tag{4.17a}$$

$$A = -\frac{i}{4}\left(|v|^2 + |u|^2 - \zeta^2 - 1/\zeta^2\right), \quad B = -\frac{i}{2}\left(\zeta v^* + u^*/\zeta\right), \quad C = -\frac{i}{2}\left(\zeta v + u/\zeta\right). \tag{4.17b}$$

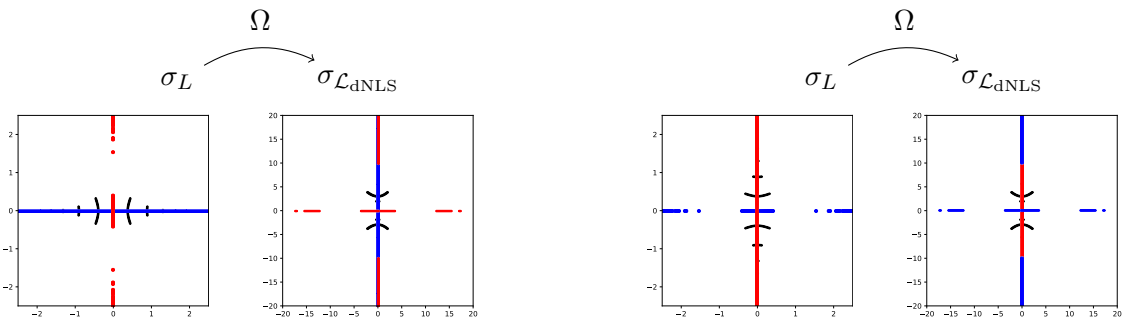

(a) (b)

Figure 4.1: The real *vs.* imaginary part of the Lax and stability spectrum (left and right respectively) for a periodic solution of (a) the focusing derivative NLS equation and (b) the defocusing derivative NLS equation. The Lax spectrum is computed numerically using [23] and the stability spectrum is the image under Ω. The Lax spectrum on the real and imaginary axes are colored blue and red respectively. Their image under the map Ω is colored in the stability spectrum accordingly. The Lax spectrum off the real and imaginary axes and its image under Ω is black.

For solutions $|u|$ and $|v|$ with common period P, Theorem 4.2.1 applies with $\mathcal{Q}_- \subset \mathbb{R}$ and $\mathcal{Q}_+ \subset i\mathbb{R}$. It follows that $\mathcal{S} = \mathbb{R} \cup (\Omega_i \cap i\mathbb{R}) \subset \sigma_L$ and $\Omega(\mathcal{S}) \subset i\mathbb{R}$. The squared-eigenfunction connection is given by [48]

$$\begin{pmatrix} \delta u \\ \delta u^* \\ \delta v \\ \delta v^* \end{pmatrix} = \begin{pmatrix} \Phi_2^2/\zeta + u\Phi_1\Phi_2 \\ \Phi_1^2/\zeta - u^*\Phi_1\Phi_2 \\ -\zeta\Phi_2^2 - v\Phi_1\Phi_2 \\ -\zeta\Phi_1^2 + v^*\Phi_1\Phi_2 \end{pmatrix}, \tag{4.18}$$

where δu, δu^*, δv, and δv^* are the linearizations of the four independent variables. Therefore $\lambda = 2\Omega(\zeta)$ so $\Omega(\mathcal{S}) \subset \sigma_{\mathcal{L}} \cap i\mathbb{R}$. This result can be used as the first step for studying stability of periodic or quasiperiodic solutions.

The O_4 nonlinear σ-model

The O_4 nonlinear σ-model,

$$u_{xx} - u_{tt} - \sin(u)\cos(u) + \frac{\cos(u)}{\sin^3(u)}\left(w_x^2 - w_t^2\right) = 0, \tag{4.19a}$$

$$\partial_x\left(w_x \cot^2(u)\right) - \partial_t\left(w_t \cot^2(u)\right) = 0, \tag{4.19b}$$

where u and w are real-valued functions, was solved on the whole line using the Inverse Scattering Transform [7] in [59]. When $\lambda = 0$, (4.19) reduces to s-G (3.50). The Lax pair for (4.19) is given by (4.1) with

$$\alpha = -\frac{i}{2}\zeta + \frac{i\cos(2u)}{8\zeta} + \frac{i}{2}w_t \cot^2(u) - \frac{i}{2}w_x, \tag{4.20a}$$

$$\beta = \frac{i}{8\zeta}\sin(2u) - \frac{1}{2}(u_x + u_t) + \frac{i}{2}(w_x + w_t)\cot(u), \tag{4.20b}$$

$$\gamma = \frac{i}{8\zeta}\sin(2u) + \frac{1}{2}(u_t + u_x) + \frac{i}{2}(w_t + w_x)\cot(u), \tag{4.20c}$$

$$A = -\frac{i}{2}\zeta - \frac{i}{8\zeta}\cos(2u) - \frac{i}{2}w_t + \frac{i}{2}w_x \cot^2(u), \tag{4.20d}$$

$$B = -\frac{i}{8\zeta}\sin(2u) - \frac{1}{2}(u_t + u_x) + \frac{i}{2}(w_x + w_t)\cot(u), \tag{4.20e}$$

$$C = -\frac{i}{8\zeta}\sin(2u) + \frac{1}{2}(u_t + u_x) + \frac{i}{2}(w_x + w_t)\cot(u). \tag{4.20f}$$

Since $\alpha(\mathbb{R})$, $A(\mathbb{R}) \subset i\mathbb{R}$ and $\beta(\mathbb{R})^* = \gamma(\mathbb{R})$, Theorem 4.2.1 applies with $\mathcal{Q}_- = \mathbb{R}$. Unlike previous examples, $i\mathbb{R} \not\subset \mathcal{Q}_+$ and no conclusions about $\mathcal{Q}_+$ or $i\mathbb{R}$ are made here. Therefore $\mathbb{R} \subset \Omega_i$ and $\mathbb{R} \subset \sigma_L$. Since the squared-eigenfunction connection is unknown, it is unclear how these results apply to stability.

Modified Vector derivative NLS equation

The Modified Vector derivative NLS equation [25] is given in polar form by

$$u_t = iu_{xx} + 2\kappa(|u|^2 u)_x + \frac{\nu}{2}(u_x + \kappa u_x^*), \tag{4.21}$$

where $\kappa = \pm 1$, $\nu \in \mathbb{R}$ is a constant, and u is a complex-valued function. Equation 4.21 is an extension of the derivative NLS equation (4.9) but is not in the Kaup-Newell hierarchy. The Lax

pair for (4.21) is given by (4.1) with

$$\alpha = \frac{i\nu^2}{32\zeta^2} - \frac{i\zeta^2}{2}, \qquad \beta = \frac{r\nu}{4\zeta} + q\zeta, \qquad \gamma = \frac{q\nu}{4\zeta} + r\zeta, \tag{4.22a}$$

$$A = \frac{i\nu^4}{512\zeta^4} + \frac{i\nu^3}{64\zeta^2} + \frac{iqr\nu^2}{16\zeta^2} - \frac{i\zeta^2\nu}{4} - \frac{i\zeta^4}{2} - iqr\zeta^2, \tag{4.22b}$$

$$B = \frac{r\nu^3}{64\zeta^3} + \frac{q\nu^2}{16\zeta} + \frac{r\nu^2}{8\zeta} + \frac{q\zeta\nu}{2} + \frac{r\zeta\nu}{4} - \frac{ir_x\nu}{4\zeta} + \frac{qr^2\nu}{2\zeta} + q\zeta^3 + 2q^2r\zeta + i\zeta q_x, \tag{4.22c}$$

$$C = \frac{q\nu^3}{64\zeta^3} + \frac{q\nu^2}{8\zeta} + \frac{r\nu^2}{16\zeta} + \frac{q\zeta\nu}{4} + \frac{r\zeta\nu}{2} + \frac{iq_x\nu}{4\zeta} + \frac{q^2r\nu}{2\zeta} + r\zeta^3 + 2qr^2\zeta - i\zeta r_x, \tag{4.22d}$$

under the reduction $q = \kappa r^* = u$. Theorem 4.2.1 applies when $|u|$ is a periodic solution of (4.21). If $\kappa = -1$, $\mathbb{R} \subset \mathcal{Q}_-$ and $i\mathbb{R} \subset \mathcal{Q}_+$, hence $\mathbb{R} \subset \Omega_i$, $i\mathbb{R} \subset \Omega_i \cup \Omega_r$, $\mathcal{S} = \mathbb{R} \cup (\Omega_i \cap i\mathbb{R}) \subset \sigma_L$, and $\Omega(\mathcal{S}) \subset i\mathbb{R}$. If $\kappa = 1$, $i\mathbb{R} \subset \mathcal{Q}_-$ and $\mathbb{R} \subset \mathcal{Q}_+$, hence $i\mathbb{R} \subset \Omega_i$, $\mathbb{R} \subset \Omega_i \cup \Omega_r$, $\mathcal{S} = i\mathbb{R} \cup (\Omega_i \cap \mathbb{R}) \subset \sigma_L$, and $\Omega(\mathcal{S}) \subset i\mathbb{R}$. Since the squared-eigenfunction connection for this equation is unknown, it is unclear at this time how these results apply to stability.

The Wadati-Konno-Ichikawa-Shimizu equation

The Wadati-Konno-Ichikawa-Shimizu (WKIS) equation,

$$iu_t + \left(\frac{u}{\sqrt{1 + |u|^2}} \right)_{xx} = 0, \tag{4.23}$$

was first solved using the Inverse Scattering Transform in [68] and has applications in theoretical physics [57]. The Lax pair for (4.23) is given by (4.1) with

$$\alpha = -i\zeta, \qquad \beta = \zeta u, \qquad \gamma = -\zeta u^*, \tag{4.24}$$

$$A = -\frac{2i}{v}\zeta^2, \qquad B = \frac{2u}{v}\zeta^2 + i\left(\frac{q}{v}\right)_x \zeta, \qquad C = -\frac{2u^*}{v}\zeta^2 + i\left(\frac{u^*}{v}\right)_x \zeta, \tag{4.25}$$

where $v = \sqrt{1 + |u|^2}$. This equation is an example of a member of the Wadati-Konno-Ichikawa (WKI) hierarchy which possesses several nonlinear evolution equations of physical significance. The orbital stability of the soliton solution obtained in [68] was established in [2]. However, no stability results exist for the case of $|u|$ periodic. When $|u|$ is periodic, Theorem 4.2.1 applies with $\mathbb{R} \subset \mathcal{Q}_-$ and $i\mathbb{R} \subset \mathcal{Q}_+$. Hence, $\mathbb{R} \subset \Omega_i$, $i\mathbb{R} \subset \Omega_i \cup \Omega_r$, $\mathcal{S} = \mathbb{R} \cup (\Omega_i \cap i\mathbb{R}) \subset \sigma_L$, and $\Omega(\mathcal{S}) \subset i\mathbb{R}$. Since the squared-eigenfunction connection is unknown for this equation, it is unclear at this time how these results apply to stability.

The methods described here directly are applicable to many, but not all equations in the WKIS hierarchy. Equations in the WKIS hierarchy do not necessarily have $\alpha(i\mathbb{R}) \subset i\mathbb{R}$, so Theorem 4.2.1 does not always apply directly. Nonetheless, the techniques here can be generalized to cover equations of this form, including extensions of the WKIS hierarchy [79].

4.3.2 Examples for which Theorem 4.2.1 does not apply directly

Vector and matrix nonlinear Schrödinger equations

The *Manakov system* or two-component Vector NLS (VNLS) equation is given by

$$\begin{aligned} i\frac{\partial q_1}{\partial t} + \frac{\partial^2 q_1}{\partial x^2} + 2(|q_1|^2 + |q_2|^2)q_1 = 0, \\ i\frac{\partial q_2}{\partial t} + \frac{\partial^2 q_2}{\partial x^2} + 2(|q_1|^2 + |q_2|^2)q_2 = 0, \end{aligned} \tag{4.26}$$

where q_1 and q_2 are complex-valued functions. The system (4.26) was shown to be integrable in [62]. Its finite-genus solutions (including its elliptic solutions) were explicitly constructed in [29]. Its Lax pair is

$$\Phi_x = \begin{pmatrix} \alpha & \beta^\intercal \\ \gamma & \rho \end{pmatrix} v = X\Phi, \qquad \Phi_t = \begin{pmatrix} A & B^\intercal \\ C & D \end{pmatrix} v = T\Phi, \tag{4.27}$$

with

$$\alpha = -i\zeta, \qquad \beta = q, \qquad \gamma = -q^*, \qquad \rho = i\zeta I_2, \tag{4.28a}$$

$$A = -2i\zeta^2 + iq^\intercal q^*, \quad B = 2\zeta q + iq_x, \quad C = -2\zeta q^* + iq_x^*, \quad D = 2i\zeta^2 I_2 - iq^* q^\intercal, \tag{4.28b}$$

where $q = (q_1, q_2)^\intercal$ and where I_n is the $n \times n$ identity matrix. This example does not fit the results found in Chapter 3 or this chapter. However, I show that similar results are found for this system: $\Omega_i = \{\zeta \in \mathbb{R} : \Omega(\zeta) \in i\mathbb{R}\} \subset \sigma_L$ and $\Omega(\Omega_i) \subset \sigma_{\mathcal{L}} \cap i\mathbb{R}$, as has been established for other examples.

The compatibility conditions are

$$A_x = \beta^\intercal C - B^\intercal \gamma, \tag{4.29a}$$

$$B_x = 2\alpha B^\intercal - 2A\beta^\intercal, \tag{4.29b}$$

$$C_x = 2\rho C + 2\gamma A, \tag{4.29c}$$

$$D_x = \gamma B^\intercal - C\beta^\intercal. \tag{4.29d}$$

As before, Ω is found by separation of variables and satisfies

$$\begin{pmatrix} A-\Omega & B^\intercal \\ C & D-\Omega I_2 \end{pmatrix} \begin{pmatrix} \Phi_1 \\ \Phi_2 \end{pmatrix} = 0, \tag{4.30}$$

for nontrivial eigenvectors $\Phi = (\Phi_1, \Phi_2)^\intercal$. Note that Ω does not have the form (3.10). Instead, Ω satisfies

$$0 = \det \begin{pmatrix} A-\Omega & B^\intercal \\ C & D-\Omega I_2 \end{pmatrix} = \begin{cases} (A-\Omega)\det\left((D-\Omega I_2) - CB^\intercal/(A-\Omega)\right), & \Omega \notin \sigma(A), \\ \det(D-\Omega I_2)\left((A-\Omega) - B^\intercal(D-\Omega I_2)^{-1}C\right), & \Omega \notin \sigma(D), \end{cases} \tag{4.31}$$

where $\sigma(L)$ represents the spectrum of L. As usual, $\Omega(\zeta)$ defines a Riemann surface. In the genus-one case [29], it is represented by

$$f(\zeta,\Omega) = (\Omega + 2i\zeta^2)(\Omega - 2i\zeta^2)^2 + (2\lambda_2\zeta + \lambda_3)(\Omega - 2i\zeta^2) + \mu_0 = 0, \tag{4.32a}$$

$$\lambda_2 = -i(q^\intercal \bar{q}_x - q_x^\intercal \bar{q}), \tag{4.32b}$$

$$\lambda_3 = q_x^\intercal \bar{q}_x + (q^\intercal \bar{q})^2, \tag{4.32c}$$

$$\mu_0 = i\left|q_{1,x}q_2 - q_{2,x}q_1\right|^2. \tag{4.32d}$$

Since

$$\det(D-\Omega I_2) = (\Omega - 2i\zeta^2)(A+\Omega), \tag{4.33}$$

I use the second expression in (4.31) only when $\Omega = 2i\zeta^2$ or $A+\Omega = 0$. But $\Omega = 2i\zeta^2$ satisfies (4.32) only if q_2 and q_1 are proportional, and $\Omega = A$ satisfies (4.32) only if $|q_1|^2 + |q_2|^2$ is constant. In the first case, (4.26) reduces to two uncoupled Schrödinger equations, for which the spectrum is known. In the second case (4.26) reduces to two uncoupled linear NLS equations, for which the spectrum is known. Therefore, I assume that $D-\Omega I_2$ is invertible.

The eigenfunctions of (4.27) are

$$\Phi(x,t) = e^{\Omega t} y_1(x) \begin{pmatrix} a \\ -(D-\Omega I_2)^{-1}Ca \end{pmatrix}, \tag{4.34}$$

where $a \in \mathbb{C}$ is an arbitrary scalar. The scalar function $y_1(x)$ is determined by substitution in the x equation (4.27):

$$y_1' = \left(\alpha - \beta^\intercal(D-\Omega I_2)^{-1}C\right) y_1, \tag{4.35}$$

so that

$$y_1 = \hat{y}_1 \exp\left(\int \left(\alpha - \beta^\intercal (D - \Omega I_2)^{-1} C \right) \, \mathrm{d}x \right), \tag{4.36}$$

where $\hat{y}_1$ is a constant. Thus, $\zeta \in \sigma_L$ provided that

$$\left| \mathrm{Re} \int \left(\alpha - \beta^\intercal (D - \Omega I_2)^{-1} C \right) \, \mathrm{d}x \right| < \infty \tag{4.37}$$

for all $x \in \overline{\mathbb{R}}$. For periodic potentials and $\zeta \in \mathbb{R}$, this becomes

$$\mathrm{Re} \left\langle \beta^\intercal (D - \Omega I_2)^{-1} C \right\rangle = 0. \tag{4.38}$$

For $\zeta \in \mathbb{R}$,

$$A^\dagger = -A, \qquad C^\dagger = -B^\intercal, \qquad D^\dagger = -D, \qquad (\beta^\intercal)^\dagger = -\gamma, \tag{4.39}$$

where $F^\dagger = (F^*)^\intercal$ is the conjugate transpose of F. It follows that T defined by (4.27) is skew-adjoint and $\Omega \in i\mathbb{R}$. Further,

$$(D - \Omega I_2)^\dagger = -(D - \Omega I_2). \tag{4.40}$$

It follows that

$$\begin{aligned}
\mathrm{Re}\, \beta^\intercal (D - \Omega I_2)^{-1} C &= \frac{1}{2} \left[\beta^\intercal (D - \Omega I_2)^{-1} C + C^\dagger ((D - \Omega I_2)^{-1})^\dagger (\beta^\intercal)^\dagger \right] \\
&= \frac{1}{2} \left[\mathrm{Tr} \left(\beta^\intercal (D - \Omega I_2)^{-1} C - B^\intercal (D - \Omega I_2)^{-1} \gamma \right) \right] \\
&= \frac{1}{2} \left[\mathrm{Tr} \left((D - \Omega I_2)^{-1} C \beta^\intercal - (D - \Omega I_2)^{-1} \gamma B^\intercal \right) \right] \\
&= \frac{1}{2} \left[\mathrm{Tr} \left((D - \Omega I_2)^{-1} \left(C \beta^\intercal - \gamma B^\intercal \right) \right) \right] \\
&= \frac{1}{2} \left[\mathrm{Tr} \left((D - \Omega I_2)^{-1} (-D_x) \right) \right] \\
&= -\frac{1}{2} \frac{\partial_x \det(D - \Omega I_2)}{\det(D - \Omega I_2)} \\
&= -\frac{1}{2} \partial_x \log \det(D - \Omega I_2),
\end{aligned} \tag{4.41}$$

so that

$$\mathrm{Re} \left\langle \beta^\intercal (D - \Omega I_2)^{-1} C \right\rangle = 0, \tag{4.42}$$

and $\Omega(\zeta) \in i\mathbb{R}$ for $\zeta \in \mathbb{R}$. This can be verified using the method described in [23].

The work above can be generalized to the Matrix NLS (MNLS) equation,

$$iU_t + U_{xx} - 2\kappa UU^*U = 0, \tag{4.43}$$

where U is an $\ell_1 \times \ell_2$ matrix for $\ell_1, \ell_2 \in \mathbb{N}$, and $\kappa = -1$ and $\kappa = 1$ correspond to the focusing and defocusing cases respectively. The Lax pair for the MNLS equation is given by

$$\Phi_x = \begin{pmatrix} -i\zeta I_{\ell_1} & Q \\ R & i\zeta I_{\ell_2} \end{pmatrix} \Phi = X\Phi, \tag{4.44a}$$

$$\Phi_t = \begin{pmatrix} A & B \\ C & D \end{pmatrix} \Phi = T\Phi, \tag{4.44b}$$

$$A = -2i\zeta^2 I_{\ell_1} - iQR, \quad B = 2\zeta Q + iQ_x, \quad C = 2\zeta R - iR_x, \quad D = 2i\zeta^2 I_{\ell_2} + iRQ. \tag{4.44c}$$

Here, Q and R are $\ell_1 \times \ell_2$ and $\ell_2 \times \ell_1$ complex-valued matrices respectively. The x equation may be written as a spectral problem,

$$\zeta\Phi = \begin{pmatrix} iI_{\ell_1}\partial_x & -iQ \\ iR & -iI_{\ell_2}\partial_x \end{pmatrix} \Psi = L\Phi. \tag{4.45}$$

L is self adjoint if $R^* = Q$, hence $\sigma_L \subset \mathbb{R}$ if $R^* = Q$. The compatibility conditions are the same as (4.29d). The steps above apply in a straightforward but cumbersome manner to establish that $\mathcal{Q} = \{\zeta \in \mathbb{R} : \Omega(\zeta) \in i\mathbb{R}\} \subset \sigma_L$ and $\Omega(\mathcal{Q}) \subset \sigma_{\mathcal{L}} \cap i\mathbb{R}$. Details are omitted here because they are very similar to the above work.

4.4 Conclusion

In this chapter, the results about the Lax spectrum for members of the AKNS hierarchy in Chapter 3 have been extended to a more general class of integrable PDEs. In particular, the real line continues to play an important role for stability. Several examples have been given to demonstrate the applicability and the ease of applying Theorem 4.2.1. The final example indicates that the framework developed here is even more general than the hypotheses used in Theorem 4.2.1.

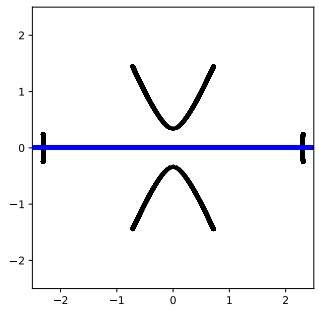

Figure 4.2: The Lax spectrum ($\mathrm{Re}(\zeta)$ *vs.* $\mathrm{Im}(\zeta)$) for the Manakov system (4.27) with initial condition $q_1(x,0) = 4\cos(x)$, $q_2(x,0) = 10\cos(x)$. The real line is colored blue. The Lax spectrum is computed numerically using the method described in [23]. The stability spectrum is not shown here because the squared-eigenfunction connection is unknown.

Chapter 5

CONCLUSION AND FUTURE WORK

The stability results in this dissertation are part of an ongoing research program of analyzing the stability of periodic solutions of integrable equations ([10, 11, 22, 24, 26, 27, 64]). The results in Chapter 2 are the first in the program to establish nonlinear stability of periodic solutions for which the underlying Lax pair is not self adjoint. The results in Chapters 3 and 4 help make sense of the similarities seen throughout this research program. This work sets up future projects on the examples listed in Chapters 3 and 4. Many other directions for future research also remain. These include:

1. **Extending the results in Chapter 4 to all integrable models.** In almost every example studied thus far, the real line maps to stable eigenvalues. This leads to the conjecture that periodic or quasiperiodic stationary solutions of integrable PDEs are stable only with respect to those perturbations that excite real elements of the Lax spectrum (except perhaps at $\{\zeta \in \mathbb{C} : \Omega(\zeta) = 0\}$). This conjecture is not straightforward to prove for many reasons. One major difficulty is that the squared-eigenfunction connection can be nontrivial to find, does not always have the same structure, and it is not always known to exist. An example where the situation is different from the results in this dissertation is the Benjamin-Ono (BO) equation,

$$u_t + \mathcal{H}u_{xx} + (u^2)_x = 0, \tag{5.1}$$

where

$$\mathcal{H}\left[f(\xi)\right](x) = \frac{1}{\pi}\int \frac{f(\xi)}{\xi - x}\,\mathrm{d}\xi. \tag{5.2}$$

Equating $(z, \tau) = (x - ct, t)$, so that z is in the traveling frame, (5.1) becomes

$$u_\tau - cu_z + \mathcal{H}u_{zz} + (u^2)_z = 0. \tag{5.3}$$

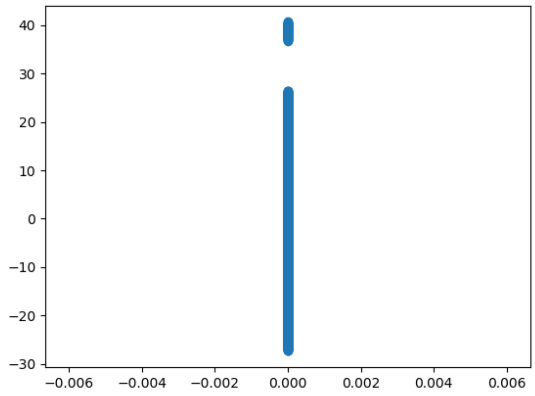

Figure 5.1: The complex Ω-plane for the Benjamin-Ono equation, found by using the method in [23] on (5.5).

Equation (5.3) possesses a 3-parameter family of stationary periodic solutions [12],

$$u(z;a,k,c) = -\frac{\frac{k^2}{\sqrt{c^2-4a-k^2}}}{\sqrt{\frac{c^2-4a}{c^2-4a-k^2}} - \cos(kz)} + \frac{1}{2}\left(\sqrt{c^2-4a}+c\right), \tag{5.4}$$

where $c<0$ and $k^2 < c^2-4a$. Finding Ω in the same way as in this dissertation gives two spectral problems for Ω,

$$\left(i\Omega + c^2/4\right) v^{\pm} = \left(-\partial_x^2 + V^{\pm}(x)\cdot\right) v^{\pm}, \tag{5.5}$$

where $v^{\pm}$ are eigenfunctions and $V^{\pm}$ are local PT-symmetric potentials with $V^{+} = (V^{-})^{*}$. As such, both potentials give the same spectrum and $i\Omega + c^2/4$ is a subset of the real-axis with bands and finite gaps (see Figure 5.1). Since the linear stability spectrum is symmetric with respect to the real and imaginary axes, it cannot be that $\lambda = 2\Omega(\zeta)$ since $\sigma_{\mathcal{L}}$ would not be symmetric with respect to the real axis.

2. **Using these same methods to study the stability of higher-genus solutions.** The periodic and quasiperiodic solutions studied in this work are usually genus-one solutions of the given equation. The genus-one solutions are a special case of the finite-genus solutions. The finite-genus solutions are a large family of periodic solutions with n-phases. The n-phase solutions are determined by a genus-n Riemann surface. The finite-genus solutions are

written in terms of the Riemann theta function [32]. When $n = 1$, the finite-genus solutions are genus-one solutions and the Riemann theta function solution is an elliptic function. To the best of my knowledge, nothing is known about the stability of higher-genus solutions of NLS. The stability of higher-genus solutions to KdV was examined in [64]. The stability of higher-genus solutions can be found using the techniques used in this dissertation along with those in [64].

3. **Using the analytic description of the stability spectrum to study the dynamics of perturbations of integrable systems.** The techniques used in this dissertation rely heavily on the integrability of the system. Many physical models are nonintegrable but are perturbations of integrable equations. An understanding of the spectrum of the unperturbed problem can be leveraged to understand the dynamics of the perturbed problem. Consider a nonlinear evolution PDE of the form

$$u_t = \mathcal{N}(u, u_x, \ldots, u_{Nx}; \epsilon), \tag{5.6}$$

where $\mathcal{N}$ is a nonlinear functional of u and N of its spatial derivatives and where ϵ is a small parameter such that when $\epsilon = 0$ (5.6) is an integrable PDE. To understand the dynamics of solutions of (5.6), consider a perturbation $u = u_0 + \epsilon u_1 + \mathcal{O}(\epsilon^2)$ where u_0 is a solution of the integrable equation. At order ϵ, this yields

$$(\partial_t - \mathcal{L}(u_0, u_{0,x}, \ldots, u_{0,Nx}))u_1 = \mathcal{F}(u_0), \tag{5.7}$$

where $\mathcal{F}(u_0)$ is a function depending only on u_0 and $\mathcal{L}(u_0, u_{0,x}, \ldots, u_{0,Nx})$ is the linearization of $\mathcal{N}$ with $\epsilon = 0$, about the solution u_0. Equation (5.7) is a non-homogeneous equation for u_1 whose left-hand side is defined by the same operator whose spectrum I have fully determined. Once u_1 is determined, a similar problem can be solved at each order of ϵ for the remaining u_n.

Appendix A

APPENDICES FOR ESTABLISHING STABILITY OF ELLIPTIC SOLUTIONS OF THE FNLS EQUATION

A.1 The fNLS equation Hierarchy

The results presented in this appendix are found in more detail in classic sources such as [7, 8]. The fNLS equation (3.14) is a Hamiltonian system with canonical variables Ψ and $i\Psi^*$, *i.e.*, it can be written as an evolution equation

$$\frac{\partial}{\partial t}\begin{pmatrix}\Psi\\ i\Psi^*\end{pmatrix} = JH'(\Psi, i\Psi^*) = J\begin{pmatrix}\delta H/\delta\Psi\\ \delta H/\delta(i\Psi^*)\end{pmatrix}, \tag{A.1}$$

for a functional H and where

$$J = \begin{pmatrix}0 & 1\\ -1 & 0\end{pmatrix}. \tag{A.2}$$

I define the variational gradient [8] of a function $F(u,v)$ by

$$F'(u,v) = \left(\frac{\delta F}{\delta u}\ ,\ \frac{\delta F}{\delta v}\right)^{\mathsf{T}} = \left(\sum_{j=0}^{N}(-1)^j\partial_x^j\frac{\partial F}{\partial u_{jx}}\ ,\ \sum_{j=0}^{N}(-1)^j\partial_x^j\frac{\partial F}{\partial v_{jx}}\right)^{\mathsf{T}}, \tag{A.3}$$

where $u_{jx} = \partial_x^j u$, and N is the highest-order x-derivative of u or v in F. The quantity $H(\Psi, i\Psi^*)$ is conserved under (3.14) and is the Hamiltonian of (3.14). The Hamiltonian is one of an infinite number of conserved quantities of the fNLS equation. I label these quantities $\{H_j\}_{j=0}^{\infty}$. The first five conserved quantites are needed here:

$$H_0 = 2\int |\Psi|^2\ \mathrm{d}x, \tag{A.4a}$$

$$H_1 = i\int \Psi_x\Psi^*\ \mathrm{d}x, \tag{A.4b}$$

$$H_2 = \frac{1}{2}\int \left(|\Psi_x|^2 - |\Psi|^4\right)\ \mathrm{d}x, \tag{A.4c}$$

$$H_3 = \frac{i}{4}\int \left(\Psi_x^*\Psi_{xx} - 3\,|\Psi|^2\,\Psi^*\Psi_x\right)\ \mathrm{d}x, \tag{A.4d}$$

$$H_4 = \frac{1}{8}\int \left(|\Psi_{xx}|^2 - \Psi^2\Psi_x^{*2} - 6\,|\Psi|^2\,|\Psi_x|^2 + |\Psi|^2\,\Psi^*\Psi_{xx} + 2\,|\Psi|^6\right)\ \mathrm{d}x. \tag{A.4e}$$

The above equations can be written in terms of Ψ and $i\Psi^*$ by using $|\Psi_{jx}|^2 = \Psi_{jx}\Psi^*_{jx}$. The above integrals are evaluated over one period $T(k)$, for periodic or quasi-periodic solutions. Each H_n defines an evolution equation with respect to a time variable τ_n by

$$\frac{\partial}{\partial \tau_n}\begin{pmatrix}\Psi\\ i\Psi^*\end{pmatrix} = JH_n'(\Psi, i\Psi^*) = J\begin{pmatrix}\delta H_n/\delta\Psi\\ \delta H_n/\delta(i\Psi^*)\end{pmatrix}. \tag{A.5}$$

When $n = 2$ and $\tau_2 = t$, $H_2 = H$ is the Hamiltonian for the fNLS equation: (A.5) is equivalent to (3.14). Letting $\Psi = (r + i\ell)/\sqrt{2}$ and $i\Psi^* = i(r - i\ell)/\sqrt{2}$, where r and ℓ are the real and imaginary parts of Ψ respectively, (A.5) becomes

$$\frac{\partial}{\partial \tau_n}\begin{pmatrix}r\\ \ell\end{pmatrix} = JH_n'(r, \ell) = J\begin{pmatrix}\delta H_n/\delta r\\ \delta H_n/\delta \ell\end{pmatrix}. \tag{A.6}$$

I use (A.5) and (A.6) interchangeably and refer to $H_n(r, \ell)$ and $H_n(\Psi, i\Psi^*)$ as H_n when the context is clear. The collection of equations (A.5) is the fNLS equation hierarchy [8, Section 1.2]. The first five members of the hierarchy are

$$\Psi_{\tau_0} = -2i\Psi, \tag{A.7a}$$

$$\Psi_{\tau_1} = \Psi_x, \tag{A.7b}$$

$$\Psi_{\tau_2} = i\,|\Psi|^2\,\Psi + \frac{i}{2}\Psi_{xx}, \tag{A.7c}$$

$$\Psi_{\tau_3} = -\frac{3}{2}\,|\Psi|^2\,\Psi_x - \frac{1}{4}\Psi_{xxx}, \tag{A.7d}$$

$$\Psi_{\tau_4} = -\frac{3}{4}i|\Psi|^4\Psi - \frac{3}{4}i\Psi^*\Psi_x^2 - \frac{i}{2}\Psi|\Psi_x|^2 - i|\Psi|^2\Psi_{xx} - \frac{i}{4}\Psi^2\Psi^*_{xx} - \frac{i}{8}\Psi_{xxxx}. \tag{A.7e}$$

Each equation obtained in this manner is integrable and shares the conserved quantities $\{H_j\}_{j=0}^{\infty}$.

Through the AKNS method, the n-th member of the fNLS equation hierarchy is obtained by enforcing the compatibility of a pair of ordinary differential equations, the n-th Lax Pair. The first equation of the pair is $\Phi_{\tau_1} = T_1\Phi$ and the second is $\Phi_{\tau_n} = T_n\Phi$, for the n-th member of the hierarchy. Here, T_1 and T_n are 2×2 matrices, the first five of which are defined in (A.8). The n-th member of the fNLS equation hierarchy is recovered by requiring $\partial_{\tau_n}\Phi_{\tau_1} = \partial_{\tau_1}\Phi_{\tau_n}$. For example, (3.14) is recovered from the compatibility condition of Φ_{τ_1} and Φ_{τ_2} with $t = \tau_2$. The collection of the Lax equations for the hierarchy is called the linear fNLS equation hierarchy. The first five

members of the linear fNLS equation hierarchy are

$$\Phi_{\tau_0} = T_0\Phi = \begin{pmatrix} -i & 0 \\ 0 & i \end{pmatrix}\Phi, \tag{A.8a}$$

$$\Phi_{\tau_1} = T_1\Phi = \begin{pmatrix} -i\zeta & \Psi \\ -\Psi^* & i\zeta \end{pmatrix}\Phi, \tag{A.8b}$$

$$\Phi_{\tau_2} = T_2\Phi = \begin{pmatrix} -i\zeta^2 + i\left|\Psi\right|^2/2 & \zeta\Psi + i\Psi_x/2 \\ -\zeta\Psi^* + i\Psi_x^*/2 & i\zeta^2 - i\left|\Psi\right|^2/2 \end{pmatrix}\Phi, \tag{A.8c}$$

$$\Phi_{\tau_3} = T_3\Phi = \begin{pmatrix} T_{3,1} & T_{3,2} \\ T_{3,3} & -T_{3,1} \end{pmatrix}\Phi, \tag{A.8d}$$

$$\Phi_{\tau_4} = T_4\Phi = \begin{pmatrix} T_{4,1} & T_{4,2} \\ T_{4,3} & -T_{4,1} \end{pmatrix}\Phi, \tag{A.8e}$$

where

$$T_{3,1} = -i\zeta^3 + i\zeta\left|\Psi\right|^2/2 + i\,\mathrm{Im}\left(\Psi\Psi_x^*\right)/2 \tag{A.9a}$$

$$T_{3,2} = \zeta^2\Psi + i\zeta\Psi_x/2 - \left|\Psi\right|^2\Psi/2 - \Psi_{xx}/4 \tag{A.9b}$$

$$T_{3,3} = -\zeta^2\Psi^* + i\zeta\Psi_x^*/2 + \left|\Psi\right|^2\Psi^*/2 + \Psi_{xx}^*/4 \tag{A.9c}$$

$$T_{4,1} = -i\zeta^4 + i\zeta^2\left|\Psi\right|^2/2 + i\zeta\,\mathrm{Im}(\Psi\Psi_x^*)/2 - 3i\left|\Psi\right|^4/8 + i\left|\Psi_x\right|^2/8 - i\,\mathrm{Re}(\Psi^*\Psi_{xx})/4, \tag{A.9d}$$

$$T_{4,2} = \zeta^3\Psi + i\zeta^2\Psi_x/2 - \zeta\left(\left|\Psi\right|^2\Psi/2 + \Psi_{xx}/4\right) - 3i\left|\Psi\right|\Psi_x/4 - i\Psi_{xxx}/8, \tag{A.9e}$$

$$T_{4,3} = -\zeta^3\Psi^* + i\zeta^2\Psi_x^*/2 + \zeta\left(\left|\Psi\right|^2\Psi^*/2 + \Psi_{xx}^*/4\right) - 3i\left|\Psi\right|\Psi_x^*/4 - i\Psi_{xxx}^*/8, \tag{A.9f}$$

and ζ is referred to as the Lax parameter.

Each of the H_n are mutually in involution under the canonical Poisson bracket (A.2) [8]. As a result, the flows of all members of the fNLS equation hierarchy commute and any linear combination of the conserved quantities gives rise to a dynamical equation whose flow commutes with all equations of the hierarchy. A family of evolution equations in t_n is defined by

$$\frac{\partial}{\partial_{t_n}}\begin{pmatrix} r \\ \ell \end{pmatrix} = J\hat{H}_n'(r,\ell) = J\left(H_n' + \sum_{j=0}^{n-1} c_{n,j}H_j'\right), \quad n \geq 0, \tag{A.10}$$

where the $c_{n,j}$ are constants. I loosely call (A.10) the "n-th fNLS equation." Similarly I define the

n-th linear fNLS equation to be

$$\Phi_{t_n} = \hat{T}_n \Phi = \left(T_n + \sum_{j=0}^{n-1} c_{n,j} T_j \right) \Phi. \tag{A.11}$$

The n-th fNLS equation is obtained by enforcing the compatibility of Φ_{τ_1} with Φ_{t_n}.

The second fNLS equation (2.2) is obtained from (A.7a) and (A.7c) and has Hamiltonian $\hat{H} = \hat{H}_2 = H_2 - \omega H_0/2$. With $\psi(x,t) = (r(x,t) + i\ell(x,t))/\sqrt{2}$, (2.2) is

$$\partial_t \begin{pmatrix} r \\ \ell \end{pmatrix} = \begin{pmatrix} -\omega\ell - \ell(r^2+\ell^2)/2 - \ell_{xx}/2 \\ \omega r + r(\ell^2+r^2)/2 + r_{xx}/2 \end{pmatrix} = J\hat{H}'(r,\ell). \tag{A.12}$$

The associated linear fNLS equation is $\hat{T}_2 = T_2 - \omega T_0/2$. Defining $\tau_1 = x$ and $t_2 = t$, (A.12) (or equivalently (2.2)) is obtained via the compatibility condition of the two matrix equations

$$\Phi_x = \Phi_{\tau_1} = T_1 \Phi, \tag{A.13a}$$

$$\Phi_t = \Phi_{\tau_2} - \frac{\omega}{2}\Phi_{\tau_0} = \left(T_2 - \frac{\omega}{2} T_0 \right) \Phi. \tag{A.13b}$$

A.2 Proofs of Lemmas in Chapter 2

Next, I present proofs for lemmas used in Section 2.2.4.

Proof of Lemma 2.2.12. Formulae for Weierstrass Elliptic functions used here and in what follows are in [1, Chapter 23] [13, 73]. I use the notation $\eta_k = \zeta_w(\omega_k)$, $k = 1, 2, 3$.

For the dn solutions, $b = 1$ and the four roots of $\Omega(\zeta)$ are

$$\zeta_1 = \frac{i}{2}(1 - \sqrt{1-k^2}), \quad \zeta_2 = \frac{i}{2}(1 + \sqrt{1-k^2}), \quad \zeta_3 = -\zeta_2, \quad \zeta_4 = -\zeta_1. \tag{A.14}$$

Since $c = \theta = 0$,

$$M(\zeta_j) = -2iI(\zeta_j) \mod 2\pi. \tag{A.15}$$

The quantities $\alpha(\zeta_j)$, $\wp'(\alpha(\zeta_j))$, and $\zeta_w(\alpha(\zeta_j))$ are needed for the computation of $I(\zeta_j)$. Using (2.9a) and (2.39),

$$\alpha(\zeta_2) = \alpha(\zeta_3) = \wp^{-1}\left(e_1 + \sqrt{(e_1-e_3)(e_1-e_2)} \right) = \sigma_1 \frac{\omega_1}{2} + 2n\omega_1 + 2m\omega_3, \tag{A.16a}$$

$$\alpha(\zeta_1) = \alpha(\zeta_4) = \wp^{-1}\left(e_3 + \frac{(e_3-e_1)(e_3-e_2)}{\wp(\omega_1/2) - e_3} \right) = \sigma_1 \left(\frac{\omega_1}{2} - \omega_3 \right) + 2n\omega_1 + 2m\omega_3, \tag{A.16b}$$

where $n, m \in \mathbb{Z}$ and σ_1 is either ± 1. From [13, equation 1033.04] and the addition formula for $\wp'(z)$,

$$\begin{aligned} \wp'(\omega_1/2) &= -2\left((e_1-e_3)\sqrt{e_1-e_2}+(e_1-e_2)\sqrt{e_1-e_3}\right) \\ &= -2(1-k^2+\sqrt{1-k^2}), \end{aligned} \tag{A.17a}$$

$$\begin{aligned} \wp'(\omega_1/2-\omega_3) &= 2\left((e_1-e_3)\sqrt{e_1-e_2}-(e_1-e_2)\sqrt{e_1-e_3}\right) \\ &= -2(1-k^2-\sqrt{1-k^2}). \end{aligned} \tag{A.17b}$$

Using the addition formula for $\zeta_w(z)$,

$$\zeta_w(\omega_1/2) = \zeta_w(-\omega_1/2+\omega_1) = -\zeta_w(\omega_1/2)+\eta_1 - \frac{1}{2}\frac{\wp'(\omega_1/2)}{\wp(\omega_1/2)-e_1}, \tag{A.18}$$

so that

$$\zeta_w(\omega_1/2) = \frac{1}{2}\left(\eta_1 - \frac{1}{2}\frac{\wp'(\omega_1/2)}{\wp(\omega_1/2)-e_1}\right) = \frac{1}{2}\left(\eta_1+1+\sqrt{1-k^2}\right), \tag{A.19a}$$

$$\zeta_w(\omega_1/2-\omega_3) = \zeta_w(\omega_1/2)-\eta_3+\frac{1}{2}\frac{\wp'(\omega_1/2)}{\wp(\omega_1/2)-e_3} = \frac{1}{2}\left(\eta_1+1-\sqrt{1-k^2}\right). \tag{A.19b}$$

Using the parity and periodicity of $\wp'(z)$, and the quasi-periodicity of $\zeta_w(z)$ I arrive at

$$\wp'(\alpha(\zeta_2)) = \sigma_1\wp'(\omega_1/2), \tag{A.20a}$$

$$\wp'(\alpha(\zeta_1)) = \sigma_1\wp'(\omega_1/2-\omega_3), \tag{A.20b}$$

$$\zeta_w(\alpha(\zeta_2)) = \sigma_1\zeta_w(\omega_1/2)+2n\eta_1+2m\eta_3, \tag{A.20c}$$

$$\zeta_w(\alpha(\zeta_1)) = \sigma_1\zeta_w(\omega_1/2-\omega_3)+2n\eta_1+2m\eta_3. \tag{A.20d}$$

Substituting the above quantities into (2.38) and using $\omega_3\eta_1 - \omega_1\eta_3 = i\pi/2$ results in $I(\zeta_j) = 0 \mod 2\pi$ for $j = 1, 2, 3, 4$. □

Proof of Lemma 2.2.13. Let $\zeta = i\xi$ with $\xi \in \mathbb{R}$. Then

$$\Omega^2(\zeta) = -\xi^4 - \frac{1}{2}(k^2-2)\xi^2 - \frac{k^4}{16} \in \mathbb{R}, \tag{A.21}$$

so $\Omega(\zeta)$ is either real or imaginary. Then $\Omega(\zeta) \in i\mathbb{R}$ if and only if

$$\xi^2 \geq \frac{1}{4}(2-k^2)+\frac{1}{2}\sqrt{1-k^2} \quad \text{or} \quad \xi^2 \leq \frac{1}{4}(2-k^2)-\frac{1}{2}\sqrt{1-k^2}, \tag{A.22}$$

which is equivalent to

$$|\xi| \leq \mathrm{Im}(\zeta_1) \quad \text{or} \quad |\xi| \geq \mathrm{Im}(\zeta_2). \tag{A.23}$$

□

Proof of Lemma 2.2.15. First, this holds for $\zeta = 0$, since

$$\alpha(0) = \wp^{-1}(e_3) = \omega_3 + 2n\omega_1 + 2m\omega_2, \tag{A.24}$$

where $m, n \in \mathbb{Z}$, so that

$$I(0) = 2\Gamma(\omega_1(\eta_3 + 2n\eta_1 + 2m\eta_3) - \eta_1(\omega_3 + 2n\eta_1 + 2m\eta_3) = -\Gamma p\pi i, \tag{A.25}$$

for $p \in \mathbb{Z}$ [1, Chapter 23]. Then

$$M(\zeta) = -2i(-\Gamma p\pi i) + \pi = \pi \mod 2\pi. \tag{A.26}$$

Since the curves for $\mathrm{Re}(I) =$ constant, given by (2.46), and for $\mathrm{Im}(I) =$ constant are orthogonal, the vector field for $\mathrm{Im}(I) =$ constant is vertical on the imaginary axis as $\Omega(\zeta) \in i\mathbb{R}$ there (2.46). Since $M(\zeta) = \pi \mod 2\pi$ at $\zeta = 0$ and is constant on the imaginary axis, it follows that $M(\zeta) = \pi \mod 2\pi$ on the imaginary axis. □

Proof of Lemma 2.2.16. For the cn solutions, $b = k^2$ and the four roots of $\Omega(\zeta)$ are

$$\zeta_1 = \frac{1}{2}\left(\sqrt{1-k^2} + ik\right), \quad \zeta_2 = \frac{1}{2}\left(-\sqrt{1-k^2} + ik\right), \quad \zeta_3 = -\zeta_1, \quad \zeta_4 = -\zeta_2. \tag{A.27}$$

Here, $c = 0$ and $\theta(T(k)) = \pi$ give

$$M(\zeta_j) = -2iI(\zeta_j) + \pi \mod 2\pi. \tag{A.28}$$

The quantities $\alpha(\zeta_j)$, $\wp'(\alpha(\zeta_j))$, and $\zeta_w(\alpha(\zeta_j))$ are needed. Using (2.9a) and (2.39),

$$\alpha(\zeta_1) = \alpha(\zeta_3) = \wp^{-1}\left(e_2 - i\sqrt{(e_1-e_2)(e_2-e_3)}\right) = \sigma_1\frac{\omega_2}{2} + 2n\omega_1 + 2m\omega_3, \tag{A.29a}$$

$$\begin{aligned}\alpha(\zeta_2) = \alpha(\zeta_3) &= \wp^{-1}\left(e_3 + \frac{(e_3-e_1)(e_3-e_2)}{e_2 - e_3 - i\sqrt{(e_1-e_2)(e_2-e_3)}}\right) \\ &= \sigma_1\left(\frac{\omega_2}{2} - \omega_3\right) + 2n\omega_1 + 2m\omega_3.\end{aligned} \tag{A.29b}$$

From [13, equation 1033.04] and the addition formula for $\wp'(z)$,

$$\begin{aligned}\wp'(\omega_2/2) &= -\wp'(\omega_1/2 + \omega_3/2) \\ &= -2\left((e_1-e_2)\sqrt{e_2-e_3} + i(e_2-e_3)\sqrt{e_1-e_2}\right) \\ &= -2k(1-k^2+ik\sqrt{1-k^2}),\end{aligned} \tag{A.30a}$$

$$\wp'(\omega_2/2 - \omega_3) = -2k(1-k^2-ik\sqrt{1-k^2}). \tag{A.30b}$$

$\zeta_w(\omega_2/2)$ is found in a similar manner to $\zeta_w(\omega_1/2)$ (Lemma 2.2.12) to be

$$\zeta_w(\omega_2/2) = \frac{1}{2}\left(\zeta_w(\omega_2) - k + i\sqrt{1-k^2}\right), \tag{A.31}$$

from which

$$\zeta_w(\omega_2/2 - \omega_3) = \frac{1}{2}\left(\zeta_w(\omega_2) - k - i\sqrt{1-k^2}\right) - \eta_3. \tag{A.32}$$

Using the parity and periodicity of $\wp'(z)$, and the quasi-periodicity of $\zeta_w(z)$ I arrive at

$$\wp'(\alpha(\zeta_1)) = \sigma_1\wp'(\omega_2/2), \tag{A.33a}$$

$$\wp'(\alpha(\zeta_2)) = \sigma_1\wp'(\omega_2/2 - \omega_3), \tag{A.33b}$$

$$\zeta_w(\alpha(\zeta_1)) = \sigma_1\zeta_w(\omega_2/2) + 2n\eta_1 + 2m\eta_3, \tag{A.33c}$$

$$\zeta_w(\alpha(\zeta_2)) = \sigma_1\zeta_w(\omega_2/2 - \omega_3) + 2n\eta_1 + 2m\eta_3, \tag{A.33d}$$

where σ_1 is either ± 1. Substituting the above quantities into (2.38) results in

$$I(\zeta_1) = I(\zeta_3) = \sigma_1\frac{i\pi}{2} + 2\pi m, \tag{A.34a}$$

$$I(\zeta_2) = I(\zeta_4) = 3\sigma_1\frac{i\pi}{2} + 2\pi m. \tag{A.34b}$$

Therefore

$$M(\zeta_1) = M(\zeta_3) = \sigma_1\pi + 4\pi m + \pi = 0 \mod 2\pi, \tag{A.35a}$$

$$M(\zeta_2) = M(\zeta_4) = 3\sigma_1\pi + 4\pi m + \pi = 0 \mod 2\pi. \tag{A.35b}$$

□

Proof of Lemma 2.2.17. Without loss of generality, let $\zeta = \zeta_r + i\zeta_i$ with $\zeta_r < 0$. The computation is the same for $\zeta_r > 0$ by symmetry of the Lax spectrum. Consider the curve in the left half plane defined by $\mathrm{Im}(\Omega^2) = 0,\ \mathrm{Re}(\Omega^2 < 0)$ (2.57). For $\zeta_i \neq 0$, this curve is defined by

$$\zeta_i^2 = Q(\zeta_r) = \zeta_r^2 - \frac{1}{4}(1-2k^2), \qquad \text{for} \qquad \zeta_r \in [-\sqrt{1-k^2}/2, 0). \tag{A.36}$$

The above parameterization is valid only when $k \geq 1/\sqrt{2}$. For $k < 1/\sqrt{2}$, ζ_r is restricted to a smaller range so that $\zeta_i \in \mathbb{R}$.

Let $G(\zeta_r) = I(\zeta_r + i\zeta_i(\zeta_r))$ where $\zeta_i(\zeta_r)$ is defined with either sign of the square root in (A.36). If I can show that $\mathrm{Re}(G(\zeta_r)) > 0$ for $\zeta_r \in (-\sqrt{1-k^2}/2, 0)$, then I have shown that $\mathrm{Re}(I(\zeta)) \neq 0$ when $\Omega(\zeta) \in i\mathbb{R} \setminus \{0\}$. A quick computation gives

$$4\Omega_i \sqrt{Q(\zeta_r)} \frac{\mathrm{d}\,\mathrm{Re}(G)}{\mathrm{d}\zeta_r} = \zeta_r P_2(\zeta_r), \tag{A.37}$$

where

$$P_2(\zeta_r) := -16K(k)\zeta_r^2 + 4(E(k) - k^2K(k)), \tag{A.38}$$

and

$$\Omega_i := \frac{1}{2}\sqrt{(4\zeta_r^2 + k^2 - 1)(k^2 + 4\zeta_r^2)}, \tag{A.39}$$

the imaginary part of Ω. Take $\Omega_i\sqrt{Q(\zeta_r)} > 0$ without loss of generality ($\Omega_i\sqrt{Q(\zeta_r)} < 0$ corresponds to a different sign for ζ_i or Ω_i or both and is a nontrivial but straightforward extension of what follows). $P_2(\zeta_r)$ and $\mathrm{d}\,\mathrm{Re}(G)/\mathrm{d}\zeta_r$ have opposite signs since $\zeta_r < 0$. Since $\mathrm{Re}(G(-\sqrt{1-k^2}/2)) = 0$ and $P_2(-\sqrt{1-k^2}/2) < 0$, it suffices to show that $\mathrm{d}\,\mathrm{Re}(G)/\mathrm{d}\zeta_r > 0$. Indeed, if this is true, then $\mathrm{Re}(G) > 0$ when $\Omega(\zeta) \in i\mathbb{R} \setminus \{0\}$. There are three cases to consider.

Case 1: $P_2(\zeta_r)$ has no negative roots or one root at $\zeta_r = 0$.

If $P_2(\zeta_r)$ is always negative, then this case is done since $\mathrm{Re}(G)$ is increasing on $(-\sqrt{1-k^2}/2, 0)$. This is the case if $E(k) - k^2K(k) \leq 0$, which is true for $k \geq \kappa$ where $\kappa \approx 0.799879$.

Case 2: $P_2(\zeta_r)$ has one negative root and $Q(\zeta_r)$ has no negative roots or a double negative root.

Let $\hat{\zeta}$ be such that $P_2(\hat{\zeta}) = 0$. Then $\mathrm{Re}(G)$ is increasing on $(-\sqrt{1-k^2}/2, \hat{\zeta})$ and decreasing on $(\hat{\zeta}, 0)$. This can only occur for $1/\sqrt{2} < k < \kappa$. Since

$$\frac{\mathrm{d}\,\mathrm{Re}(I)}{\mathrm{d}\zeta_i} = -\,\mathrm{Im}\left(\frac{\mathrm{d}I}{\mathrm{d}\zeta}\right), \tag{A.40}$$

$\mathrm{d}\,\mathrm{Re}(I)/\mathrm{d}\zeta_i > 0$ for $\zeta = i\zeta_i$. Since $\mathrm{Re}(G(\zeta_r))$ must be minimized in the limit $\zeta_r \to 0^-$, it follows from continuity and the fact that $\mathrm{Re}(G) > 0$ on the imaginary axis that $\mathrm{Re}(G) > 0$ for $\zeta_r \in (-\sqrt{1-k^2}/2, 0)$.

Case 3: $P_2(\zeta_r)$ and $Q(\zeta_r)$ both have one negative root.

Let $\hat{\zeta}$ be as above and let $\hat{\xi}$ be the negative root of Q. Then $\mathrm{Re}(G)$ is increasing on $(-\sqrt{1-k^2}/2, \hat{\zeta})$ and decreasing on $(\hat{\zeta}, \hat{\xi})$ at which $\mathrm{Re}(G(\hat{\xi})) = 0$. Since the parameterization is not valid on $(\hat{\xi}, 0)$, $\mathrm{Re}(G) > 0$ for $\zeta_r \in (-\sqrt{1-k^2}/2, \hat{\xi})$ which are all allowed ζ values for which $\zeta \notin \mathbb{R} \cup i\mathbb{R}$.

It follows that $\mathrm{Re}(G) > 0$ when $\Omega(\zeta) \in i\mathbb{R} \setminus \{0\}$. □

Proof of Lemma 2.2.20. I establish that $M_j = 0 \mod 2\pi$ on the boundary of the parameter space by establishing this fact for the Stokes waves ($k = 0$) and using Lemmas 2.2.12 and 2.2.16.

Setting $\lambda = 0$ in (2.23) shows that $\mu = -2n$. Since $T(k) = \pi$ for Stokes waves, $T(k)\mu = 0 \mod 2\pi$ whenever $\Omega = 0$. Next, I compute directly that $\partial_b M_j = 0$ for the nontrivial-phase solutions. In what follows I use that

$$\zeta_j = \frac{1}{2}\left(\sigma_1\sqrt{1-b} + i\sigma_2\left(\sqrt{b} - \sigma_1\sqrt{b-k^2}\right)\right), \tag{A.41}$$

so that $\zeta_1,\ \zeta_2,\ \zeta_3$, and ζ_4 correspond to $(\sigma_1, \sigma_2) = (1,1),\ (-1,1),\ (-1,-1),\ (1,-1)$ respectively. Defining

$$e_{p,j} = \wp(\alpha_j) - e_0 = -2\zeta_j^2 + \omega, \tag{A.42}$$

where e_0 is defined in (2.52), gives

$$\frac{\partial \zeta_j}{\partial b} = \frac{e_{p,j}}{4c}, \tag{A.43a}$$

$$\frac{\partial \alpha_0}{\partial b} = \frac{1}{\wp'(\alpha_0)} = -\frac{i}{2c}, \tag{A.43b}$$

$$\frac{\partial \alpha_j}{\partial b} = -\frac{c + 2\zeta_j e_{p,j}}{2c\wp'(\alpha_j)} = \frac{4\zeta_j^3 - 2\zeta_j\omega - c}{2c\wp'(\alpha_j)}. \tag{A.43c}$$

From the definition of Γ and (2.40),

$$\frac{(4\zeta_j^3 - 2\zeta_j\omega - c)\Gamma}{\wp'(\alpha_j)} = \frac{2i(4\zeta_j^3 - 2\zeta_j\omega - c)^2}{\wp'(\alpha_j)^2} = -\frac{i}{2}. \tag{A.44}$$

Using the above calculations, the expression (2.41), and (2.49) with $\theta(T(k))$ defined in (2.51), I compute

$$\begin{aligned}\frac{\partial}{\partial b}M_j &= -2i\left(\frac{\partial I(\zeta_j)}{\partial b} + \frac{\partial}{\partial b}(\alpha_0\eta_1 - \omega_1\zeta_w(\alpha_0))\right)\\ &= -2i\left(-\frac{i}{2c}e_{p,j}\omega_1 - \frac{(4\zeta_j^3 - 2\zeta_j\omega - c)\Gamma}{c\wp'(\alpha_j)}(\eta_1 + \omega_1(e_{p,j} + e_0)) - \frac{i}{2c}(\eta_1 + \omega_1 e_0)\right) = 0\end{aligned} \tag{A.45}$$

by direct computation. Since $M_j = 0 \mod 2\pi$ along the boundaries of the parameter region (Figure 2.1) and $\partial_b M_j = 0$ on the interior of the parameter space, it follows that M_j is constant (0 mod 2π) in the whole parameter space.

□

A.3 Necessity of stability condition (2.73), proof of Lemma 2.2.8, and proof of Theorem 2.2.24

In this appendix I present progress made towards showing that (2.73) is not only a sufficient but also a necessary condition for spectral stability. A theorem is introduced which shows that $|\mathrm{Re}(\lambda)| > 0$ on the complex bands of the spectrum. For part of the parameter space, the proof of this theorem is complete. For a different part of parameter space, the proof relies upon a numerical check over a bounded region of parameter space (see Figure A.2a). The numerical check consists of finding a root of a degree-six polynomial and evaluating Weierstrass elliptic functions at that root. Numerical checks of this kind are not uncommon (see *e.g.*, the non-degeneracy condition for the fNLS equation in [36]). Similar arguments are used in Lemma A.3.1 to prove Theorem 2.2.24 and Lemma 2.2.8.

Lemma A.3.1. *Let $c \neq 0$ and $\zeta \in (\mathbb{C}^- \cap \sigma_L) \setminus (\mathbb{R} \cup i\mathbb{R} \cup \{\zeta_2, \zeta_3\})$ where $\mathbb{C}^-$ is the left half plane. Then $\Omega(\zeta) \notin i\mathbb{R}$.*

Proof. Let $c \neq 0$ and $\zeta = \zeta_r + i\zeta_i$ with $\zeta_r < 0$. Consider the curve in the left half plane defined by $\mathrm{Im}(\Omega^2) = 0$. For $\zeta_i \neq 0$, this curve is defined by

$$\zeta_i^2 = \zeta_r^2 - \frac{\omega}{2} - \frac{c}{4\zeta_r}. \tag{A.46}$$

The condition $\mathrm{Re}(\Omega^2) \leq 0$ implies $|\zeta_r| \leq \sqrt{1-b}/2$ with equality attained at the roots of Ω^2. Let

$$Q(\zeta_r) := 4\zeta_r^3 - 2\omega\zeta_r - c. \tag{A.47}$$

Then $\zeta_i \in \mathbb{R}$ only if $Q(\zeta_r) \leq 0$ and $Q(\zeta_r)$ has two roots with negative real part. If both roots are complex or there is a double root, then the parameterization (A.46) is valid for all $-\sqrt{1-b}/2 \leq \zeta_r < 0$. This is the case if the discriminant of Q is nonpositive, which is true when

$$b \geq \begin{cases} k^2, & k > 1/\sqrt{2}, \\ F(k), & k \leq 1/\sqrt{2}, \end{cases} \tag{A.48}$$

with

$$F(k) := \frac{(1+k^2)^3}{9(1-k^2+k^4)}. \tag{A.49}$$

It is interesting to note that the condition $b < F(k)$ is the same condition as [27, equation (85)] which determines when the imaginary Ω axis is quadruple covered by the map $\Omega(\zeta)$.

Define $G(\zeta_r) = I(\zeta_r + i\zeta_i(\zeta_r))$, where $\zeta_i(\zeta_r)$ is defined with either sign of the square root in (A.46). The goal is to show that $\operatorname{Re} G(\zeta_r) = 0$ only when $\zeta_i = 0$ or $\zeta_r = -\sqrt{1-b}/2$, which corresponds to one of the roots of Ω^2. Along the solutions of (A.46),

$$\Omega_i \zeta_r \sqrt{Q(\zeta_r)} \frac{\mathrm{d} \operatorname{Re} G}{\mathrm{d}\zeta_r} = P_6(\zeta_r), \tag{A.50}$$

where

$$\Omega_i = \pm \frac{1}{4\,|\zeta_r|} \sqrt{(4\zeta_r^2 + b - 1)(b + 4\zeta_r^2)(b - k^2 + 4\zeta_r^2)}, \tag{A.51}$$

the imaginary part of Ω (and $\Omega = \Omega_i$ because of the parameterization). The polynomial P_6 is given by

$$\begin{aligned} P_6(x) = -64K(k)x^6 + 16(E(k) + (k^2 - 2b)K(k))x^4 + 8cK(k)x^3 \\ + 2c(E(k) + (b-1)K(k))x - c^2K(k). \end{aligned} \tag{A.52}$$

I let $\Omega_i \sqrt{Q(\zeta_r)} > 0$, without loss of generality. ($\Omega_i \sqrt{Q(\zeta_r)} < 0$ corresponds to a different sign for ζ_i or Ω_i or both and is a nontrivial but straightforward extension of what follows). Therefore, $P_6(\zeta_r)$ has the opposite sign of $\mathrm{d}\operatorname{Re}(G)/\mathrm{d}\zeta_r$ and $\operatorname{Re}(G(\zeta_r)) \to +\infty$ as $\zeta_r \to 0^-$ since $\Omega_i \zeta_r \sqrt{Q(\zeta_r)} \to 0^-$ and $P_6 \to -c^2K(k) < 0$. Since $\zeta_r = -\sqrt{1-b}/2$ corresponds to a root of Ω and the roots of Ω are in the Lax spectrum, $\operatorname{Re} G(-\sqrt{1-b}/2) = 0$. I wish to show that $\mathrm{d}\operatorname{Re}(G)/\mathrm{d}\zeta_r \geq 0$, which guarantees that $\operatorname{Re}(G(\zeta_r)) = 0$ only when $\Omega(\zeta_r) = 0$.

Consider the polynomial

$$\tilde{P}_6(x) = P_6(-x) = a_6x^6 + a_4x^4 + a_3x^3 + a_1x + a_0. \tag{A.53}$$

It is clear that $a_6 < 0, a_3 < 0, a_0 < 0$ and a_4 changes sign depending on b and k. Then

$$a_1 = -2c\,(E(k) + (b-1)K(k)) \leq -2c\,\big(E(k) + (k^2-1)K(k)\big) = -2c\frac{\mathrm{d}K(k)}{\mathrm{d}k} \leq 0. \tag{A.54}$$

By Descartes' sign rule, an upper bound on the number of negative roots of P_6 is either 2 or 0, depending on the sign of a_4. Since $P_6(\zeta_r) \to -\infty$ as $\zeta_r \to -\infty$ and $P_6(0) < 0$, $P_6(\zeta_r)$ has an even number of negative roots, either 2 or 0.

I consider four cases.

Case 1: $P_6(\zeta_r)$ has no negative roots or a double negative root.

If $P_6(\zeta_r)$ has no negative roots or a double negative root, then $P_6(\zeta_r) \leq 0$ and $\mathrm{Re}(G(\zeta_r)) > 0$ so $\mathrm{Re}(G(\zeta_r))$ is bounded away from 0 (see Figure A.1a).

Case 2: $P_6(\zeta_r)$ has two distinct negative roots, $Q(\zeta_r)$ has no negative roots.

Let ξ_1 and ξ_2 be the two roots of P_6 with $\xi_1 < \xi_2 < 0$ (see Figure A.1b). Then $\mathrm{Re}(G)$ is increasing on $(-\sqrt{1-b}/2, \xi_1)$, decreasing on (ξ_1, ξ_2), and increasing again on $(\xi_2, 0)$. If $\mathrm{Re}(G(\xi_2)) > 0$, then $\mathrm{Re}(G)$ is bounded away from 0 and this case is done. I do not know how to verify this condition analytically, so I check it numerically. It is found to always hold.

Case 3: $P_6(\zeta_r)$ has two distinct negative roots, $Q(\zeta_r)$ has a double negative root.

Let ξ_1 and ξ_2 be as above and let ζ_1 be the negative double root of Q (see Figure A.1c). It must be the case that $\zeta_1 > \xi_1$ since $\mathrm{Re}(G)$ is initially increasing and I know that $\mathrm{Re}(G) \to 0$ as $\zeta \to \zeta_1$. However, since ζ_1 is a double root of Q, it is also a root of $\mathrm{Re}(G)$ so it must be that $\zeta_1 = \xi_2$. This means that $\mathrm{Re}(G)$ is tangent to 0 at $\zeta = \zeta_1$. This corresponds to $\zeta \in \mathbb{R}$.

Case 4: $P_6(\zeta_r)$ and $Q(\zeta_r)$ have two distinct negative roots

Let ξ_1 and ξ_2 be as before and let ζ_1 and ζ_2 be the two negative roots of Q with $\zeta_1 < \zeta_2$. As before, it must be that ξ_1 is smaller than each of ξ_2, ζ_1, and ζ_2. The next largest root may be either ξ_2 or ζ_1.

- An illustration of this case is found in Figure A.1d. If ξ_2 is the next largest root, then there is a $\hat{\zeta} \in (\xi_1, \xi_2)$ such that $\mathrm{Re}(G(\hat{\zeta})) = 0$. For ζ_r greater than ξ_2, $\mathrm{Re}(G)$ increases to 0 at $\zeta_r = \zeta_1$. For $\zeta \in (\zeta_1, \zeta_2)$, nothing can be said about $\mathrm{Re}(G)$ since the parameterization is not valid. For $\zeta \in (\zeta_1, 0)$, $\mathrm{Re}(G) > 0$ is increasing since $P_6(\zeta) < 0$ in this range. Thus if the ordering is $\xi_1 < \xi_2 < \zeta_1 < \zeta_2$, there is a $\hat{\zeta} \in \sigma_L$ such that $\mathrm{Re}(G(\hat{\zeta})) = 0$ and $\Omega(\hat{\zeta}) \in i\mathbb{R}$.
- An illustration of this case is found in Figure A.1e. If ζ_1 is the next largest root, there are no zeros on $(-\sqrt{1-b}/2, \zeta_1)$. If there were, there would be another zero of P_6 in (ξ_1, ζ_1) (so that $\mathrm{Re}(G)$ can increase back to zero) but there is not, by assumption. For $\zeta_r \in (\zeta_1, \zeta_2)$, the parameterization is not valid. $\mathrm{Re}(G(\zeta_2)) = 0$ and is increasing if $\xi_2 < \zeta_2$ and is decreasing if $\xi_2 > \zeta_2$. If $\mathrm{Re}(G)$ is increasing at ζ_2, this case is done. If $\mathrm{Re}(G)$ is decreasing at ζ_2, then since $\mathrm{Re}(G) \to \infty$ as $\zeta_r \to 0$, there must be another zero of $\mathrm{Re}(G)$ in $(\zeta_2, 0)$.

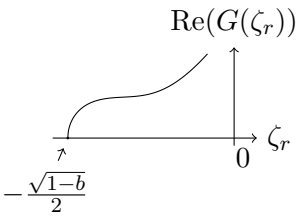

(a) Illustration for Case 1

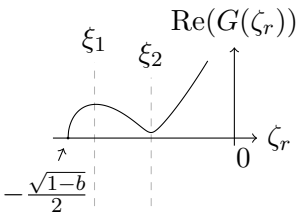

(b) Illustration for Case 2

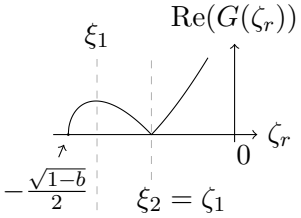

(c) Illustration for Case 3

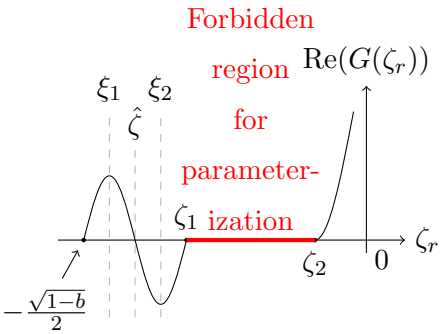

(d) Illustration for Case 4, option 1

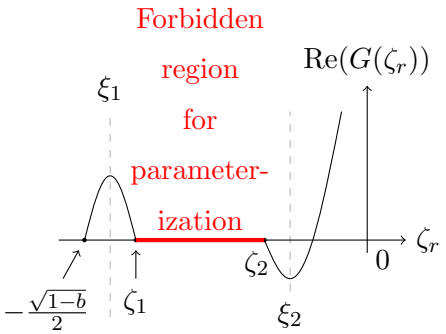

(e) Illustration for Case 4, option 2

Figure A.1: Illustrations of ζ_r *vs.* $\mathrm{Re}(G(\zeta_r))$ for the four cases in the proof of Lemma A.3.1.

In either of the two subcases of Case 4, there can be at most one $\zeta_r = \hat{\zeta}_r$ with $\operatorname{Re} G(\hat{\zeta}_r) = 0$. However, Lemma A.3.3 below shows that there must be an even number of zeros of $\operatorname{Re}(G(\zeta_r))$ for $\zeta_r < 0$. It follows that there must be 0 intersections and Case 4 is eliminated. Since Case 1 and Case 3 also do not pose any problems, only Case 2 is left to verify. This check is done numerically for some parameters, which completes the proof of Lemma A.3.1. □

Remark A.3.2. The numerical search required for Lemma A.3.1 need not take place over the whole parameter space. Case 2 can only occur when (A.48) holds with strict inequality ($b = F(k)$ corresponds to Case 3). Thus the search region covers only those b values satisfying $b > \max(k^2, F(k))$. The search space is shrunk further by looking only for those (b, k) pairs satisfying $a_4 > 0$ in (A.53). $a_4 \leq 0$ if and only if $b \geq G(k)$, where

$$G(k) := \frac{E(k) + k^2 K(k)}{2K(k)}. \tag{A.55}$$

The search region is further shrunk by first checking whether or not P_6 has two negative roots, counted with multiplicity. This check needs to be done numerically since the roots cannot be found analytically. The search region shown in Figure A.2a indicates where P_6 has two negative roots. From the numerical tests, fewer than 4% of the grid points in the search region give rise to P_6 with negative roots, independent of grid spacing. Therefore, fewer than 4% of the points are checked to satisfy $\operatorname{Re}(G(\xi_2)) > 0$. Representative plots of $\operatorname{Re}(G(\zeta_r))$ near $b = F(k)$ are shown in Figure A.2b. It is verified that, for a grid spacing of 10^{-10}, the condition $\operatorname{Re}(G(\xi_2)) > 0$ is satisfied in the necessary domain. The numerical check can be removed if it can be shown that the minimum of $\operatorname{Re}(G(\zeta_r))$ at ξ_2 is monotonically increasing as b increases from $F(k)$. I am not, however, able to prove that at this time.

A.3.1 $\zeta_c \in \mathbb{R}$: an extension of Theorem 2.2.21

I first look at cases when $b \leq B(k)$ (2.55) so that $\zeta_c \in \mathbb{R}$.

Lemma A.3.3. *Let $b \leq B(k)$ so that $\zeta_c \in \mathbb{R}$. Then for $\zeta \in (\mathbb{C}^- \cap \sigma_L) \setminus \mathbb{R}$, $\Omega(\zeta)$ has an even number of intersections with the imaginary Ω axis.*

Proof. Note that for $\zeta \in (\mathbb{C}^- \cap \sigma_L) \setminus \mathbb{R}$, $\Omega(\zeta)$ has 0, 1, or 2 intersections with the imaginary axis by Lemma A.3.1. The tangent line to $\sigma_{\mathcal{L}}$ at the origin is given by [27, equation (104)],

$$\frac{\mathrm{d}\Omega_i}{\mathrm{d}\Omega_r} = \pm \frac{(2c - \sqrt{1-b}(k^2 - 2b))E(k)}{(\sqrt{b-k^2} + \sqrt{b})(1 + \sqrt{b(b-k^2)} - b)E(k) + (1-k^2)K(k)}, \tag{A.56}$$

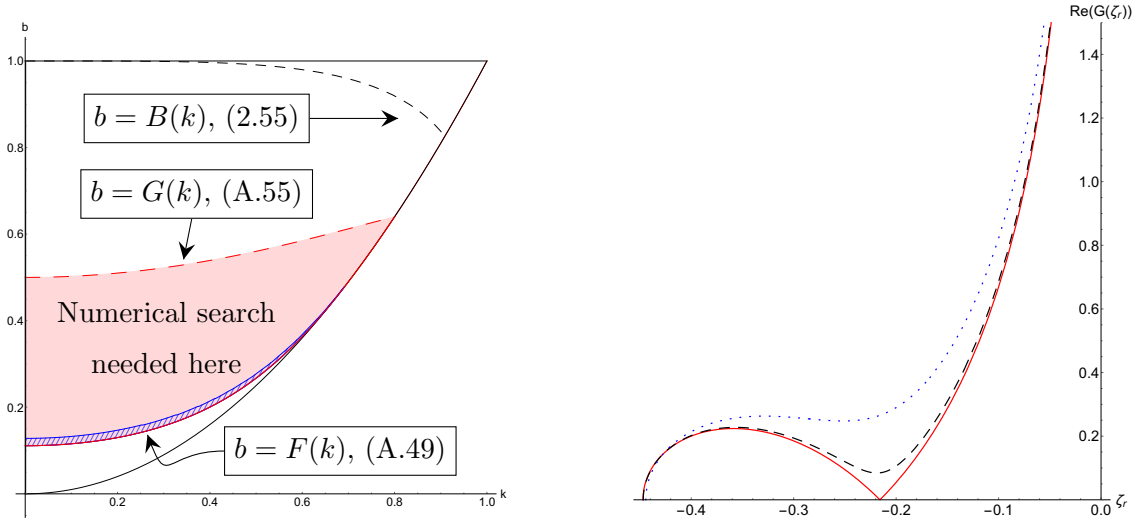

(a) (b)

Figure A.2: (a) The parameter space with curves indicating when a numerical check to show that the condition (2.73) in Theorem 2.2.21 is both necessary and sufficient. For more details, see Lemma A.3.1. The dashed blue region just above the line $b = F(k)$ indicates where P_6 has either 1 or 2 negative roots and hence where the numerical check takes place. (b) Plots of ζ_r *vs.* $\mathrm{Re}(G(\zeta_r))$ near $b = F(k)$ for $k = 0.4$. The curve $b = F(k)$ is shown in solid red, $b = F(k) + 0.001$ in dashed black, and $b = F(k) + 0.01$ in dotted blue. See Cases 2 and 3 in the proof of Lemma A.3.1. The numerical check in case 2 is to determine whether $\mathrm{Re}(G(\zeta_r)) = 0$ anywhere for $b > F(k)$.

with + corresponding to ζ_3 and − corresponding to ζ_2. It follows that for ζ near ζ_3 on σ_L, the stability spectrum enters the 1st quadrant of the λ plane. For $\zeta \in \sigma_L \setminus \mathbb{R}$ near $-\zeta_c \in \mathbb{R}$, $\zeta = -\zeta_c + i\delta_i + \mathcal{O}\left(\delta_i^2\right)$ where $\delta_i \in \mathbb{R}$ is a small perturbation parameter [27, equation (150)]. A short calculation gives

$$\Omega(-\zeta_c + i\delta_i) = \Omega(-\zeta_c) + \frac{i}{2}\frac{\delta_i}{\Omega(-\zeta_c)}(4\zeta_c^3 - 2\omega\zeta_c + c), \tag{A.57}$$

where $\Omega(-\zeta_c) \in i\mathbb{R}$. Then

$$\begin{aligned} 4\zeta_c^3 - 2\omega\zeta_c + c &= \sqrt{\frac{2E(k) - (b - k^2 + 1)K(k)}{2K^3(k)}}\left(4E(k) + K(k)(b + k^2 - 3)\right) \\ &= \sqrt{\frac{2E(k) - (b - k^2 + 1)K(k)}{2K^3(k)}}\left(k(k')^2\frac{\mathrm{d}K(k)}{\mathrm{d}k} + 2E(k) - K(k)\right) \\ &\geq 0, \end{aligned} \tag{A.58}$$

since $b < B(k)$. Since $\sigma_{\mathcal{L}}$ enters the first quadrant from the origin and enters the imaginary axis from the first quadrant, it must have an even number of crossings with the imaginary axis. In particular there must be either 0 or 2 crossings. □

Using Theorem 2.2.21, Lemmas A.3.1 and A.3.3 imply that the condition (2.73) is both a necessary and sufficient condition for spectral stability when $2E(k) - (1 + b - k^2)K(k) \geq 0$ by following the exact same proof as for Theorem 2.2.18.

Theorem A.3.4. *The sufficient condition for spectral stability* (2.73) *given in Theorem 2.2.21 is also necessary.*

Proof. Using Lemma A.3.1 notice that $\Omega(\zeta) \in i\mathbb{R}$ for $\zeta \in \sigma_L \cap \mathbb{C}^-$ if and only if $\zeta \in \mathbb{R} \cup \{\zeta_1, \zeta_2\}$. This means that the bound (2.73) is a necessary and sufficient condition for spectral stability. When $\max(k^2, F(k)) < b < G(k)$, Lemma A.3.1 relies upon a numerical check. □

Remark A.3.5. If one is not pleased working with the numerical check, then the results in this appendix only change in the following manner. The bound (2.73) still determines which solutions are spectrally stable with respect to perturbations of period $PT(k)$. It still follows that if $Q < P$ and a solution is stable with respect to perturbations of period $PT(k)$, then this solution is also spectrally stable with respect to perturbations of period $QT(k)$. The results in the appendix are only needed to rule out spectral stability with respect to other perturbations, *e.g.*, perturbations with period $RT(k)$ for $R > P$.

A.3.2 A proof of Theorem 2.2.24, $\zeta_c \in i\mathbb{R}$

In this subsection I present the details needed to establish Theorem 2.2.24.

Lemma A.3.6. *Let $c \neq 0$, $\zeta_c \in i\mathbb{R}$, and $\zeta \neq \zeta_1$ be in the open first quadrant. Then $\Omega(\zeta) \in i\mathbb{R}$ for at most one value of $\zeta \in \sigma_L$.*

Proof. The proof is similar to that of Lemma A.3.1 with the following changes. Here $Q(\zeta_r)$ always has one zero for $\zeta_r > 0$. Call this zero $\hat{\zeta}$. Then the parameterization (A.46) is valid for $\zeta_r \in [\hat{\zeta}, \sqrt{1-b}/2]$. Note that $P_6(\zeta_r)$ has at most two positive zeros by Descartes' sign rule. Since $P_6(\zeta_r)$ has at most two positive zeros and $\mathrm{Re}(G(\hat{\zeta})) = \mathrm{Re}(G(\sqrt{1-b}/2)) = 0$, it follows that there is at most one other ζ_r value at which $\mathrm{Re}(G) = 0$. □

Proof of Theorem 2.2.24. Note that if $2E(k) - (1+b-k^2)K(k) < 0$, then $\zeta_c \in i\mathbb{R}$ and it must be that σ_L intersects $i\mathbb{R} \setminus \{0\}$ (Lemma 2.2.6, see Figure 2.3(iv)). Let $\hat{\zeta} \in i\mathbb{R} \setminus \{0\}$ be the intersection point of σ_L and $i\mathbb{R} \setminus \{0\}$. Since $\mathrm{Re}(\hat{\zeta}) = 0$ and $\mathrm{Im}(\hat{\zeta}) \neq 0$, (2.57) implies that $\Omega(\hat{\zeta}) \notin i\mathbb{R}$. By (2.58), $M(\zeta)$ is increasing on (ζ_2, ζ_1) except perhaps at ζ_c if $\zeta_c \in \sigma_L$. In any case, since $M(\zeta_2) = M(\zeta_1) = 0$ mod 2π, $M(\zeta)$ traces out all of $T(k)\mu \in (0, 2\pi)$. By Lemma A.3.1, $\mathrm{Re}(\lambda) > 0$ for $\zeta \in (\zeta_2, \hat{\zeta}]$. By Lemma A.3.6, $\mathrm{Re}(\lambda) = 0$ at most at one point in the band connecting ζ_2 to ζ_1. Since I need $\mathrm{Re}(\lambda) = 0$ for $P-1$ different μ values different from 0 for stability by (2.16), it follows that there can be stability at most for $P = 2$. Since $P = 2$ corresponds to perturbations of twice the period, the desired result is established.

Finally, note that the above proof does not rely on the numerical check in Lemma A.3.1 since the curve $b = B(k)$ (2.55) always lies above the curve $b = G(k)$ (A.55) for $k^2 < b < 1$. To see this, note that $B(k) > G(k)$ if and only if

$$3E(k) - 2(k')^2 K - k^2 K(k) > 0. \tag{A.59}$$

But

$$3E(k) - 2(k')^2 K(k) - k^2 K(k) > \frac{\pi k^2}{4} \frac{2(1-k^2)^{-3/8} - (1-k^2/4)^{-1/2}}{(1-k^2/4)^{1/2}(1-k^2)^{3/8}} > 0 \tag{A.60}$$

for $0 < k < \tilde{k} \approx 0.941952$, where all estimates are found in [1, Section 19.4]. It can be verified that both $B(\tilde{k}) < \tilde{k}^2$ and $G(\tilde{k}) < \tilde{k}^2$, so $B(k) > G(k)$ everywhere in the domain $k^2 < b < 1$, hence no numerical check is needed for solutions satisfying $b > B(k)$. □

A.3.3 A proof of Lemma 2.2.8

Proof of Lemma 2.2.8. For the cn solutions and the NTP solutions with $b \leq F(k)$ (A.49) or $b \geq G(k)$ (A.55), Lemmas 2.2.17 and A.3.1 imply that every $\zeta \in (\mathbb{C}^- \cap \sigma_L) \setminus \mathbb{R}$ gives rise to an unstable eigenvalue $\lambda(\zeta)$. By [36], the elliptic solutions are spectrally stable with respect to coperiodic perturbations. Since coperiodic perturbations correspond to $T(k)\mu = 0 \mod 2\pi$, I conclude that in the cases above $M(\zeta) \neq 0$ for ζ on the complex bands of the Lax spectrum in the left half plane. It is left to show that the same result holds for the NTP solutions with $F(k) < b < G(k)$.

By continuity, an eigenvalue with $T(k)\mu = 0 \mod 2\pi$ (hereafter called a *periodic eigenvalue*) can only enter a complex band by passing through the intersection of the complex band with the real axis. Since a periodic eigenvalue has $\mathrm{Re}(\Omega(\zeta)) = 0$ by [36], it must be the case that the curve (A.46) intersects the complex band at a periodic eigenvalue. Since the intersection of (A.46) and the complex band must occur immediately upon the periodic eigenvalue entering the band, it must be that the curve (A.46) and the complex band intersect the real axis at the same location, $\zeta = -\zeta_c$ (2.54). The curve (A.46) intersects the real axis when $Q(\zeta_r) = 0$ (A.47). But $Q(\zeta_r) = 0$ only at the boundary of the region $F(k) < b < G(k)$, when $b = F(k)$. Therefore, in order to establish that no periodic eigenvalues enter the complex band, I must establish that the zero of $Q(\zeta_r)$ mentioned above is not equal to $-\zeta_c$.

When $b = F(k)$, $Q(\zeta_r)$ has a double zero at $\zeta_r = \tilde{\zeta}_1 < 0$:

$$Q(\zeta_r) = 4(\zeta_r - \tilde{\zeta}_1)^2(\zeta_r - \tilde{\zeta}_2). \tag{A.61}$$

Comparing the above expression to (A.47), I find that $\tilde{\zeta}_1^2 = \omega/6$. But

$$\begin{aligned} \zeta_c^2 - \tilde{\zeta}_1^2 &= 2\left(E(k) - \frac{1}{3}(2-k^2)K(k)\right) \\ &\geq E(k) - \frac{2}{3}K(k) > \sqrt{1-k^2}K(k) - \frac{2}{3}K(k) > 0, \end{aligned} \tag{A.62}$$

for $k^2 < 5/9$ (the inequality used for $E(k)$ comes from [1, Section 19.9]). Since $b = F(k) < k^2$ only when $k^2 < 1/2 < 5/9$, I find that the intersection of $Q(\zeta_r)$ with the real line is well separated from the intersection of the complex band with the real line for all allowed k. It follows that no periodic points can enter the complex band in the left half plane. The proof is finished by noting that since $2\pi > M(-\zeta_c) > M(\zeta_c)$, periodic points also can not enter the complex band in the right half plane.

□

A.3.4 A proof of Theorem 2.2.2

Proof of Theorem 2.2.2. The proof is similar to the proof of [11, Theorem 2]. I provide details omitted there.

For every $\lambda \in \mathbb{C}$, (2.11) can be written as a four-dimensional first-order system of ordinary differential equations. For each $\lambda \in \mathbb{C}$, one value of Ω is obtained through $\Omega = \lambda/2$. Defining

$$\tilde{Q}_4(\zeta) := -\zeta^4 + \omega\zeta^2 + c\zeta - \frac{1}{16}\left(4\omega b + 3b^2 + (1-k^2)^2\right), \tag{A.63}$$

and

$$Q_4(\Omega, \zeta) := \Omega^2 - \tilde{Q}_4(\zeta), \tag{A.64}$$

let

$$\mathcal{B} := \{\lambda \in \mathbb{C} : \text{ the discriminant of } Q_4 \text{ with respect to } \zeta \text{ vanishes}\}. \tag{A.65}$$

For $\lambda \in \mathbb{C} \setminus \mathcal{B}$, the zeros of $Q_4(\Omega, \zeta)$ give four values of $\zeta \in \mathbb{C}$. It is not necessary that each of these four values of ζ are in the Lax spectrum since this counting argument is independent of the Lax spectrum. The squared-eigenfunction connection (2.47) gives a solution to (2.11) for each of the four $\zeta \in \mathbb{C}$. Therefore, (2.47) gives four solutions of the fourth-order problem (2.11) for each $\lambda \in \mathbb{C} \setminus \mathcal{B}$. I first show that the four solutions obtained through (2.47) are linearly independent for $\lambda \in \mathbb{C} \setminus \mathcal{B}$, then later I will look at $\lambda \in \mathcal{B}$.

Using the fact that

$$B_x = 2(-i\zeta B - \phi A), \tag{A.66}$$

the eigenfunctions (2.36) may be written as

$$\begin{aligned} \chi(x,t) &= e^{\Omega t}\begin{pmatrix} -B \\ A - \Omega \end{pmatrix} y_0 \exp\left(-\int \left(\frac{B_x}{2B} + \frac{\phi\Omega}{B}\right) \, \mathrm{d}x\right) \\ &= e^{\Omega t}\begin{pmatrix} -B \\ A - \Omega \end{pmatrix} \frac{y_0}{B^{1/2}} \exp\left(-\int \frac{\phi\Omega}{B} \, \mathrm{d}x\right). \end{aligned} \tag{A.67}$$

When $\lambda \in \mathbb{C} \setminus (\mathcal{B} \cup \{0\})$, the above gives four eigenfunctions, one for each ζ. The four eigenfunctions have singularities at the zeroes of B. Since the zeros of B depend on ζ, the four eigenfunctions have different singularities in the complex x plane for the four different values of ζ. When $\Omega = 0$,

there exist two bounded eigenfunctions [36, Proposition 3.2]. Only one of these is obtained through (2.36).

Now consider the six values of $\lambda \in \mathcal{B}$. The discriminant can only vanish in one of the following cases:

1. $Q_4 = (\zeta - \hat{\zeta}_1)(\zeta - \hat{\zeta}_2)(\zeta - \hat{\zeta}_3)^2 = 0$,
2. $Q_4 = (\zeta - \hat{\zeta}_1)^2(\zeta - \hat{\zeta}_2)^2 = 0$,
3. $Q_4 = (\zeta - \hat{\zeta}_1)(\zeta - \hat{\zeta}_2)^3 = 0$, or
4. $Q_4 = (\zeta - \hat{\zeta}_1)^4 = 0$.

The zeros of Q_4 come from level sets of $\tilde{Q}_4(\zeta)$. Case 4 can only occur when the graph of $\tilde{Q}_4(\zeta)$ has one maximum. However, since I know from (2.53) that all four roots of $\tilde{Q}_4(\zeta)$ cannot be equal, case 4 is not possible. Case 3 can also be ruled out since the four roots (2.53) of $\tilde{Q}_4(\zeta)$ are real. Case 2 can only occur when two roots of (2.53) collide, which can only occur for the cn or dn solutions. The stability of these cases has been determined [42] so they are not a concern here. Finally, case 1 is possible. In case 1, only three values of ζ are determined from Ω. In such a case, three linearly independent solutions of (2.11) are found. The fourth is obtained using reduction of order and introduces algebraic growth so it is not an eigenfunction. Therefore in this case, all eigenfunctions are found using the squared-eigenfunction connection.

□

Appendix B

COMPUTING THE FLOQUET DISCRIMINANT

A common tool for characterizing the Lax spectrum for periodic potentials is the Floquet discriminant [4, 14, 31, 58]. The Floquet discriminant is typically approximated numerically since the eigenfunctions of the x equation are unknown for generic potentials. Using the framework laid out in Chapters 3 and 4, I obtain explicit expressions for the eigenfunctions (3.27). Since $\Omega(\zeta)$ is defined by its square, (3.10) defines two different values of Ω for every value of ζ for which $\Omega(\zeta) \neq 0$. Hence (3.27) defines two linearly independent solutions of (4.5) except for when $\Omega(\zeta) = 0$. When $\Omega(\zeta) = 0$, only one solution is generated by (3.27) and a second solution is found using the method of reduction of order. The solution found by reduction of order is algebraically unbounded so it is not an eigenfunction. For $\Omega(\zeta) \neq 0$, the two eigenfunctions of (4.5) are

$$\phi_{\pm}(x,t) = e^{\pm\Omega t} y_{\pm}(x) \begin{pmatrix} -\hat{B}(x) \\ \hat{A}(x) - \Omega_{\pm} \end{pmatrix}. \tag{B.1}$$

One choice of (3.27) and y_1 are used here. The following computations proceed similarly for the other choices. A fundamental matrix solution (FMS) of the x-equation of (4.5) is

$$M(x) = \begin{pmatrix} -\hat{B}(x)y_{+}(x) & -\hat{B}(x)y_{-}(x) \\ (\hat{A}(x) - \Omega_{+})y_{+}(x) & (\hat{A}(x) - \Omega_{-})y_{-}(x) \end{pmatrix}, \tag{B.2}$$

where dependence on t has been omitted. The FMS normalized to the identity is given by

$$\tilde{M}(x; x_0) = M^{-1}(x_0)M(x). \tag{B.3}$$

To simplify notation, define

$$I_{\pm}(x;\zeta) = -\int \left(\hat{\alpha} + \frac{\hat{\beta}\hat{C}}{\hat{A} - \Omega_{\pm}} \right) \, \mathrm{d}x. \tag{B.4}$$

In this section Assumption B.0.1 is used instead of assuming that $\alpha \in i\mathbb{R}$.

Assumption B.0.1. $\hat{\alpha}$ and $\hat{\beta}C/(\hat{A} - \Omega)$ are periodic in x with the same period P as the solution.

Under Assumption B.0.1, each of the integrands in (4.7) is P-periodic, and any of the representations may be used for I. It follows that

$$I_{\pm}(x+P;\zeta) = I_{\pm}(x;\zeta) + I_{\pm}(P;\zeta). \tag{B.5}$$

Then

$$y_{\pm}(x+P) = y_{\pm}(x)e^{I_{\pm}(x;\zeta)}e^{I_{\pm}(P;\zeta)} = y_{\pm}(x)\Gamma_{\pm}(P), \tag{B.6}$$

and

$$\tilde{M}(x+P;x_0) = M^{-1}(x_0)M(x+P) = M^{-1}(x_0)M(x)\Gamma(P) = \tilde{M}(x;x_0)\Gamma(P), \tag{B.7}$$

where

$$\Gamma(P) = \begin{pmatrix} \Gamma_+(P) & 0 \\ 0 & \Gamma_-(P) \end{pmatrix} \tag{B.8}$$

is the transfer matrix. In order for solutions to be bounded in space, it must be that the eigenvalues of the transfer matrix have unit modulus. Thus,

$$\mathrm{Re}\left(I_{\pm}(P;\zeta)\right) = 0. \tag{B.9}$$

If Assumption B.0.1 holds, this is equivalent to (4.7). The Floquet discriminant is defined by

$$\Delta(\zeta) = \mathrm{tr}(\Gamma(P)) = \Gamma_+(P) + \Gamma_-(P), \tag{B.10}$$

and

$$\sigma_L = \left\{\zeta \in \mathbb{C} : \mathrm{Im}(\Delta(\zeta)) = 0 \quad \text{and} \quad |\Delta(\zeta)| \leq 2\right\}. \tag{B.11}$$

Both definition (B.11) and (4.7) require numerical computation or the use of special functions. I prefer working with (4.7) directly, but I present the Floquet discriminant because of its popularity.

BIBLIOGRAPHY

[1] *NIST Digital Library of Mathematical Functions*. http://dlmf.nist.gov/, Release 1.0.14 of 2016-12-21. F. W. J. Olver, A. B. Olde Daalhuis, D. W. Lozier, B. I. Schneider, R. F. Boisvert, C. W. Clark, B. R. Miller and B. V. Saunders, eds.

[2] R. A. Van Gorder. Orbital stability for stationary solutions of the Wadati–Konno–Ichikawa–Shimizu equation. *Journal of the Physical Society of Japan*, 82(6):064005, 2013.

[3] M. J. Ablowitz and P. A. Clarkson. *Solitons, nonlinear evolution equations and inverse scattering*, volume 149 of *London Mathematical Society Lecture Note Series*. Cambridge University Press, Cambridge, 1991.

[4] M. J. Ablowitz, B. M. Herbst, and C. M. Schober. Computational chaos in the nonlinear Schrödinger equation without homoclinic crossings. *Phys. A*, 228(1-4):212–235, 1996.

[5] M. J. Ablowitz and Z. H. Musslimani. Inverse scattering transform for the integrable nonlocal nonlinear Schrödinger equation. *Nonlinearity*, 29(3):915–946, 2016.

[6] M. J. Ablowitz and Z. H. Musslimani. Integrable nonlocal nonlinear equations. *Stud. Appl. Math.*, 139(1):7–59, 2017.

[7] M.J. Ablowitz, D.J. Kaup, A.C. Newell, and H. Segur. The inverse scattering transform-Fourier analysis for nonlinear problems. *Studies in Appl. Math.*, 53(4):249–315, 1974.

[8] M.J. Ablowitz and H. Segur. *Solitons and the inverse scattering transform*, volume 4 of *SIAM Studies in Applied Mathematics*. Society for Industrial and Applied Mathematics (SIAM), Philadelphia, Pa., 1981.

[9] M. Antonowicz and A. P. Fordy. Hamiltonian structure of nonlinear evolution equations. In *Soliton theory: a survey of results*, Nonlinear Sci. Theory Appl., pages 273–312. Manchester Univ. Press, Manchester, 1990.

[10] N. Bottman and B. Deconinck. KdV cnoidal waves are spectrally stable. *Discrete Contin. Dyn. Syst.*, 25(4):1163–1180, 2009.

[11] N. Bottman, B. Deconinck, and M. Nivala. Elliptic solutions of the defocusing NLS equation are stable. *J. Phys. A*, 44(28):285201, 24, 2011.

[12] J. C. Bronski, V. M. Hur, and M. A. Johnson. Modulational instability in equations of kdv type. In *New approaches to nonlinear waves*, pages 83–133. Springer, 2016.

[13] P.F. Byrd and M.D. Friedman. *Handbook of elliptic integrals for engineers and physicists*, volume 67. Springer, 2013.

[14] A. Calini, S.F. Keith, and S. Lafortune. Squared eigenfunctions and linear stability properties of closed vortex filaments. *Nonlinearity*, 24(12):3555–3583, 2011.

[15] T. Cazenave and P.-L. Lions. Orbital stability of standing waves for some nonlinear Schrödinger equations. *Comm. Math. Phys.*, 85(4):549–561, 1982.

[16] F.F. Chen. *Introduction to plasma physics*. Springer Science & Business Media, 2012.

[17] J. Chen and D.E. Pelinovsky. Rogue periodic waves of the focusing nonlinear Schrödinger equation. *Proceedings of the Royal Society A: Mathematical, Physical and Engineering Sciences*, 474(2210):20170814, 2018.

[18] J. Chen and D.E. Pelinovsky. Rogue periodic waves of the modified KdV equation. *Nonlinearity*, 31(5):1955, 2018.

[19] J. Chen, D.E. Pelinovsky, and R.E. White. Periodic standing waves in the focusing nonlinear schrödinger equation: Rogue waves and modulation instability. *Physica D: Nonlinear Phenomena*, 405:132378, 2020.

[20] Xiang-Jun Chen and Jianke Yang. Direct perturbation theory for solitons of the derivative nonlinear schrödinger equation and the modified nonlinear schrödinger equation. *Physical Review E*, 65(6):066608, 2002.

[21] R. Conte and M. Musette. *The Painlevé handbook*. Springer, Dordrecht, 2008.

[22] B. Deconinck and T. Kapitula. The orbital stability of the cnoidal waves of the Korteweg-de Vries equation. *Phys. Lett. A*, 374(39):4018–4022, 2010.

[23] B. Deconinck and J.N. Kutz. Computing spectra of linear operators using the Floquet-Fourier-Hill method. *J. Comput. Phys.*, 219(1):296–321, 2006.

[24] B. Deconinck, P. McGill, and B. L. Segal. The stability spectrum for elliptic solutions to the sine-Gordon equation. *Phys. D*, 360:17–35, 2017.

[25] B. Deconinck, P. Meuris, and F. Verheest. Oblique nonlinear Alfvén waves in strongly magnetized beam plasmas. part 1. nonlinear vector evolution equation. *Journal of plasma physics*, 50(3):445–455, 1993.

[26] B. Deconinck and M. Nivala. The stability analysis of the periodic traveling wave solutions of the mKdV equation. *Stud. Appl. Math.*, 126(1):17–48, 2011.

[27] B. Deconinck and B. L. Segal. The stability spectrum for elliptic solutions to the focusing NLS equation. *Phys. D*, 346:1–19, 2017.

[28] B. Deconinck and J. Upsal. The Orbital Stability of Elliptic Solutions of the Focusing Nonlinear Schrödinger Equation. *SIAM J. Math. Anal.*, 52(1):1–41, 2020.

[29] J.N. Elgin, V.Z. Enolski, and A.R. Its. Effective integration of the nonlinear vector Schrödinger equation. *Physica D: Nonlinear Phenomena*, 225(2):127–152, 2007.

[30] V. Z. Enolskii, F. Gesztesy, and H. Holden. The classical massive Thirring system revisited. In *Stochastic processes, physics and geometry: new interplays, I (Leipzig, 1999)*, volume 28 of *CMS Conf. Proc.*, pages 163–200. Amer. Math. Soc., Providence, RI, 2000.

[31] N.M. Ercolani and D.W. McLaughlin. Toward a topological classification of integrable PDEs. In *The geometry of Hamiltonian systems (Berkeley, CA, 1989)*, volume 22 of *Math. Sci. Res. Inst. Publ.*, pages 111–129. Springer, New York, 1991.

[32] H. M. Farkas and I. Kra. *Riemann surfaces*, volume 71 of *Graduate Texts in Mathematics*. Springer-Verlag, New York, second edition, 1992.

[33] M. G. Forest and D. W. McLaughlin. Spectral theory for the periodic sine-Gordon equation: a concrete viewpoint. *J. Math. Phys.*, 23(7):1248–1277, 1982.

[34] J. Frenkel and T. Kontorova. On the theory of plastic deformation and twinning. *Acad. Sci. U.S.S.R. J. Phys.*, 1:137–149, 1939.

[35] T. Gallay and M. Hărăguş. Stability of small periodic waves for the nonlinear Schrödinger equation. *J. Differential Equations*, 234(2):544–581, 2007.

[36] T. Gallay and M. Hărăguş. Orbital stability of periodic waves for the nonlinear Schrödinger equation. *J. Dynam. Differential Equations*, 19(4):825–865, 2007.

[37] T. Gallay and D. Pelinovsky. Orbital stability in the cubic defocusing NLS equation: I. Cnoidal periodic waves. *J. Differential Equations*, 258(10):3607–3638, 2015.

[38] R. A. Gardner. Spectral analysis of long wavelength periodic waves and applications. *J. Reine Angew. Math.*, 491:149–181, 1997.

[39] V. Gerdjikov, G. Vilasi, and A. B. Yanovski. *Integrable hamiltonian hierarchies: Spectral and geometric methods*, volume 748. Springer Science & Business Media, 2008.

[40] M. Grillakis, J. Shatah, and W. Strauss. Stability theory of solitary waves in the presence of symmetry, i. *Journal of Functional Analysis*, 74(1):160–197, 1987.

[41] E. P. Gross. Structure of a quantized vortex in boson systems. *Nuovo Cimento (10)*, 20:454–477, 1961.

[42] S. Gustafson, S. Le Coz, and T. Tsai. Stability of periodic waves of 1D cubic nonlinear Schrödinger equations. *Appl. Math. Res. Express. AMRX*, (2):431–487, 2017.

[43] T. Hada, CF Kennel, and B. Buti. Stationary nonlinear Alfvén waves and solitons. *Journal of Geophysical Research: Space Physics*, 94(A1):65–77, 1989.

[44] M. Hărăguş and T. Kapitula. On the spectra of periodic waves for infinite-dimensional Hamiltonian systems. *Phys. D*, 237(20):2649–2671, 2008.

[45] T. Ivey and S. Lafortune. Spectral stability analysis for periodic traveling wave solutions of NLS and CGL perturbations. *Phys. D*, 237(13):1750–1772, 2008.

[46] Christopher K. R. T. Jones, R. Marangell, P. D. Miller, and R. G. Plaza. On the stability analysis of periodic sine-Gordon traveling waves. *Phys. D*, 251:63–74, 2013.

[47] T. Kapitula. On the stability of N-solitons in integrable systems. *Nonlinearity*, 20(4):879–907, 2007.

[48] D. J. Kaup and T. I. Lakoba. The squared eigenfunctions of the massive Thirring model in laboratory coordinates. *J. Math. Phys.*, 37(1):308–323, 1996.

[49] D.J. Kaup. Perturbation theory for solitons in optical fibers. *Physical Review A*, 42(9):5689, 1990.

[50] D.J. Kaup and A.C. Newell. An exact solution for a derivative nonlinear Schrödinger equation. *Journal of Mathematical Physics*, 19(4):798–801, 1978.

[51] A. Khare and A. Saxena. Periodic and hyperbolic soliton solutions of a number of nonlocal nonlinear equations. *J. Math. Phys.*, 56(3):032104, 27, 2015.

[52] Y.S. Kivshar and G. Agrawal. *Optical solitons: from fibers to photonic crystals*. Academic press, 2003.

[53] Y. Kodama and A. Hasegawa. Nonlinear pulse propagation in a monomode dielectric guide. *IEEE Journal of Quantum Electronics*, 23(5):510–524, 1987.

[54] R. Kollár and P. D. Miller. Graphical Krein signature theory and Evans-Krein functions. *SIAM Rev.*, 56(1):73–123, 2014.

[55] E. A. Kuznetsov, A. M. Rubenchik, and V. E. Zakharov. Soliton stability in plasmas and hydrodynamics. *Phys. Rep.*, 142(3):103–165, 1986.

[56] S. Lafortune. personal communication, 2018.

[57] M Lakshmanan and S Ganesan. Equivalent forms of a generalized hirota's equation with linear inhomogeneities. *Journal of the Physical Society of Japan*, 52(12):4031–4033, 1983.

[58] J. J. Lee. *The inverse spectral solution, modulation theory and linearized stability analysis of n-phase, quasi-periodic solutions of the nonlinear Schrodinger equation.* PhD thesis, The Ohio State University, 1986.

[59] F. Lund. Example of a relativistic, completely integrable, Hamiltonian system. *Physical Review Letters*, 38(21):1175, 1977.

[60] Y.C. Ma and M.J. Ablowitz. The periodic cubic Schrödinger equation. *Stud. Appl. Math.*, 65(2):113–158, 1981.

[61] J.H. Maddocks and R.L. Sachs. On the stability of KdV multi-solitons. *Comm. Pure Appl. Math.*, 46(6):867–901, 1993.

[62] S. V. Manakov. On the theory of two-dimensional stationary self-focusing of electromagnetic waves. *Soviet Physics-JETP*, 38(2):248–253, 1974.

[63] A. S. Markus. *Introduction to the spectral theory of polynomial operator pencils*, volume 71 of *Translations of Mathematical Monographs*. American Mathematical Society, Providence, RI, 1988. Translated from the Russian by H. H. McFaden, Translation edited by Ben Silver, With an appendix by M. V. Keldysh.

[64] M. Nivala and B. Deconinck. Periodic finite-genus solutions of the KdV equation are orbitally stable. *Phys. D*, 239(13):1147–1158, 2010.

[65] L.P. Pitaevskii. Vortex lines in an imperfect Bose gas. *Sov. Phys. JETP*, 13(2):451–454, 1961.

[66] G. Rowlands. On the stability of solutions of the non-linear Schrödinger equation. *IMA Journal of Applied Mathematics*, 13(3):367–377, 06 1974.

[67] B. Sandstede and A. Scheel. On the stability of periodic travelling waves with large spatial period. *J. Differential Equations*, 172(1):134–188, 2001.

[68] T. Shimizu and M. Wadati. A new integrable nonlinear evolution equation. *Progress of Theoretical Physics*, 63:808–820, 1980.

[69] C. Sulem and P.-L. Sulem. *The nonlinear Schrödinger equation: self-focusing and wave collapse*, volume 139. Springer Science & Business Media, 2007.

[70] F. Tisseur and K. Meerbergen. The quadratic eigenvalue problem. *SIAM review*, 43(2):235–286, 2001.

[71] J Upsal and B Deconinck. Real lax spectrum implies spectral stability. *In preparation*, 2019.

[72] M.I. Weinstein. Lyapunov stability of ground states of nonlinear dispersive evolution equations. *Comm. Pure Appl. Math.*, 39(1):51–67, 1986.

[73] E.T. Whittaker and G.N. Watson. *A course of modern analysis*. Cambridge university press, 1996.

[74] S. Wiggins. *Introduction to applied nonlinear dynamical systems and chaos*, volume 2 of *Texts in Applied Mathematics*. Springer-Verlag, New York, 1990.

[75] Z. Yang and K. Zumbrun. Convergence as period goes to infinity of spectra of periodic traveling waves toward essential spectra of a homoclinic limit. *arXiv preprint arXiv:1802.02830*, 2018.

[76] V. E. Zakharov and E. I. Schulman. Integrability of nonlinear systems and perturbation theory. In *What is integrability?*, Springer Ser. Nonlinear Dynam., pages 185–250. Springer, Berlin, 1991.

[77] V. E. Zakharov and A. B. Shabat. Exact theory of two-dimensional self-focusing and one-dimensional self-modulation of waves in nonlinear media. *Ž. Èksper. Teoret. Fiz.*, 61(1):118–134, 1971.

[78] V.E. Zakharov. Stability of periodic waves of finite amplitude on the surface of a deep fluid. *Journal of Applied Mechanics and Technical Physics*, 9(2):190–194, 1968.

[79] H. Zhu, Sh. Yu, S. Shen, and W. Ma. New integrable sl (2,R)-generalization of the classical Wadati–Konno–Ichikawa hierarchy. *Communications in Nonlinear Science and Numerical Simulation*, 22(1-3):1341–1349, 2015.